AD_____

Award Number: W81XWH-04-1-0068

TITLE: Cell Therapy to Obtain Spinal Fusion

PRINCIPAL INVESTIGATOR: Elizabeth A. Olmsted-Davis, Ph.D.
Alan R. Davis, Ph.D.
Kevin M. Moran, M.D.
Jennifer West, Ph.D.

CONTRACTING ORGANIZATION: Baylor College of Medicine
Houston TX 77030

REPORT DATE: March 2007

TYPE OF REPORT: Final

PREPARED FOR: U.S. Army Medical Research and Materiel Command
Fort Detrick, Maryland 21702-5012

REPORT DOCUMENTATION PAGE

Form Approved
OMB No. 0704-0188

1. REPORT DATE *(DD-MM-YYYY)*	**2. REPORT TYPE**	**3. DATES COVERED** *(From - To)*
01-03-2007	Final	02 Jan 04 – 28 Feb 07

4. TITLE AND SUBTITLE
Cell Therapy to Obtain Spinal Fusion

5a. CONTRACT NUMBER

5b. GRANT NUMBER
W81XWH-04-1-0068

5c. PROGRAM ELEMENT NUMBER

6. AUTHOR(S)
Elizabeth A. Olmsted-Davis, Ph.D.; Alan R. Davis, Ph.D.; Kevin M. Moran, M.D.
Jennifer West, Ph.D.

E-Mail: edavis@bcm.tmc.edu

5d. PROJECT NUMBER

5e. TASK NUMBER

5f. WORK UNIT NUMBER

7. PERFORMING ORGANIZATION NAME(S) AND ADDRESS(ES)

Baylor College of Medicine
Houston TX 77030

8. PERFORMING ORGANIZATION REPORT NUMBER

9. SPONSORING / MONITORING AGENCY NAME(S) AND ADDRESS(ES)
U.S. Army Medical Research and Materiel Command
Fort Detrick, Maryland 21702-5012

10. SPONSOR/MONITOR'S ACRONYM(S)

11. SPONSOR/MONITOR'S REPORT NUMBER(S)

12. DISTRIBUTION / AVAILABILITY STATEMENT
Approved for Public Release; Distribution Unlimited

13. SUPPLEMENTARY NOTES

14. ABSTRACT:
Surgery of the spine to fuse the vertebral bones is one of the most commonly performed operations with an estimated 350,000 Americans undergoing this surgery annually with estimated costs of $60 billion. Current procedures are highly invasive with limited success. The goal of this study is to develop a safe efficacious system for inducing spine fusion which will eliminate the need for invasive surgery. We have currently developed a cell based gene therapy system that can induce rapid bone formation at a targeted location which is independent of immune status of the model. This system relies on adenovirus transduced cells expressing bone morphogenetic protein 2 to induce bone formation leading to vertebral fusion after delivery into the paraspinous musculature. To prolong cell survival and insure cells are maintained at the target site, we have encapsulated them in a non-degradable hydrogel material. This provides additional safety by eliminating direct injection of the virus through cell delivery, and prevention of cell diffusion, through encapsulation. Here we provide preliminary data; demonstrating spine fusion using this system at 6 weeks after induction. This is the first step in demonstrating efficacy, a critical component of preclinical testing. Thus with validation of our hypothesis, this approach can now be developed as a safe and efficacious gene therapy system for spine fusion, thus circumventing the need for costly invasive surgery.

15. SUBJECT TERMS
BMP2, Spine fusion, Hydrogel, Gene Therapy, Adenovirus

16. SECURITY CLASSIFICATION OF:			**17. LIMITATION OF ABSTRACT**	**18. NUMBER OF PAGES**	**19a. NAME OF RESPONSIBLE PERSON**
a. REPORT	**b. ABSTRACT**	**c. THIS PAGE**			USAMRMC
U	U	U	UU	104	**19b. TELEPHONE NUMBER** *(include area code)*

Table of Contents

Introduction: Surgery of the spine to fuse the vertebral bones is one of the most commonly performed operations with some 400,000 Americans undergoing this type of surgery annually in the United States. The estimated cost associated with such procedures exceeding $60 billion annually demonstrating this to be a significant problem. In the most common form, posterolateral fusion, the paraspinous musculature is stripped and the bone decorticated, resulting in significant pain, reduced stability afforded by these muscles, and disruption of the blood supply to both bone and muscle. Further, success rates for fusion range from 50-70% depending on how many levels are fused and the number and types of attendant complications. We recently demonstrated that transduced cells expressing high levels of bone morphogenetic protein 2 (BMP2) in skeletal muscle could rapidly recruit and expand endogenous cell populations to initiate all stages of endochondral bone formation, with mineralized bone forming within one week of implantation. The central hypothesis of this application is that posterolateral spine fusion can be successfully achieved with only minimally invasive percutaneous techniques and without a scaffold, by collecting cells from patient's, transducing them to express BMP2, encapsulating the cells with hydrogel material, and then delivering them to the fusion site. If added structural stability is required, the injectable hydrogel will be crosslinked *in vivo* with a small fiber-optic light source. Successful completion of this project would advance the current state of gene therapy in this field by eliminating the search for an optimal osteoprogenitor cell and scaffolding.

Body: The central hypothesis of this application is that posterolateral spine fusion can be successfully achieved with only minimally invasive percutaneous techniques and without a scaffold, by collecting cells from patient's peripheral blood, transducing them to express an osteoinductive factor (bone morphogenetic protein 2 or BMP2), encapsulating the cells with hydrogel material, and then delivering them to the fusion site. We have developed three specific tasks to accomplish our goals.

Task 1: To produce high levels of BMP2 from human peripheral blood cells transduced with the Ad5F35BMP2 chimeric adenovirus. (Months 7-14). These tasks were reviewed in our last update. We have included the previous data reported last year, but also provided additional data that has led to a recent publication in *Human Gene Therapy* (Fouletier-Dilling *et al*, 2005). Since our previous studies (first progress report) demonstrated a significant reduction (≥50%) in the amount of BMP2 secreted from human peripheral blood mononuclear cells transduced with adenovirus vectors, as compared to similar numbers of other fibroblast cell lines transduced in parallel, we focused on improving the transduction efficiency. In these studies using a variety of cells rather than human peripheral blood we developed a novel method for improving transduction efficiency with our chimeric virus.

a. ***Determine the viral transduction efficiency of human peripheral blood with Ad5F35 chimeric adenovirus, and compare this to the efficiency of transduction in purified human peripheral blood mononuclear cells. (Months 1-4).*** Briefly, our results indicated that a small amount of BMP2 was detected in the media in both concentrations of purified mononuclear cells, but this was greatly reduced to that which is found with other fibroblasts (Figure 1). However, in the whole blood samples with the same number of white cells, BMP2 activity was equal to the control suggesting that either the vector was not able to efficiently transduce the cells, or the BMP2 was being rapidly degraded. **Results indicate that we must purify mononuclear cells if we continue to use human peripheral blood.**

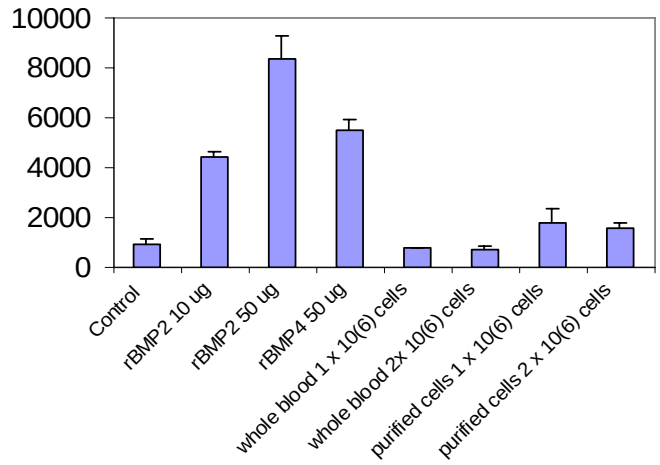

Figure 1: Alkaline phosphatase induction in W20-17 cells after exposure to BMP2. BMP2 activity in was assessed in culture supernatant taken from either whole peripheral or purified mononuclear cells from blood 48 hours after transduction with Ad5F35BMP2 (2500 vp/cell).

b. ***BMP2 levels will be determined by Western blot analysis of human peripheral blood cells transduced with the chimeric adenovirus. (Months 5-8).***

From our results described in the above section, we chose to pursue improving the transduction in purified mononuclear cells. We therefore isolated peripheral blood, purified the mononuclear cells as described above, and plated them directly into a 24 well dish in varying concentrations (10^6,10^7,10^8) in DMEM supplemented with 2% FBS, with antibiotic-antimycotic. Since we previously determined that the critical factor for inducing bone formation is the level of BMP2 secretion (Olmsted-Davis *et al* 2002, Gugala *et al*, 2003) expression by escalating both the cell number and adenovirus dose. Therefore the cells were transduced with Ad5F35BMP2 with varying MOI of (2500 vp/cell, 5000 vp/cell, and 10,000 vp/cell) and placed in a humid chamber at 37°C and 5% CO_2 for 72 hours prior to collection of the culture supernatant. Cells were also transduced with Ad5F35GFP (10,000 vp/cell) as a control. We have chosen to assay the BMP2 by an ELISA (R&D systems, Inc., Minneapolis, MS) rather than western blot in that it is a more rapid, quantitative method for large numbers of samples. Briefly, the culture supernatant was added to the ELISA assay according to manufacturer's specifications. rBMP2, of known concentrations, was used to generate a standard curve which was then used to quantify the amount of BMP2 in culture supernatant. Figure 2, shows the results of the BMP2 quantification.

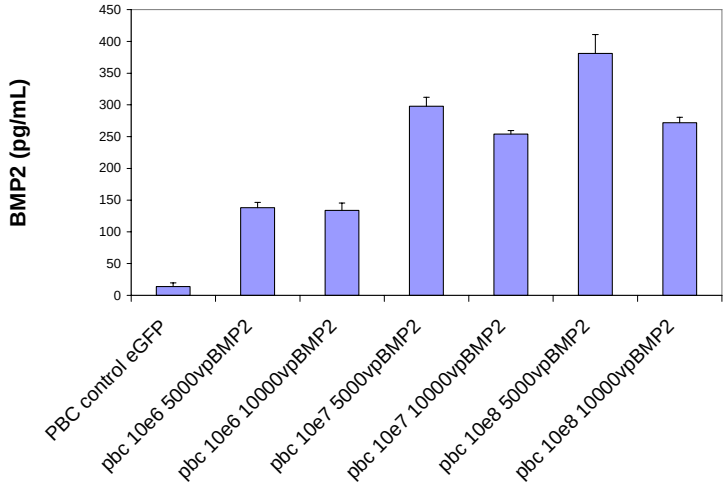

Figure 2: Analysis of BMP2 protein in conditioned media from purified mononuclear cells in peripheral blood. Mononuclear cells were purified on a Ficoll-Paque™ PLUS (Amersham Pharmacia Biotech, Piscatawy, NJ) and transduced with Ad5F35BMP2 virus (5000 vp/cell and 10,000 vp/) or Ad5F35GFP (10,000 vp/cell). Cell number was also varied from 10^6, 10^7, 10^8 cells/ml as indicated and culture supernatant was collected 72 hours after initial transduction. Cell viability in these experiments was determined to be greater than 90%.

As can bee seen in figure 2, escalation of virus dose did not appear to enhance the BMP2 expression, suggesting that the cellular internalization mechanism may be saturated, and hence no more virus can be taken up by the cells. As expected we did see an elevation of BMP2 in culture supernatant with increasing number of transduced cells. However, this level of expression is still significantly lower than what we achieve with the fibroblasts; therefore we may need to consider some alternatives beyond escalation of cell number. Please see the conclusions **section d, *Task 1*** for alternative strategies.

In an attempt to improve the transduction efficiency of the Ad5F35BMP2 we chose to compare the normal adenovirus infection methods to that obtained when the lipid-polyamine known as GeneJammer® Transfection Reagent (Stratagene, La Jolla, CA) was included in the infection. Although this is currently

marketed for DNA rather than virus transfer, we have determined that this reagent greatly enhances the transduction of cells with adenovirus (Fouletier-Dilling *et al*, 2006, see appendix).

- ***Enhanced viral transduction in the presence of GeneJammer®***

Adenovirus transduction of coxackie-adenovirus receptor (CAR)-negative cell lines is extremely inefficient requiring large amounts of virus, and resulting in low level expression of the desired transgene. To enhance virus uptake into the cells, we tested the ability of the commercially available polyamine complex, GeneJammer® to enhance virus transduction. Accordingly, CAR-negative hBM-MSCs (10^6 cells) were transduced with Ad5eGFP virus at three different concentrations (2500 vp/cell, 5000 vp/cell, and 10000 vp/cell) in the presence or absence of GeneJammer® (Fig. 3A). An adenovirus type 5 lacking any transgene (Ad-empty) was used as a negative control. As seen in Fig. 3A, the presence of the polyamine, GeneJammer® increases the number of the hBM-MSCs transduced cells for all concentrations of virus. The lowest MOI of 2500 vp/cell resulted in the most dramatic increase in number of transduced cells, with 15% in the absence of GeneJammer® and 95% transduced in the presence of the polyamine. Further we observed an increase in the number of transduced cells with a corresponding increase in virus MOI in the absence of GeneJammer®, however, in the presence GeneJammer®, the maximum number of transduced cells (95-100%) was found for all virus concentrations.

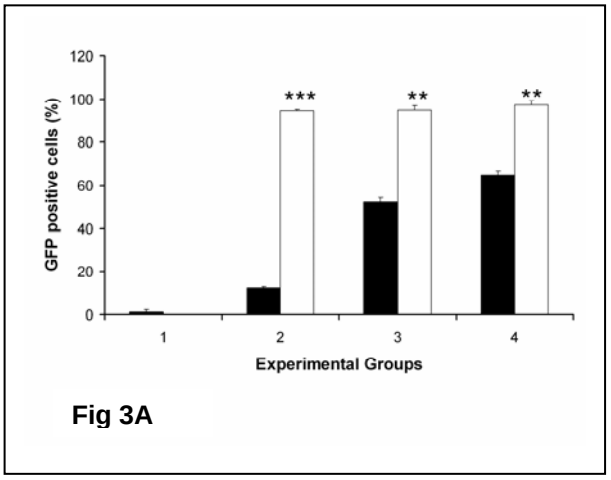

Fig 3A

Since multiple virus particles can enter the same cell, we also analyzed the samples transduced in the presence of GeneJammer®, in which we obtained 95-100% cell transduction, to determine if the intensity of GFP expression increased with virus concentration. As can be seen in Figure 3B, the intensity of GFP expression from the cells transduced with GeneJammer®, increased with virus dose. Since 100% of the cells were transduced at all virus doses in this population, the increase in GFP intensity presumably represents an increase in the number of virus particles each cell is taking up. The data suggests that GeneJammer® not only enhances the number of cells taking up the virus (Fig. 3A) but also the total amount of virus entering any given cell (Fig. 3B).

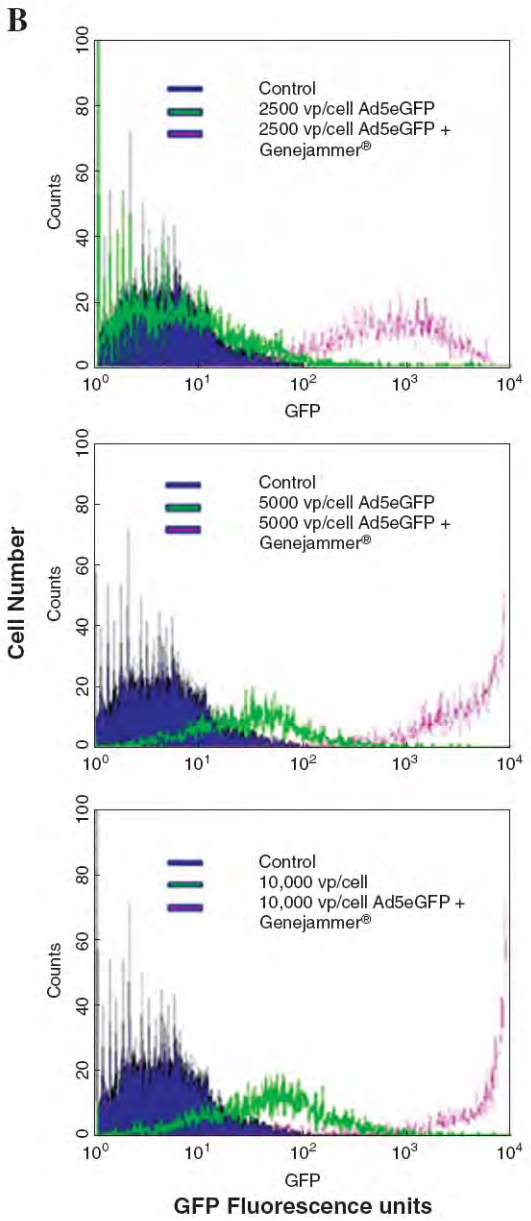

Figure 3: (A) Flow cytometric quantification of GFP expression after transduction of hBM-MSCs with (1) Ad5-empty, (2) Ad5eGFP 2,500vp/cell, (3) Ad5eGFP 5,000vp/cell, or (4) Ad5eGFP 10,000vp/cell in the absence (solid columns) or presence (open columns) of GeneJammer®. The percentage of GFP-positive cells is depicted as the average eGFP fluorescence, where n=3. Columns and error bars represent means ± standard deviation for n=3. *** represent p<0.001 and ** represent p<0.01 (Student t test). **(B)** GFP fluorescence intensity shifts in the flow cytometry profiles of eGFP expression in the hBM-MSCs transduced with either 2,500 vp/cell, 5,000 vp/cell, or 10,000 vp/cell Ad5GFP in the presence of GeneJammer® shown in **(A)**. In all samples 100% of the cells were found to express eGFP.

The compound GeneJammer® allows adenovirus to enter cells lacking the receptor for fiber

Two potential models exist as to the mechanism by which the polyamine enhances virus uptake. First, GeneJammer® may aid in virus binding to its receptor, therefore potentially acting as a co-receptor for the virus internalization. Alternatively, this compound may bind to the virus and promote a novel entry route into the cell. To determine which of these is most likely, we compared the transduction efficiency of various cell types known to have differential expression levels of CAR and αV integrin (Ad5) or CD46 (Ad5F35), in the presence or absence of GeneJammer®. The three cells lines chosen have the following receptor characteristics: A549 cells express high levels of CAR, αV integrin, and CD46; hBM-MSCs lack CAR but express αV integrin, and express moderate levels of CD46, and CHO cells express little to no adenovirus receptors (Table 1). As expected, Ad5eGFP (2500 vp/cell) transduced 100% of the receptor positive A549 cells, while less than 15% of the receptor negative CHO cells were transduced (Fig. 4A and C).

TABLE 1. ADENOVIRUS RECEPTOR EXPRESSION ON SELECTED CELL LINES[a]

	Expression (%) of cell surface receptor		
Cell line	*CAR*	*Integrin α_v*	*CD46*
A549	93.28 ± 1.28	99.26 ± 0.53	99.27 ± 0.79
hBM-MSCs	0.34 ± 0.50[b]	87 ± 4.70[b]	31.78 ± 3.54
CHO	1.77 ± 0.27	2.04 ± 0.16	0.19 ± 0.05

Abbreviations: CAR, coxsackievirus–adenovirus receptor; CHO, Chinese hamster ovary; hBM-MSCs, human bone marrow mesenchymal stem cells.

[a]Numbers represent the mean percentage of cells expressing each receptor ± SD ($n = 3$).

[b]From Olmsted-David *et al.* (2002).

The hBM-MSCs which are αV integrin positive-CAR negative yielded approximately 10% of the cells expressing GFP at this same MOI (Fig. 2B). Parallel transductions done in the presence of GeneJammer® showed significant enhancement in transduction in both the cells lacking CAR but expressing αV integrin, as well as the receptor negative cells (Fig. 4B and C). The results (Fig. 4C) show approximately 95% of the transduced CHO cells were expressing GFP when the adenovirus was delivered in the presence of the polyamine, suggesting that the molecular mechanism is not adenovirus receptor associated but rather, a novel pathway for virus entry into the cell. We did not see any significant changes between the groups in the A549 cells (Fig. 4A) due to the fact that the cells in the absence of GeneJammer® have been maximally transduced. However, the data suggests that these two systems for virus entry do not appear to inhibit one another (Fig. 4A).

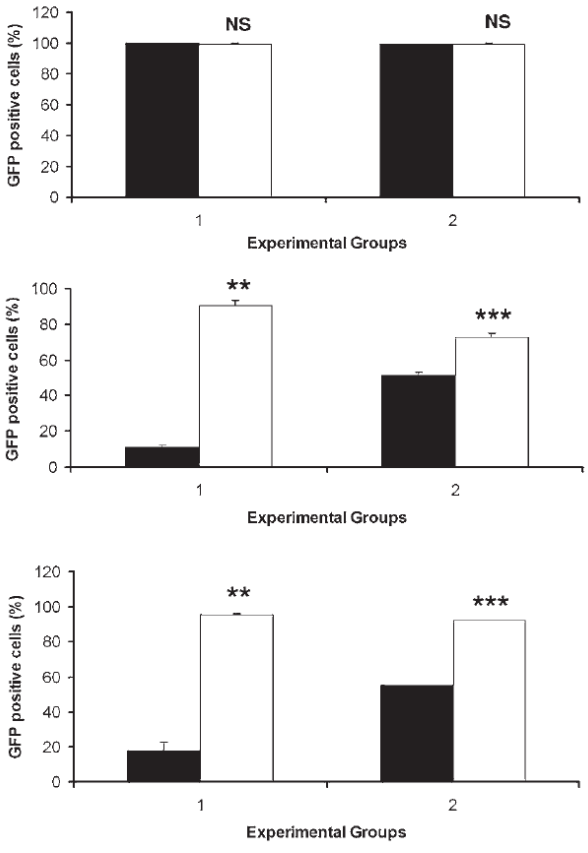

Next we chose to determine if the virus entry into the cells via the polyamine was specific to the adenovirus type 5 capsid, so similar experiments were conducted using the altered fiber virus Ad5F35eGFP. The results were similar to those obtained with the Ad5 vector, suggesting similar mechanism that is not dependant on adenovirus type 5 fiber for entry into the cell (Figure 4).

Figure 4: Flow cytometry analysis of GFP expression of A549 cells **(A)**, hBM-MSCs (B) and CHO cells **(C)** transduced with Ad5eGFP 2,500 vp/cell (bar 1), Ad5F35eGFP 2,500 vp/cell (bar 2). In the absence ■ or presence □ of GeneJammer®. The percentage of GFP positive cells was depicted as the average GFP fluorescence where n=3. Errors bars represent means ± standard deviation for n=3. *** represent $p<0.001$ and ** represent $p<0.01$; Student *t* test.

Since the GeneJammer® allowed for adenovirus entry in the absence of receptor, we tested whether it could improve the transduction efficiency of human peripheral blood mononuclear cells. Briefly, the cells were isolated and purified as described above, a 24 well dish was plated at a cell density of 1 x 10^6 cells per well. Cells were then either transduced with Ad5F35GFP, or no additions, in DMEM + 2% FBS and antibiotic-antimycotic for 24 hours, prior to increasing the serum, or in DMEM + 10% FBS and a antibiotic-antimycotic and the 1.2% polyamine GeneJammer® Transfection Reagent (Stratagene, La Jolla, CA) according to manufacturers specifications for approximately 4 hours, prior to addition of more media to dilute the polyamine. The percentage of Ad5F35eGFP positively transduced cells was determined using flow cytometry. Briefly, cells were washed and resuspended in phosphate buffered saline (PBS). Dead cells and debris were excluded from analysis by using propidium iodide (PI). Samples were run on a FACSCalibur cytometer (Becton Dickinson, San Jose, CA). Percentage of cells transduced to express GFP was determined as relative fluorescence intensity (RFI) of the total viable cell population. Cell viability was determined by addition of propidium Iodide (50 µ/mL) to the cells, and detection using the FACScan Analyzer. Transduction of the purified blood mononuclear cells was enhanced as can be seen in figure 5.

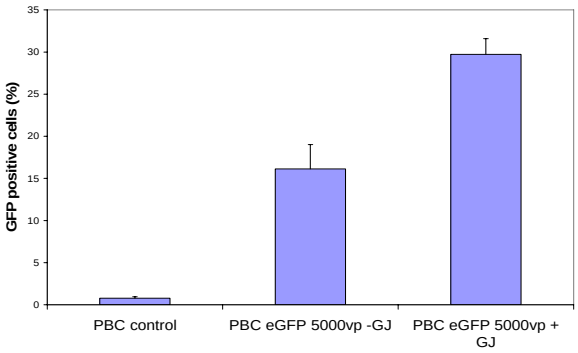

Figure 5: Flow cytommetray analysis of GFP expression in purified mononuclear cells after transduction with Ad5F35GFP in the presence and absence of GeneJammer® Transfection Reagent (Stratagene, La Jolla, CA). Control cells represent those which were not transduced with virus.

Next we looked at BMP2 expression from the peripheral blood mononuclear cells 72 hours after transduction with Ad5F35BMP2 in the presence or absence of GeneJammer®. Media was collected and the level of BMP2 determined by an ELISA assay described above to detect BMP2,

As can be seen in figure 6A, when the polyamine was included during the transduction, there was a significant enhancement (approximately 40%) in BMP2 expression from the same number of cells, hence allowing us to increase the amount of BMP2 being produced per individual cell.

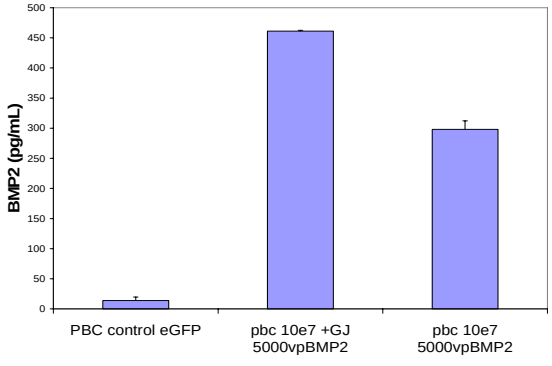

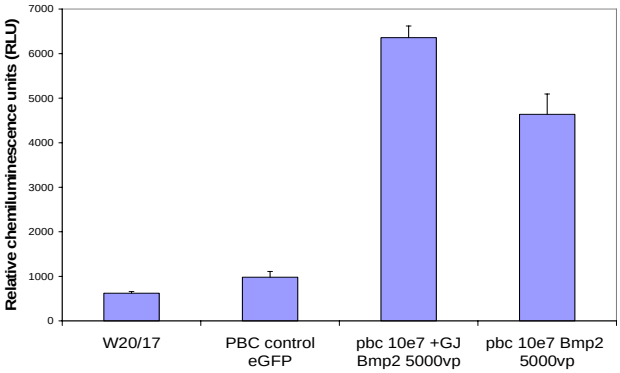

Figure 6: Comparison of standard adenovirus transduction methods versus transduction using GeneJammer® Transfection Reagent (Stratagene, La Jolla, CA). (A) Transduction efficiency of purified mononuclear cells using Ad5F35BMP2 in the presence and absence of the polyamine GeneJammer®. Approximately 10^7 cells were transduced with Ad5F35BMP2 (5000 vp/cell) and 72hrs later, BMP2 was measured in the culture supernatant using an ELISA assay (R&D Systems, Inc. Minneapolis, MN). **(B)** Analysis of BMP2 activity in the media as detected by the level of alkaline phosphatase induction in W20-17 cells after exposure to the culture supernatants collected from cells transduced with either Ad5F35BMP2 or Ad5F35eGFP

To determine the level of BMP2 activity within the culture supernatant after transduction of the purified mononuclear cells with Ad5F35BMP2, we used the murine bone marrow cells known as W20-17. These cells have previously been shown to respond to active BMP2 by elevating the level of alkaline phosphatase activity (Thies *et al.*, 1992). Briefly, culture supernatant from the samples described above, was added to the W20-17 cells, and alkaline phosphatase activity was assayed using a chemiluminescent detection system (Olmsted *et al.*, 2001), (Blum *et al*, 2001). Cellular alkaline phosphatase was extracted by three freeze-thaw cycles in 100 $\mu l/cm^2$ of 25mM Tris-HCl, pH 8.0 and 0.5% Triton X-100 and the activity was then measured by addition of CSPD® Ready-to-use with Sapphire II enhancer (Tropix, Bedford, MA) to the samples. The light output from each sample was integrated for 10 seconds after a 2 second delay using a luminometer (TD-20/20, Turner Designs, Sunnyvale, CA). Alkaline phosphatase levels were recorded in relative luminescence units (RLU) and normalized to protein content with the BCA assay using bovine serum albumin to derive a standard curve. Data are presented as percent induction above unstimulated basal control cells.

However, the purified peripheral blood mononuclear cells, still produced significant less BMP2 per 10^7 cell 450 pg/ml as compared to 15,000 pg/ml observed when other fibroblast were transduced in parallel with Ad5F35BMP2 (2500 vp/cell) in the presence of the polyamine, suggesting that the apparent enhancement may not be sufficient to produce bone formation *in vivo*.

c. Transduced peripheral blood cells will then be tested *in vitro* with a heterotopic bone assay to verify their ability to induce bone formation *in vivo*. (months 8-12).

We next tested whether the purified peripheral blood mononuclear cells (10^7 cells) transduced with Ad5F35BMP2 (5000 vp/cell) in the presence of GeneJammer® could produce heterotopic bone when delivered to a mouse quadriceps muscle. Briefly, the cells were isolated, transduced as described in the previous section and cultured for 24 hours prior to injection into the mouse. Cell viability was examined prior to injection and found to be 95%. The quadriceps muscles were analyzed two weeks after the induction, for the presence of bone or cartilage. In all cases, we observed no bone or cartilage formation with the Ad5F35BMP2 transduced human peripheral blood mononuclear cells even with inclusion of GeneJammer® during the transduction, thus confirming that the level of BMP2 expression was not sufficient to induce bone formation.

d. Alternative strategy:

We propose to circumvent this problem by adapting our studies to bone marrow mesenchymal stem cells. These cells are easily obtained from human bone marrow, are readily expanded, and are routinely manufactured in most GMP cell processing facilities. The mesenchymal stem cells have previously been shown to be versatile jn that they do not launch a graft versus host response when used in an autologous setting. Thus a single lot of cells can be used for multiple patients. These cells are readily transduced with our Ad5F35BMP2 virus, and encapsulated with hydrogel, injected into the paraspinous musculature and photopolymerized into place. Hence this approach would be readily adaptable to the operating room.

Task 2: To ensure the production of high levels of BMP2 at local fusion sites, by delivering the osteoinductive factor via hydrogel-encapsulated Ad5F35BMP2 transduced peripheral blood cells. (Months 12-26). Development and implementation of hydrogel materials for encapsulation of the Ad5F35BMP2 transduced cells will provide essential safety with the sequestration of the cells, as well as provide ability to direct the location of BMP2 expression, and bone formation. Further, hydrogel encapsulation provides immunoprotection to the transduced cells, potentially extending BMP2 expression as compared with the transduced cells delivered through direct injection that are rapidly cleared by the immune system.

The optimal hydrogel formulation would provide an adequate environment for the transduced cells to both survive and continue to synthesis and secrete the BMP2. Therefore we tested several different molecular weights of the polymer, each having slightly different pore sizes as well as structural properties. Since compression of the material may reduce cell viability as well as disrupt the encapsulation, we tested both properties of the different gel formulations. This work has since been published (Bikram *et al*, 2007).

a. Perform *in vitro* testing of hydrogels containing Ad5F35BMP2 transduced human peripheral blood. Various hydrogel formulations will be tested to determine the optimal conditioned for BMP2 diffusion. (Months 12-20).

Comparison BMP2 release from PEG-DA hydrogels of varying molecular weight.

Hydrogels were synthesized as follows (Cruise *et al*, 1998).

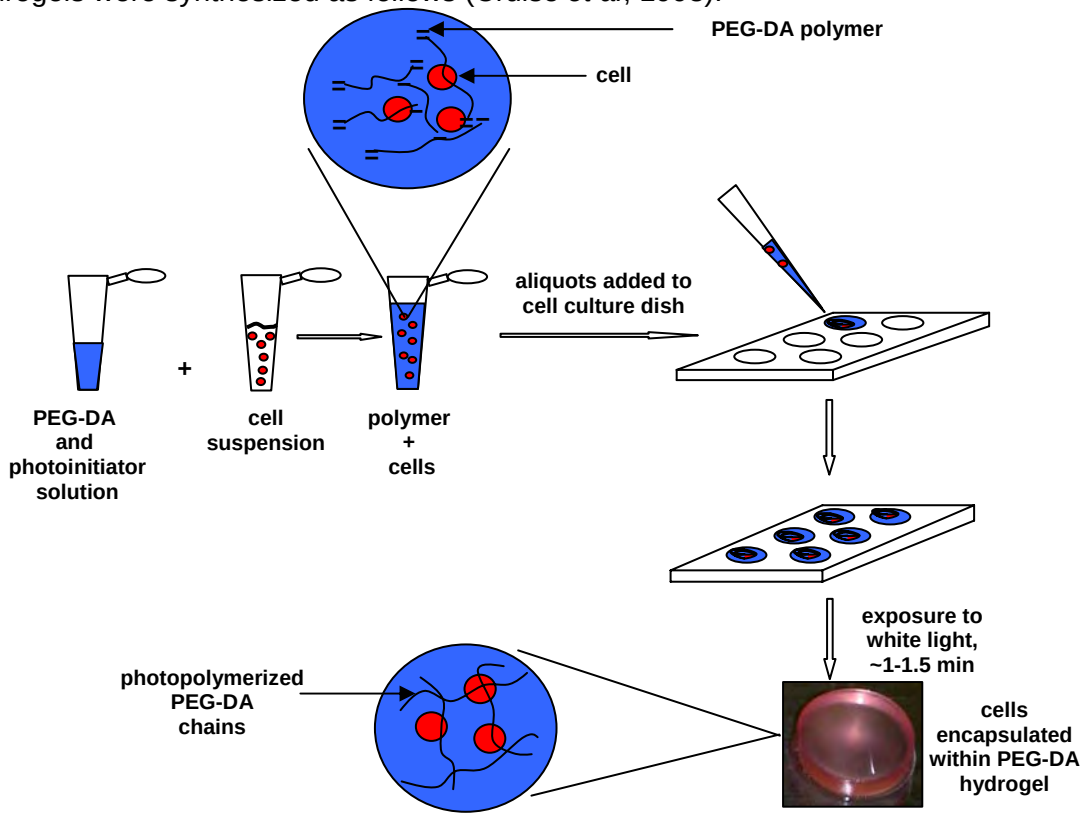

PEG-DA (6000 Da, 10000 Da, 20000 Da) was synthesized from PEG (Fluka, Milwaukee, WI) as previously described (DeLong SA *et al*, 2005). Covalently immobilized gradients of bFGF were linked to the hydrogel scaffolds for directed cell migration. The dried polymers were then dissolved in 10 mL of ultrapure water and purified by dialysis (MWCO 3500 Da; Fisher Scientific, Pittsburg, PA) against deionized water for 3 days. The purified polymers were then lyophilized and stored at -20 ºC. The hydrogel disks (11.5 mm × 0.5 mm) were photopolymerized by combining filter sterilized (0.2 µm filter; Gelman Sciences, Ann Arbor, MI) 0.1 g/mL PEG-DA (10 % w/v) with 1.5 % (v/v) triethanolamine/hepes buffered saline (HBS, pH 7.4), 37 mM 1-vinyl-2-pyrrolidinone, 10 mM eosin Y as the initiator, and MRC-5 or MRC-5 cells transduced with Ad5F35-BMP-2 viral vectors (tMRC-5) for hydrogels with cells for a final concentration of 1, 5, or 10 million cells/disk. For characterization of the prepared hydrogels, photopolymerized PEG-DA hydrogels were dried in a vacuum oven for 1 week, after which the dry weights were recorded and then the hydrogels were reswollen in 1X PBS buffer and the swollen weights were recorded. The swelling ratio, water content, molecular weight of the crosslinks, M_c, and the mesh sizes of the prepared hydrogels were then determined. A volume of 150 µL of the reaction solution was pipetted into the wells of a 48-well cell culture dish that was exposed to surgical white light for 2 min. The hydrogels were then transferred to 150 mm × 25 mm cell culture dishes (Corning Inc., Corning, NY) to which 35 mL cell culture media was added. Control cells were plated onto either 75 cm^2 or 225 cm^2 tissue culture flasks (Fisher Scientific; Pittsburg, PA) that were pretreated with filter sterilized 1% gelatin solution (w/v) (Sigma, St. Louis, MO) and maintained in 35 mL of media with the antibiotic-antimycotic.

The molecular weight of the PEG-DA polymers determines the mesh or pore size of the hydrogel, which can impact both diffusion of essential nutrients and oxygen through the materials for cell survival, as well as release of BMP2 for induction of bone. Therefore we tested three different molecular weights; 6 kDa, 10 kDa and 20 kDa of PEG-DA. Table 2 shows the molecular weights (M_c) of the crosslinked PEG-DA and the resulting mesh sizes of the 6kDa, 10 kDa, and 20 kDa hydrogels.

Table 2	Swelling Ratio	Water Content (%)	M_c (g mol^{-1})	Mesh size (Å)
10 % PEG-DA 6 kDa	9 ± 0.7	89 ± 0.7	617 ± 98	34 ± 3
10 % PEG-DA 10 kDa	11 ± 0.4	91 ± 0.3	780 ± 54	39 ± 2
10 % PEG-DA 20 kDa	17 ± 0.2	94 ± 0.1	1556 ± 24	65 ± 1

Varying amounts of BMP2 protein was found to be released from the different hydrogels depending on their molecular weights. As can be seen in Figure 7, BMP2 protein was significantly inhibited by the hydrogel encapsulation as compared to the plated cells, regardless of the molecular weight of the polymer. Encapsulation of 1 million cells within the hydrogels resulted in ~20-fold reduction in BMP-2 protein compared with the controls ($p < 0.001$) and the expression was biphasic over the 15 d period with highest expression observed on day 5. In addition, BMP-2 levels from cells within the different molecular weight hydrogels for each time interval were the same except for days 3 and 9 in which expression from the PEG-DA (20 kDa) hydrogel was higher than both the 6 kDa and 10 kDa hydrogels for day 3 ($p < 0.01$) and expression from PEG-DA (6 kDa) was higher in comparison with PEG-DA 10 kDa and 20 kDa for day 9 ($p < 0.05$). Since the hydrophobic properties of the polymer are not conducive to protein binding, these results are somewhat surprising. One possible explanation is that the BMP2 protein may be forming structures that are much larger than the pore sizes in any of the polymers since even the 20 kDA polymer pore sizes are smaller than many large protein complexes. Alternatively, these numbers may represent cell death, suggesting that only a small percentage of the encapsulated cells are still viable.

We next escalated the cell number per mL of gel to determine if we could increase the amount of BMP2 secreted into the media (Figure 7 A, B, C). We observed a significant increase in BMP2 which correlated with the increase in cell number. We obtained ~600 pg/mL, ~4600 pg/mL, ~8000 pg/mL of BMP2 protein when 1, 5, and 10 million cells respectively, were encapsulated, as determined by ELISA (Figure 7). However, in all cases we observed a ≥60% drop in BMP2 within the media collected from the encapsulated cells versus the plated. Interestingly, the results do not suggesting that the loss of BMP2 is due to overcrowding of the cells within the polymer because we see significantly more BMP2 produced when more cells are added to the same volume of polymer. Since we routinely use 5 million cells to induce bone formation comparison between of BMP2 release between the plated cells (approximately 15,000 pg/mL) and our optimal encapsulation conditions 10 millions cells (approximately 8000), is still significant at 50% drop, but was still sufficient to produce heterotopic bone (see *Task 2 section b*). Further escalation of the cell number above 10 million within this volume of hydrogel, resulted reduced BMP2 expression presumably due to cell death from overcrowding (data not shown).

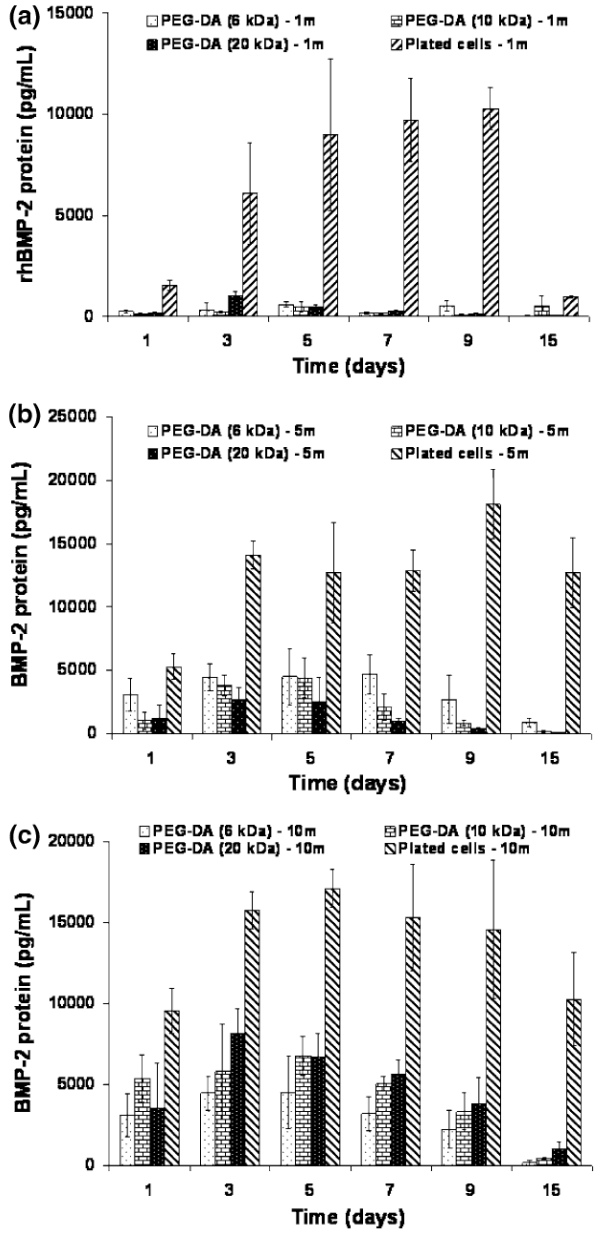

Figure 7: Evaluation of BMP2 expression from Ad5F35BMP2 transduced MRC-5 (tMRC-5) (A) 1 million, (B) 5 million and (C) 10 million cells encapsulated within PEG-DA (6 kDa, 10 kDa, 20 kDa) hydrogels. BMP2 was quantified by ELISA (R&D Systems Inc). Negative hydrogel and plated controls were below the level of detection for this assay. Data reported as mean ± SD, n = 5.

Surprisingly, the expression of BMP2 from the encapsulated cells appears to decrease with time as compared to the cells directly plated, which suggests the

conditions for the cells may be suboptimal. Since the cells cannot bind the hydrogel material, perhaps this is a direct response to their lack of adherence, since these are fibroblasts. One method which would circumvent this problem is to introduce binding sites within the hydrogel materials that would provide the cells attachment sites to better enhance their survival and transgene expression. Alternatively, we propose to also re-engineer the BMP2 protein to remove a stretch of amino acids known to cause nonspecific cellular binding of secreted proteins. Similar experiments with other proteins has shown significant enhancement in their diffusion without altering their biological function.

Mechanical testing of PEG-DA hydrogels

To assess the compressive strength of the PEG-DA hydrogels after encapsulation with tMRC-5 cells and to select the hydrogel with the best mechanical property that supports the highest gene expression, we performed compressive testing with the PEG-DA hydrogels of various molecular weights containing 10 million tMRC-5 cells. Briefly, PEG-DA (10 kDa and 20 kDa) hydrogel solution with and without 10 million tMRC-5 cells were formulated as described above. The solution was then placed in a rectangular glass mold (~1.4 mm thickness) and exposed to surgical white light for 2 min. The faceplate was removed and a cork borer was used to cut out 11.5 mm diameter disks that corresponded to a final volume of 150 µL. The disks were then transferred to cell culture plates to which 35 mL of complete media was added and the plates were incubated overnight. Prior to analysis, the hydrogels were dabbed with a Kimwipe to remove excess surface media and placed between two parallel platens mounted on an Instron® 3342 (Canton, MA) mechanical tester and the compression modulus of the hydrogels were determined with a 10 N load cell at a crosshead speed of 1 mm/min using the Instron® Series IX software.

The compressive modulus of the PEG-DA hydrogels only was 454 kPa, 395 kPa, and 155 kPa for the 6 kDa, 10 kDa, and 20 kDa hydrogels respectively (Figure 4). Encapsulation of the hydrogels with 10 million tMRC-5 cells resulted in a decrease in compressive modulus of 153 kPa ($p < 0.001$), 236 kPa ($p < 0.01$), and 90 kPa ($p < 0.05$) for PEG-DA 6 kDa, 10 kDa, and 20 kDa respectively.

Figure 8

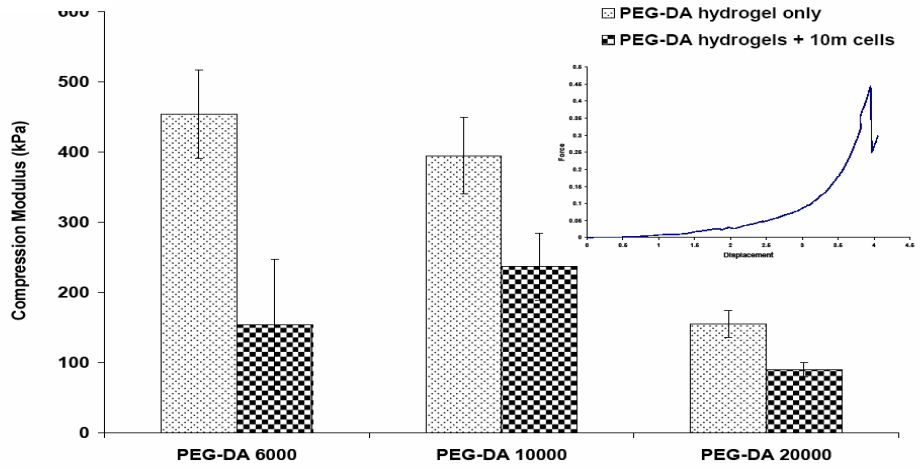

Figure 8: Compression modulus for prepared PEG-DA hydrogels of varying molecular weights with and without 10 million tMRC-5 encapsulated cells after 24 h.

Cell viability of encapsulated cells

The cell viability of MRC-5 and tMRC-5 cells was determined after encapsulation in PEG-DA (10 kDa) hydrogels after 1 and 7 days according to manufacturer's specifications using a LIVE/DEAD® Viability/Cytotoxicity (Molecular Probes; Eugene, OR) kit. Briefly, hydrogel disks with 10 million MRC-5 and tMRC-5 cells were formulated and photopolymerized in 48-well cell culture plates as described above. The hydrogels were then transferred to cell culture dishes to which 35 mL of media was added. On days 1 and 7, the media was removed and the hydrogels were transferred to 6-well plates. The disks were washed with sterile tissue culture grade phosphate buffered saline (PBS) (1X) three times for 10 min each. The fluorophore solution was then prepared by adding 20 µL ethidium homodimer (2 mM) and 5 µL calcein AM (4 mM) to 10 mL 1X PBS. The resulting solution was vortexed and 2 mL was then added to each well containing the hydrogels. The plate was incubated for 45 min at 37 ºC after which the hydrogels were washed as previously described (Cruise *et al* 1998) and the

fluorescence of the live and dead cells were analyzed using a Zeiss LSM 510 confocal microscope (Thornwood, NY). Results suggest little change in cell viability in either population between 1 and 7 days in culture (Table 3).

Table 3: Results of Cell Viability	24 hours		7 days	
	Live Cells	**Dead Cells**	**Live Cells**	**Dead Cells**
tMRC	71% ± 9%	29% ± 9%	69% ± 8%	31% ± 8%
encapMRC	58% ± 7%	42% ± 7%	60% ± 14%	40% ± 14%

The data suggests that the cells are surviving for at least one week, although this does not rule out that cell death is responsible for the drop in BMP2 expression at two weeks. We propose to further analyze cell viability at longer time points, and compare the results to those when cellular binding sights are engineered into the material. We also propose to measure and compare the release of BMP2 the non-dissociated skin fibroblasts in the presence of and absence of hydrogel encapsulation.

Characterization of secreted BMP-2

In order to verify that the secreted BMP-2 protein from the PEG-DA hydrogels was present, functional, and intact, alkaline phosphatase activity was investigated in W20-17 cells and Western blot analysis was performed with conditioned media from cultured tMRC-5 cells and PEG-DA hydrogels with 10 million tMRC-5 cells. Results from the Western blot analysis showed that not only was the secreted BMP-2 protein from the hydrogels the same as the secreted BMP-2 from the plated controls but that only cells transduced with the Ad5F35-BMP2 produced detectable BMP-2 (Figure 9A). The results from the alkaline phosphatase data showed that the conditioned media from the hydrogels produced similar levels of alkaline phosphatase activity as the media from the plated cells except for day 1 ($p < 0.001$) (Figure 9B).

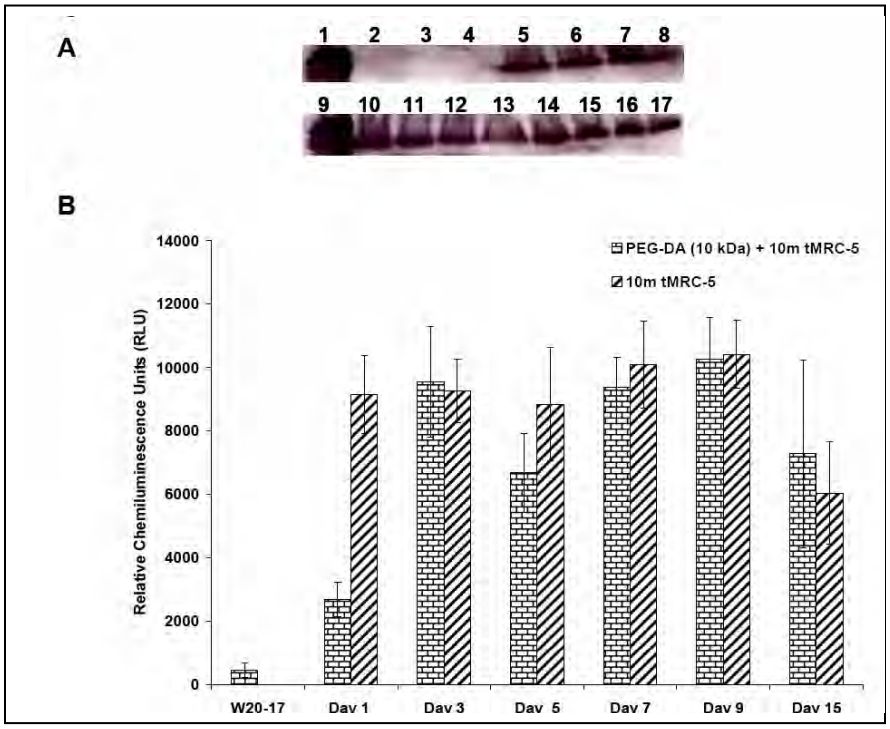

Figure 9: Detection of BMP2 protein and activity. (A) Western blot analysis for the detection of BMP-2 protein. Human recombinant BMP2 (lane 1), conditioned medium from PEG-DA (10 kDa) hydrogels only (lane 2), conditioned medium from 10 million MRC-5 cells encapsulated within PEG-DA (10 kDa) hydrogels (lanes 3 and 4), conditioned medium from 10 million tMRC-5 cells control (lanes 5-8), human recombinant BMP2 (lane 9) conditioned medium from 10 million tMRC-5 cells encapsulated within PEG-DA (kDa)

b. Perform *in vivo* testing of hydrogels containing Ad5F35BMP2 transduced human peripheral blood in heterotopic bone formation. Radiological and histological analysis will be done to confirm that the resultant bone formation is local rather than progressive (Month 20-26).

Optimization of hydrogel shape for in vivo implantation

In our first preliminary experiments, the 150 uL hydrogel disks were implanted into the rear quadriceps muscle in a mouse and endochondral bone formation was allowed to progress for two weeks prior to analysis. Although in these experiments we did observe bone formation, however due to their large size we experienced difficulty in maintaining the integrity of the hydrogel during implantation, and the large volume left little room in the tissues for extensive bone formation. Hence we developed an alternative structure for the hydrogel material, which utilized the same number of cells, but were in smaller "bead-like" structures that were formed along a surgical thread which allowed for easier transfer into the mice. However, prior to implantation we confirmed that the new structure had not significantly altered either BMP2 release (Figure 10), structural integrity, or cell viability (data not shown).

The results of the ELISA data for the polymerized "beads-on-a-string" showed that the plated tMRC-5 controls produced ~2.5-fold higher BMP-2 levels as compared with both the hydrogel beads and disks (Figure 10). However, the tMRC-5 cells within the hydrogel beads produced peak levels of ~7600 pg/mL BMP-2 on day 5 as opposed to ~6800 pg/mL ($p>0.005$) from the tMRC-5 cells within the hydrogel disks with a similar biphasic profile that was previously observed for the hydrogel disks. This slight increase in BMP-2 levels for the hydrogel beads as compared with the disks (~800 pg/mL difference) was maintained over the 15 day period except for day 1 ($p<0.01$) (~4000 pg/mL difference).

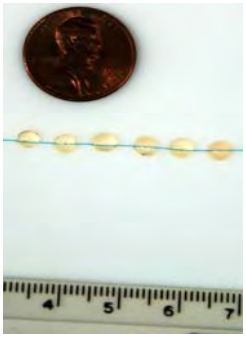

25 uL beads

150 uL disk

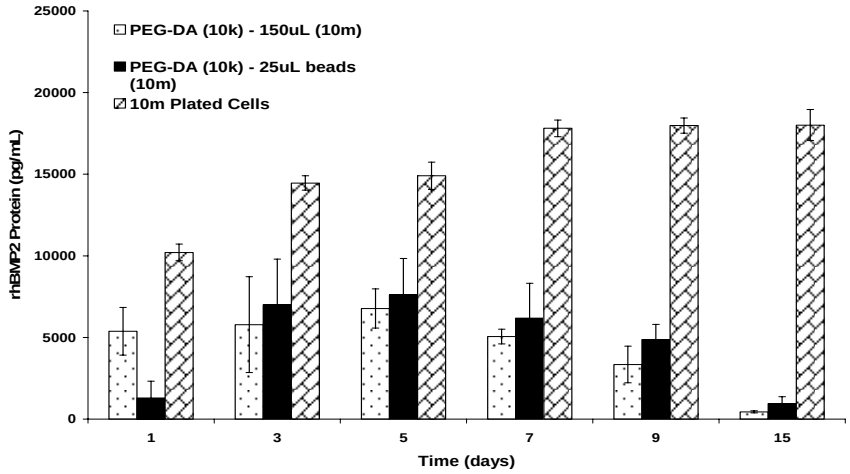

Figure 10: Comparison of gene expression from 10 million adenovirus transduced MRC-5 cells (tMRC-5) in PEG-DA (10 kDa) hydrogels disks with 10 million tMRC-5 cells in PEG-DA (10 kDa) hydrogels beads with ELISA assay. Negative hydrogel and plated controls were less than 100 pg/ mL BMP-2 detected. Data reported as mean ± SD, n = 5

Micro-CT analysis of bone

To determine the amount of ectopic bone formed in NOD/SCID mice with implanted PEG-DA hydrogels containing tMRC-5 cells, the volume of mineralized ectopic tissue in the muscle was evaluated.

Approximately three weeks after implantation, the rear hind limbs NOD/SCID mice were scanned at 14 µm resolution with a commercial micro-CT system (GE Locus SP, GE Heathcare, London, Ontario). Three-dimensional reconstructions of the lower limb bones and any mineralized tissue in the surrounding muscle were created at 29 µm resolution to visualize ectopic mineralized tissues. A complex volume of interest was defined for each specimen to include only the ectopic mineralized tissue, and a threshold was chosen to exclude any non-mineralized tissue. The total volume of ectopic bone was then measured (eXplore MicroView, v. 2.0, GE Healthcare, London, Ontario).

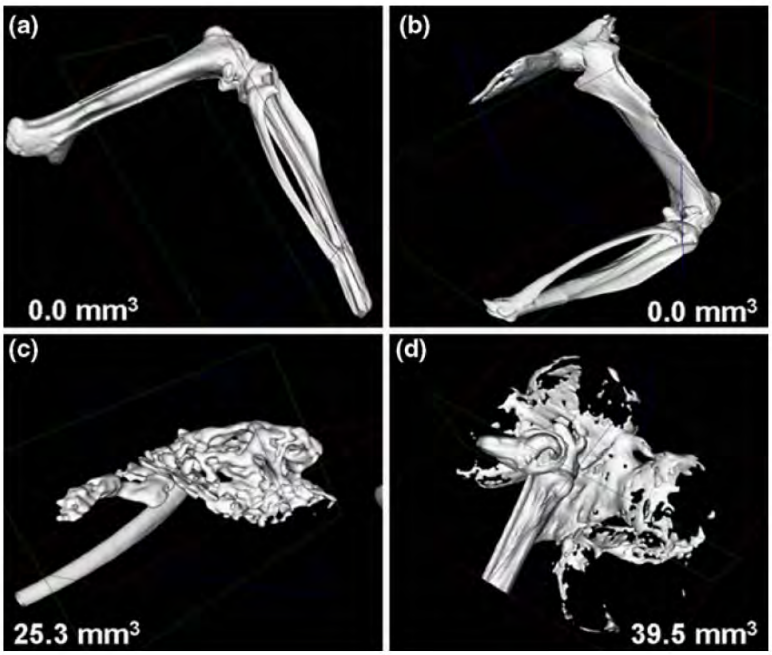

Figure 11: Micro-CT analysis of ectopic bone formation at 3 weeks. Representative image of bone formation from (a) 10 million MRC-5 cells transduced with AdHM4, (b) PEG-DA (10kDa) hydrogels with 10 million MRC-5 cells transduced with Ad5HM4 (c) 10 million MRC-5 cells transduced with Ad5BMP2 (d) PEG-DA hydrogels with 10 million MRC-5 cells transduced with Ad5BMP2 administered via intramuscular (i.m.) injection and (a, c) or following surgical implantation (b,d). Measurements from the femur or tibia shown in the panel were not included in the volume calculations and the values of mineralized tissues shown in the figure are only depicted for the image. Data reported as mean ± SD, *n=6.*

The mean amount of mineralized tissue in the muscle of the mice was 31.8 ± 7.8 mm^3 and 39.5 ± 5.0 mm^3 for mice injected with tMRC-5 cells only and mice implanted with the PEG-DA hydrogels encapsulated with tMRC-5 cells respectively (*n=6*). There was no ectopic bone detected in the mice that were administered untransduced MRC-5 cells or those transduced with Ad5F35-HM4 viral vectors. Surprisingly, the volume of mineralized tissue between the samples was approximately equivalent. Presumably this was due in part to the fact that all the beads had bone surrounding them whereas in delivery of the cells directly, bone formed only around the area of the initial injection. This finding is significant in that the animals receiving the injected cells received 50-60% more BMP2 than those that got the hydrogel beads suggesting that placement of the BMP2 may be a critical to inducing robust bone formation as a threshold amount. Further this finding suggests that the bone reaction can only occur within a limited distance from the BMP2 itself even in these systems with sustained expression.

We have obtained similar results in C57BL/6 (immunocompetent) mice. Early radiological analysis suggests similar results to those obtained with the Nod/Scid. In these studies we encapsulated a fibroblast cell line derived from C57BL/6 mice that had been transduced with Ad5BMP2 in the presence of GeneJammer. We have developed a protocol in which we can obtain the same level of BMP2 expression as that obtained when we transduce human fibroblasts with Ad5F35BMP2. The results are identical to those presented here. (see third aim, comparison of immune competent and immune incompetent models).

Histological analysis

To demonstrate the physiology of the ectopic bone formed in the muscle as well as to assess the biocompatibility of the PEG-DA hydrogels as a result of surgical implantation, sections of the muscle tissue was stained with hematoxylin and eosin. The stained sections showed that there was bone as well as cartilage formed in the muscles of the mice implanted with the hydrogels that was comparable to injected tMRC-5 transduced cells only. In addition, there were little or no immunological reactions due to the presence of the PEG-DA hydrogels as shown from the negative hydrogel control, whereas there were noticeable amounts of recruited cells in the area of the injection site (Figure 12).

In addition, the cell viability of tMRC-5 cells encapsulated within PEG-DA (10 kDa) hydrogels two weeks after surgical implantation was evaluated. The LIVE/DEAD staining of the cells showed that 72% ± 22% and 28% ± 22% of the cells were live and dead respectively in the left leg. This data was consistent with the right leg that had 75% ± 3% and 25% ± 23% live and dead cells respectively.

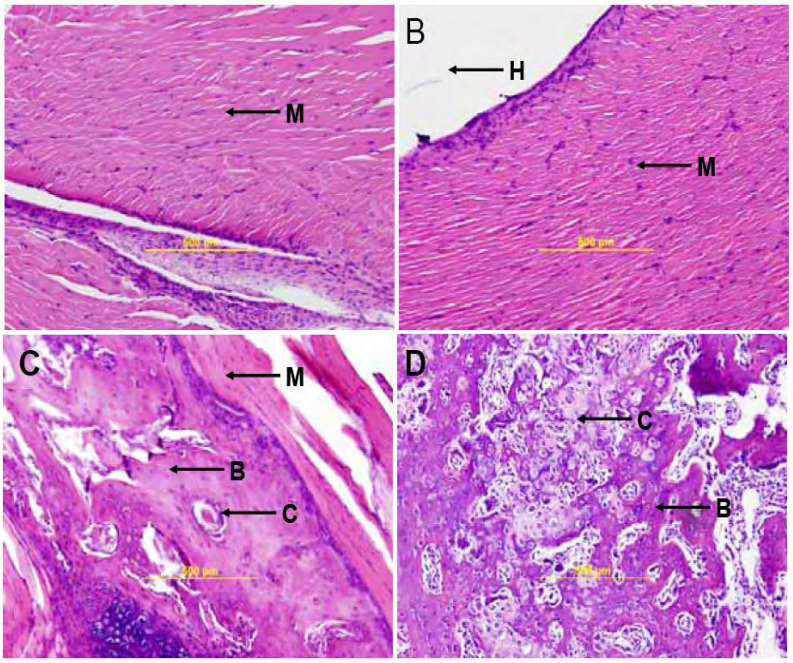

Figure 12: Histological evaluation of ectopic bone formation at 3 weeks. (A) 10 million MRC-5 cells transduced with HM4-1; (B) PEG-DA (10 kDa) hydrogels with 10 million MRC-5 cells transduced with HM4-1; (C) 10 million tMRC-5 cells; (D) PEG-DA (10 kDa) hydrogels with 10 million tMRC-5 cells. M-Muscle, H-Hydrogel, C-Cartilage, B-Bone

Task 3: To achieve posterolateral spine fusion by percutaneous injection of the encapsulated Ad5F35BMP2 transduced human peripheral blood cells, into the paraspinous musculature of rats. (Months 24-36).

a. Confirm spine fusion using Ad4F35BMP2 transduced human peripheral blood cells encapsulated in hydrogels using an athymic rat model for spine fusion. Spine fusion in the rat model will be assessed by both histological and radiological analysis. (Months 24-30).

To confirm that our heterotopic bone formation assay could form bone in the paraspinous musculature that would fuse into the adjacent vertebral bone and thus fuse the spine, we next analyzed bone formation in our NOD/Scid mouse model, when injected into this new location. Experiments were initiated in NOD/Scid mice since we had recently optimized the hydrogel materials for this system. For these initial tests we chose to compare the Ad5F35BMP2 transduced cells encapsulated in hydrogel, and preformed into bead-like structures, to the same numbers of cells directly injected into the same location. Since the size of the bead structure was limited to the size of the fusion distance (roughly two vertebra), we reduced the numbers of cells delivered to the muscle from 5×10^6 to 1×10^5 to maintain the optimal cell number per volume of hydrogel as described in section 2b. We set up four groups of mice ($n = 9$); (Group 1) 1×10^5 MRC5 cells transduced with Ad5F35BMP2 (2500 vp/cell), (Group 2) 1×10^5 MRC5 cells transduced with control vector (2500 vp/cell), (Group 3)1×10^5 MRC5 cells transduced with Ad5F35BMP2 and then hydrogel encapsulated, (Group 4) 1×10^5 MRC5 cells transduced with control vector and hydrogel encapsulated. These were implanted into the paraspinous musculature in accordance with our IUCAC and DOD approved protocol, and mice were allowed euthanized 6 weeks later for analysis of the bone formation. Since the bead structures were pre-formed, the paraspinous musculature was exposed by opening the skin and the beads stitched into place or cells directly injected, however, we did not further decorticate or injure the adjacent periosteum surrounding the vertebral bones, nor did we purposely remove or disrupt further any of the musculature, thus attempting to keep this as non-invasive as possible. Further, with the placement and lack of exposure of the vertebral bone surfaces, we expected the bone to form initially through heterotopic processes, thus a six week time point was chosen rather than a two week point, because we wanted to ensure adequate time for both the bone to form but also remodel into the vertebra skeletal bone or fuse. Since we were adding approximately one log fewer transduced cells, we extended our previous pilot four week studies, to 6 weeks. However, we propose in future studies that a more rigorous time course will be performed to determine the rate of fusion. The results are reported in Table 4 below.

Table 4: Results of	Fusion of two vertebra	Fusion with one	Heterotopic bone in	No bone

Spine Fusion Study		vertebra	adjacent tissues	formation
Group 1	2	5	1	1
Group 2	0	0	0	9
Group 3	4	2	1	2
Group 4	0	0	0	9

The hydrogel group had fewer samples fusing two vertebras, the overall bone formation and fusion to the skeletal bone and bone formation was equivalent to or greater than the cells directly injected. Most likely these results reflect placement of the cells versus the hydrogel bead structures in the spine. For example, when the cells were directly injected into the musculature, the limited numbers of cells were free to diffuse, perhaps a portion of the cells were more capable of diffusing towards the spine and thus fusing two vertebra, but alternatively, more were also free to diffuse away from the spine, resulting in the 2 which had no apparent bone formation. However, in the case of the beads, the cells were not free to move, so BMP2 secretion was more uniform, but perhaps more distal to the vertebral bones, and thus resulted in more samples forming bone, but less capable of undergoing fusion of two or more vertebra. Interestingly, the hydrogel group overall made more total bone, as depicted in Figure 13, but this most likely is due to the heterotopic nature of the bone formation, and the lack of remodeling once it fuses with the skeletal bone. Further, since these are six weeks after induction of the bone formation, they most likely will have undergone bone remodeling, and resorption (See next section for long term studies). Most likely the BMP2 is expressed longer from the cells encapsulated in hydrogel since they are not rapidly cleared which may result in the greater volume of bone produced.

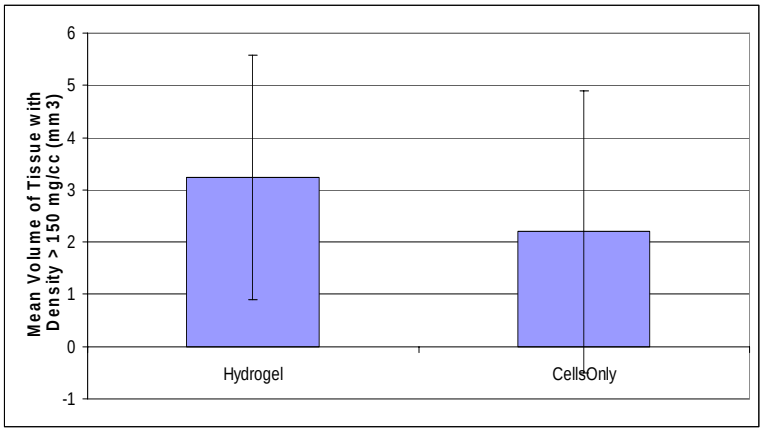

Figure 13: Comparison of bone volumes generated in paraspinous musculature of NOD/Scid mice (*n = 9*) six weeks after induction of bone formation by implantation of cells transduced to express BMP2 either directly or encapsulated in hydrogel.

Figure 14 shows three dimensional reconstruction of the microcomputed tomographic analysis of representative samples in which the heterotopic bone formation was found to fuse two of the mice vertebras both after induction with either direct injection of transduced cells (Panel A) or implantation of transduced cells after encapsulation in hydrogel (Panel C). Panels B and D are representative control samples, which consistently lacked any new bone formation.

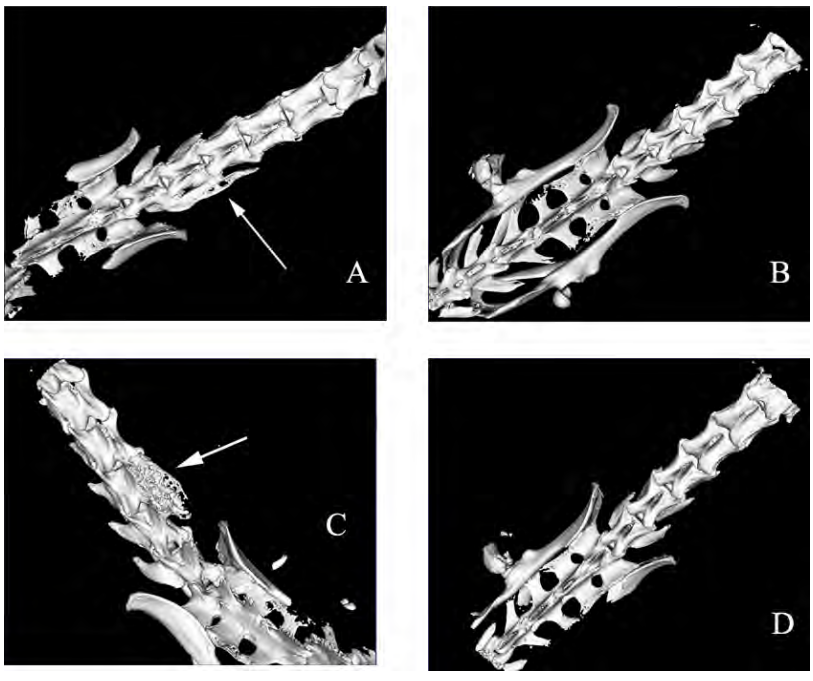

Figure 14: MicroCT Analysis of bone formation in the paraspinous musculature in NOD/Scid mice. Representative three dimensional reconstruction of bone formation six weeks after direct injection of **(A)** Ad5F35BMP2 transduced cells or **(B)** Ad5F35HM4 transduced cells (Control), and implantation of hydrogel encapsulated cells transduced with **(C)** Ad5F35BMP2 or **(D)** Ad5F35HM4. Arrows indicate the fusion site.

b. Compare resultant spine fusion using the encapsulated transduced cells in both immuno-incompetent and

immunocompetent rats. (Months 30-36).

Before initiating experiments in the rat model, we needed to demonstrate that the two systems are comparable in both timing of bone formation as well as the total bone volume made, and define the essential parameters. Therefore we performed a detailed comparison of bone formation in similar murine models of heterotopic bone formation in the muscle.

For comparison, the two cell-based gene therapy systems were evaluated for their ability to secrete BMP2, so that in future analysis both systems would be producing equivalent amounts of BMP2. Thus, BMP2 expression was measured by quantifying the amount of protein secreted into the culture supernatant after transduction of the cells with the respective adenoviruses at varying multiplicity of infections (MOIs). Culture supernatants were collected 72 hours after initial transduction and BMP2 was quantified by an enzyme-linked immunosorbent assay (ELISA). MOIs were adjusted so that the expression level of BMP2 between the MC3T3 cells transduced by Ad5BMP2 and MRC5 cells transduced by Ad5F35BMP2 were the same (Figure 15A). Based on these findings, all other subsequent studies were done using these doses so as to have comparable expression of BMP2.

We next determined the functional activity of BMP2 protein using a W20-17 cell-based assay (Thies *et al*, 1992) which measures the induction of alkaline phosphatase in response to active BMP2. In this assay, the murine bone marrow cell line W20-17 was exposed to culture supernatant from the MC3T3 cells or MRC5 cells that had been transduced respectively with Ad5BMP2 at a concentration of 5000vp/cell or Ad5F35BMP2 at a concentration of 2500vp/cell. Culture supernatants from MC3T3 and MRC5 cells transduced with control viruses were also included to verify that the W20-17 response was specific to BMP2. Cell lysates were assayed for alkaline phosphatase activity approximately three days after addition of the tentative BMP2 containing supernatant. In all cases in which cells were transduced with AdBMP2 viruses, the cells secreted active BMP2, with no significant differences (*p* value is 0.6985) (Figure 15B), whereas supernatants from cells transduced with control viruses did not induce alkaline phosphatase activity.

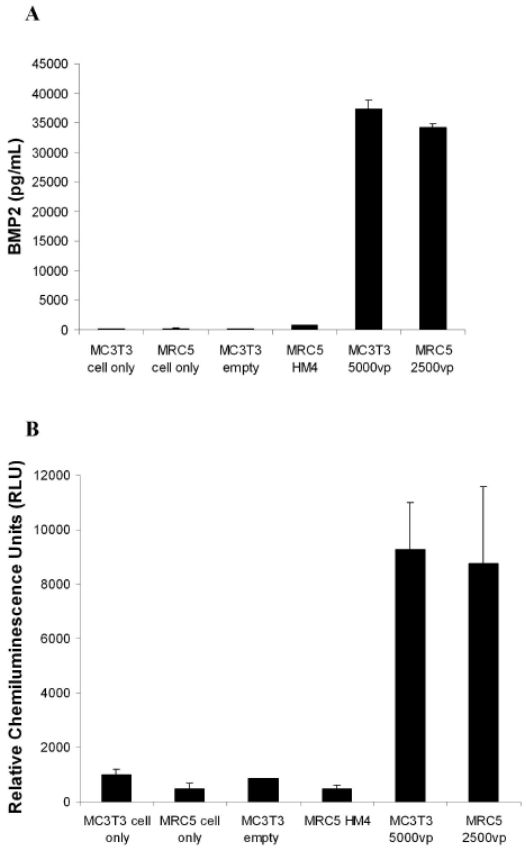

Figure 15: Quantification of BMP2 *in vitro* **(A)** and activity of BMP2 **(B)**. **(A)** The quantity of BMP2 was measured in culture supernatant taken from MC3T3 cells transduced with Ad5BMP2 (5000vp/cell) and MRC5 cells transduced with Ad5F35BMP2 (2500vp/cell) and MRC5 cells transduced with Ad5F35BMP2 (2500vp/cell) using the Quantikine assay (R&D systems). The concentration of BMP2 was extraplolated from a standard curve based on known concentrations of recombinant BMP2. BMP2 concentrations in the supernatant are reported as picograms per millilieter, $n = 3$. $p>0.5$ (Student *t* test). **(B)** BMP2 activity was measured in culture supernatant from MC3T3 transduced with Ad5BMP2 (5000 vp/cell) and MRC 5 cells transduced with Ad5F35BMP2 (2500 vp/cell) by determining the increase in alkaline phosphatase activity in W20-17 cells 72hs after exposure. Alkaline phosphatase activity is depicted as average relative chemiluminescence units (RLU), where $n = 3$. Columns and error bars represent means ± standard deviation, respectively, for $n = 3$ experiments, $p>0.5$ (Students *t* test).

Delivery cells are not longer present by day 6

With establishment of the transduction criteria essential for each system to make equivalent active BMP2, these transduced cells were then tested for their engraftment potential in the corresponding mouse models. The Ad5BMP2 model was developed to efficiently transduce the C57BL/6 autologous cells for

induction of bone in an immune competent setting (Fouletier-Dilling *et al*, 2005), we next measured the engraftment of these cells into the site of bone formation and compared this to the Ad5F35BMP2 transduced human cells delivered to immune incompetent NOD/SCID mice. Even though the MC3T3 cells are considered to be "osteoblastic", no bone formation was ever observed using non-transduced cells or those cells transduced with control vector. Since both cell types possess adenovirus antigens as a result of the transduction using first-generation adenoviral vectors, we were interested in determining if the human cells would have similar survival rates in NOD/SCID mice which lack the lymphocytic arm of the immune system, as compared to the cells delivered to wild type mice.

The cells were tracked by two different systems. In the NOD/SCID (immune incompetent) model, the human cells were detected by immunohistochemical staining for the expression of a protein specific to human mitochondria. We observed positive staining for the human cells in tissues isolated from 1-5 days after induction (Figure 16A), but were completely absent by day 6 after their initial injection into the muscle. In the C57BL/6 (immune competent) model, we looked for the expression of the hexon protein, the largest and most abundant of the structural proteins in the icosahedral adenoviral capsid, by immunohistochemistry as a means of locating the transduced cells. As seen in Figure 16B, transduced cells were still present at day 6 after induction, but had not engrafted into any of tissue structures associated with the newly forming bone. Although the original report that first generation adenovirus vectors elicted production of virus neutralizing antibodies against capsid antigens was presented over a decade ago (Yang *et al*, 1996), the study presented here directly shows the production of a capsid viral antigen *in vivo.* By 7 days post-induction, the transduced cells were completely absent in all tissue sections encompassing the reaction site. These results demonstrate that the transduced cells are cleared prior to bone formation. However, in all cases the cells did not appear to be associated with any of the newly forming cartilage and bone. Interestingly, the cells were cleared at the same rate in both systems, seemingly independent of the immune status of the animal.

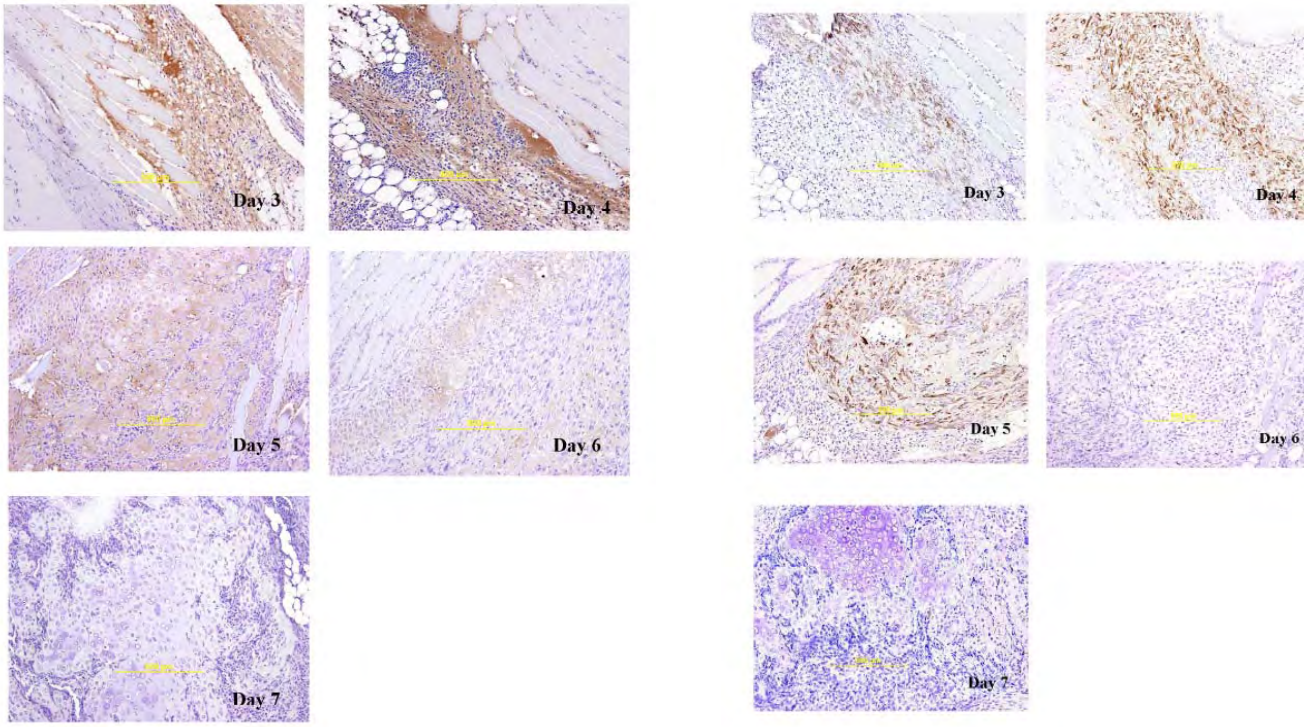

Figure 16: Immunohistochemistry for human mitochondria (A) and hexon (B) proteins. (A) Staining for human mitochondria on NOD/Scid sections from day 3-7 demonstrates positive staining within the transduced cells from days 3-5 while the sections from days 6 and 7 are negative indicating absence of the delivery cells. (B) Positive staining for hexon was noted within the transduced cells from days 3-5 days, weakly positive staining on day 6 sections, and was completely absent on day 7 tissues indicating the absence of the delivery cells. (Immunohistochemistry, maginification 40.5X).

Stage by stage comparison of bone formation in immune-competent and immune-deficient

We have recently characterized through immunohistochemical phenotyping and cell tracking, the initial stages of endochondral bone formation in the NOD/SCID model (Olmsted-Davis *et al*, 2007; Shafer *et al*, 2007). These stages are extremely reproducible and include the appearance of brown adipocytes on days 1-2, new vessels on days 3-4, cartilage on days 4-6, and bone on days 6-8. These previous studies have linked the early mesenchymal precursors for chondrocytes and osteoblasts to be of a myelo-monocytic origin (Shafer *et al*, 2007).

Here we compared these stages of endochondral bone formation between the two murine models given that both systems are capable of producing equivalent functional BMP2, as well as with control mice that received cells transduced with an empty cassette vector. The emphasis is to detect any differences in the progression of endochondral bone formation including temporal changes that may be resulting from the difference in immunological backgrounds of the animals. Figure 17 shows resultant photomicrographs from the immune-competent model (C57BL/6), the immune-incompetent model (NOD/SCID) and the control section at days 2, 4, 6 and 7. The images are representative of the reaction within the tissues for each of the days. As can be seen in Figure 17, day 2, the sections look similar with both the delivery cells and visible inflammation present in the tissues regardless of whether the cells were expressing BMP2. However, by four days after the initial injection, the experimental sections for both models no longer match the control sections. The tissues receiving the cells transduced to express BMP2, showed a significant increase in the number of cells within the tissues. Our previous studies have shown these to be a myelo-monocytic precursor both migrating into the tissues as well as proliferating, to form the new cartilage (Shafer *et al*, 2007). Alternatively, the inflammatory response is essentially gone by day 4 in the control sections. Both the transduced cells as well as the host-derived cells are greatly reduced in volume compared to the previous days (see Figure 17) and these results confirm earlier data showing the disappearance of the delivery cells in both systems (Figure 16). The cartilage is well established and similar in the experimental sections in both models at day 6; however the control section demonstrates a complete absence of both inflammatory cells and the injected cells. By day 7 newly formed bone is observed in both models that received the BMP2 transduced cells, suggesting that the presence of a complete immune system did not reduce the rapid nature of the endochondral bone formation previously reported in the immune competent model.

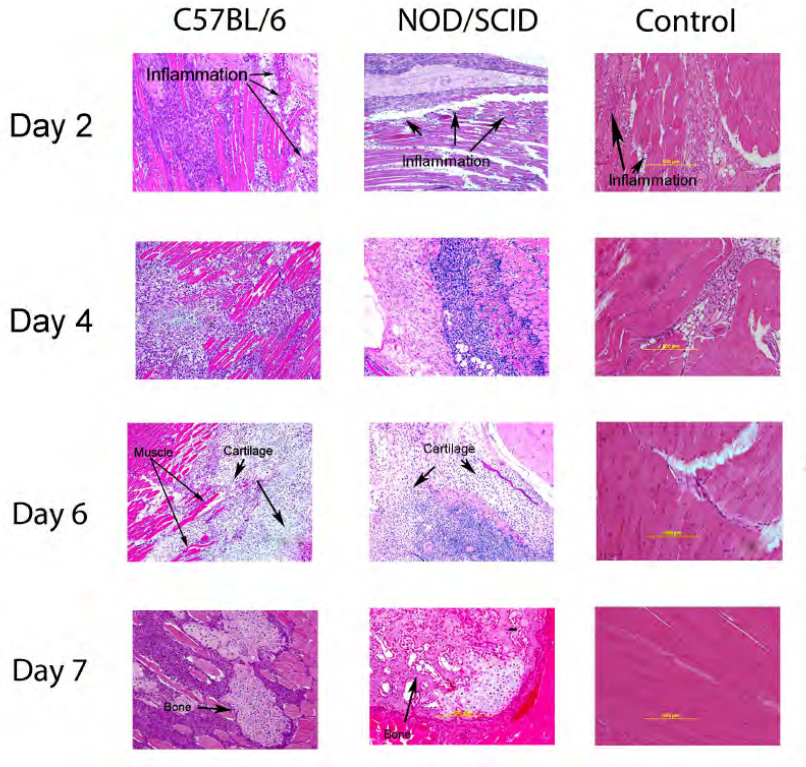

Figure 17: Photomicrographs from the first week in both experimental (NOD/SCID and C57BL/6) and control animals. Day 2, an inflammatory infiltrate is observed in both experimental and control animals; Day 4 the experimental sections for both models no longer match the control sections. The experimental sections showed a significant increase in the number of cells within the tissues while cell numbers appear greatly reduced in volume in the control section; Days6-7 show an orderly maturation of the cartilage component with progression to bone in both experimental sections while cell numbers in the control section steadily decline.

Long term bone expression

While the endochondral bone formation during the first 7 days was histologically similar in both systems, we wanted to compare long term bone formation, and/or retention. Figure 18 represents the Hematoxylin and Eosin stained photomicrographs taken of tissues isolated from the immune-incompetent

model (NOD/SCID) and immune-competent (C57BL/6) 2 weeks, 3 weeks and 4 weeks after injection of the BMP2 producing cells. The histological analysis of the sections are dramatically different from a 2 week time point to the 4 week time point but remains similar between the two systems. As expected the bone appears to be remodeling into a more hollow structure, but surprisingly, a large amount of fat cells are appearing over time in the central compartment or presumptive marrow cavity of this tissue.

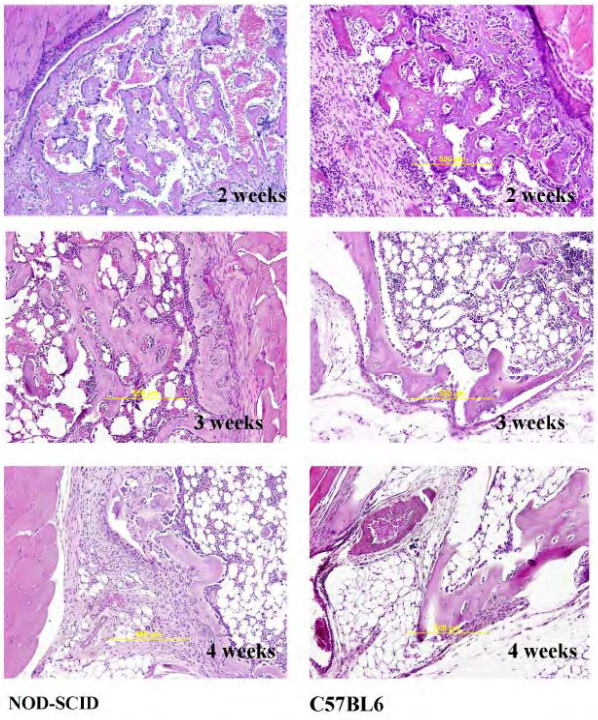

Figure 18: Histological analysis of long term bone formation (2-4 weeks). NOD/Scid sections (left column) demonstates well-formed bone with osteoblastic and osteoclastic activity that result in a presumptive marrow cavity by 4 weeks (bottom left image). C57BL/6 sections (right column) follow an identical patterning and remodeling that also results in a presumptive marrow cavity. (Hematoxylin and Eosin, magnification 100X)

Microcomputed tomographic analysis was performed on tissues (*n*=6) isolated 2, 3 and 4 weeks after induction of bone formation to compare total bone volume between the two model systems (Figure 19A).

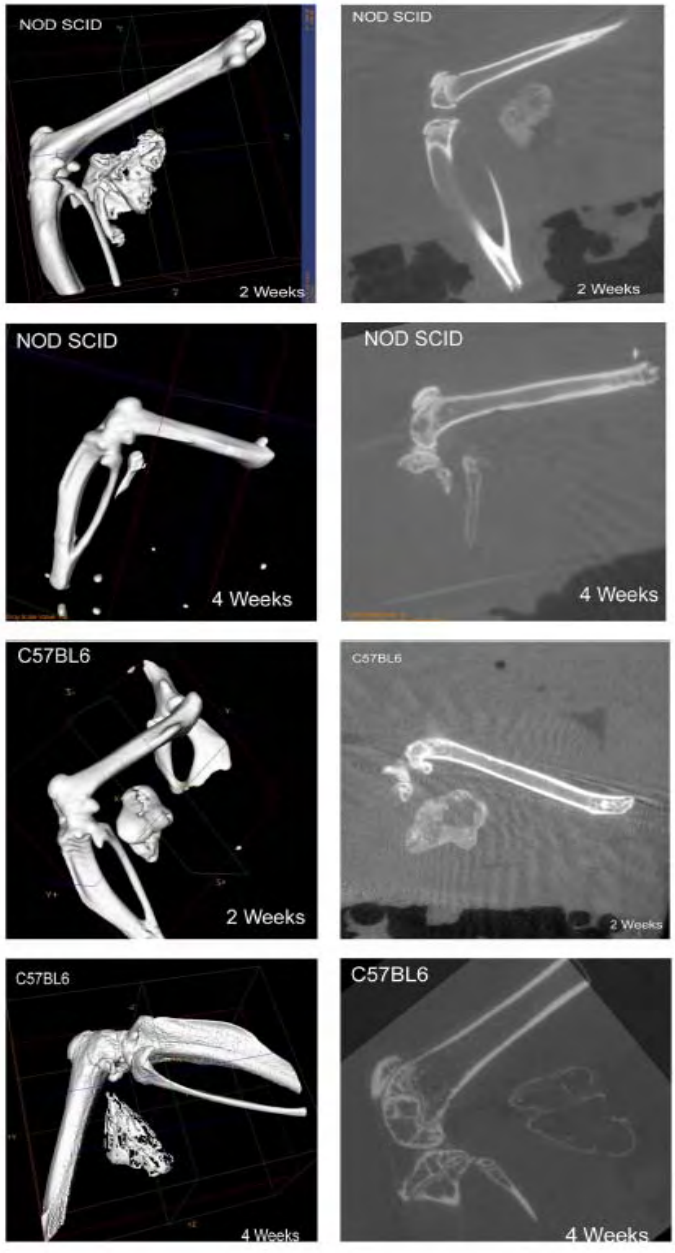

Figure 19: MicroCT analysis of long term bone formation. Graphical representation of the heterotopic bone volumes measured by MicroCT. **(A)** The bone volumes in both systems remain relatively similar and both systems show a significant decrease in overall bone volume from 2 to 4 weeks. **(B)** Three and two dimensional reconstructed images of the bone formed at 2 and 4 weeks by post injection with BMP2 in NOD/Scid and C57BL/6 mice.

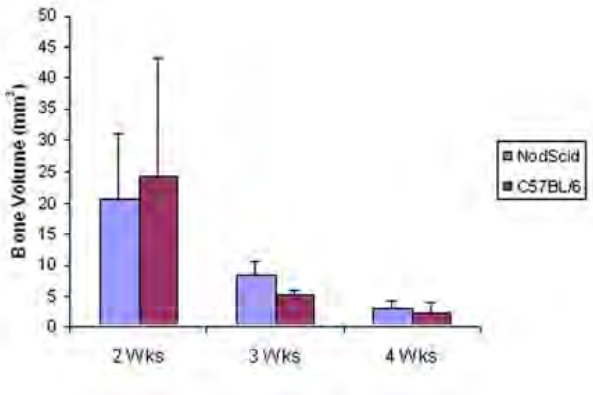

The results show similar bone volume at all time periods with no significant difference between the two systems, however there was a significant decrease in the overall bone volume in both systems when samples were compared temporally (Figure 19A). The

bone volume peaked at two weeks and decreased significantly by 4 weeks in both models (Figure 19A). Heterotopic bone is apparent in all samples, regardless of the model. Three dimensional reconstruction of heterotopic bone from representative NOD/SCID and C57BL/6 (Figure 19B) tissue samples are shown. Two dimensional cross-sectional analysis of the three dimensional reconstruction show thicker bone that is less well mineralized in both NOD/SCID and C57BL/6 at two weeks which becomes much thinner and more well mineralized by four weeks. This change in overall bone volume may reflect both the remodeling of the presumptive marrow cavity as well as the lack of weight bearing forces on the heterotopic bone.

Summary

Both systems employ the efficient but transient expression of BMP2 through a cell based gene therapy approach, and appears to produce localized bone capable of remodeling into a mature structure. Interestingly, both the immune compromised (NOD/SCID) and an immune competent (C57BL/6) models yielded identical temporal, morphologic and volumetric measurements of the bone formation. In all cases transient expression of BMP2 within the tissues led to rapid endochondral bone formation in which mineralized bone was detected by 7 days after induction.

Previous studies delivering BMP2 through a cell based gene therapy approach in which the cells were transduced with first generation adenoviral vectors demonstrated bone formation only in immune compromised animals (Alden *et al*, 1999). Similar results were observed by Okubo *et al*, 2000 and Sonobe *et al*, 2002 who observed endochondral bone formation only in immunosuppressed rats but not in immune-competent animals. In more recent studies, Sonobe *et al* 2004, used collagen as a biomaterial to mask the host immune response and suggested this was a requirement for bone formation in immune-competent animals. In other studies investigators attempted to mask severe inflammatory responses by inclusion of immunosuppressant's such as FK506 or Cyclosporin A (Kaihara *et al*, 2004; Okubo *et al*, 2000).

Here we compare endochondral bone formation in both immune compromised and immune competent mice and demonstrate the equivalent nature of these systems. Our data suggests that immunogenicity and clearance of the adenovirus transduced cells does not interfere with the osteoinductive nature of BMP2. Using set parameters to obtain equivalent functional BMP2 production in the two systems, we injected the MRC5 into the NOD/SCID animals and the MC3T3 cells into the C57BL/6 mice. We then compared the temporal formation of bone and morphologic features in the two different models. The bone formation was essentially the same in each of the models.

Thus this cell based BMP2 gene therapy system has several unique properties which set it apart from other cell and gene therapies. First, long-term expression of the transgene is not a requirement, as evidenced by the significant endochondral bone formation, even with rapid clearing of the BMP2 transduced delivery cells. The ability of BMP2 to induce endochondral bone formation through a trigger-type mechanism has also been demonstrated by others (Koh *et al*, 2006). This property provides significant advantages over other gene therapy targets which require long term persistence of the transgene and have limited ability for readministration. Even the helper dependent adenovirus with its lessened immunogenicity has not solved the problem (Koehler *et al*, 2003).

However, here we present data that demonstrates the ability of BMP2 to rapidly form bone without requiring a specific delivery cell. Thus the choice of delivery cells can be based on other factors than those associated with bone formation. This finding greatly enhances the versatility of the system, in that one can select a cell type based on manufacturing properties as well as versatility to the general population. The ability to develop a single qualified cell type such as a bone marrow mesenchymal stem cell that can be used universally in the population without leading to significant immune responses to the foreign cells, and this greatly reduces the cost and time associated with manufacturing this therapy, thus allowing for more widespread applications.

Key Research Accomplishments

- We have developed a novel non-receptor mediated delivery system for adenovirus, to provide for higher level transduction efficiency.
- We have developed a formulation of hydrogel that provides for sufficient BMP2 expression to induce *in vivo* bone formation. In experiments in which one large 150 ul disk was implanted, we had a very thin shell of bone surrounding the material. To circumvent this we went ahead and pre-formed the hydrogel encapsulated cells into 25 uL bead structures. These were then implanted thus allowing more room for

bone formation to occur between the beads. Micro-CT analysis of the bone formation 2 and 3 weeks after injection showed significant amounts of mineralization that was confirmed to be mature bone via histology.

- The area of new bone formation as determined by microCT was equivalent between the animals receiving the hydrogel beads as compared to those that received the direct injection of cells. Presumably this was due in part to the fact that all the beads had bone surrounding them whereas in the direct injection, bone formed only around the area of the initial injection. This finding is significant in that the animals receiving the injected cells received 50-60% more BMP2 than those that got the hydrogel beads suggesting that placement of the BMP2 may be as critical to inducing robust bone formation as a threshold amount. Further this finding suggests that the bone reaction can only occur within a limited distance from the BMP2 itself even in these systems with sustained expression.
- We have demonstrated similar temporal and rate of bone formation in comparison studies between C57BL/6 (immunocompetent) mice and the NOD/Scid (immune incompetent) mouse model. In these studies we encapsulated a fibroblast cell line derived from C57BL/6 mice that had been transduced with Ad5BMP2 in the presence of GeneJammer. We have developed a protocol in which we can obtain the same level of BMP2 expression as that obtained when we transduce human fibroblasts with Ad5F35BMP2.
- We have demonstrated in a detailed comparison that bone formation induced by this type of cell based gene therapy system proceeds through similar temporal stages of formation, independent of the immune status. Further, we demonstrate that stem cells are not required for the production of bone formation in these systems, but rather are rapidly cleared most likely due to the first generation adenovirus vector used in the studies. However, bone formation in both models rapidly forms, and eventually remodels into a hollow structure reminiscent of skeletal bone, with an active marrow cavity.
- We have initiated studies in the spine, to obtain fusion. We have preliminary data which demonstrated rapid spine fusion in mice that received either direct injection of the AdBMP2 transduced cells into the paraspinous musculature or implantation of the same cells after encapsulation within the hydrogel material. Although the hydrogel encapsulated cells more consistently formed bone within the spine, less samples went on to fuse two vertebras within the time period. One of the main reasons for this was the difficult challenge of accurately placing the hydrogel bead structures. They were quite large compared to the murine spine, and we were unable to place them internal in the paraspinous musculature. However, we were encouraged by the robust bone formation in the area. To circumvent this problem in the future we will move towards a photopolymerizable form which can eventually be remodeled away by the bone formation. Further, we will start the rat model that will provide for a larger spine model for testing and placement of the materials.

Reportable Outcomes:

Abstracts:

1. Hydrogel Encapsulation of Adenovirus-transduced Cells Expressing BMP2 for Local Osteoinduction. Malavosklish Bikram, Christine Dilling, André M. Gobin, Elizabeth A. Olmsted-Davis, Alan R. Davis and Jennifer L. West. American Society of Gene Therapy 8th Annual Meeting, St Louis Missouri 2005.
2. Novel Compound Enables Transduction in the Absence of an Adenovirus-Specific Receptor. Christine M. Fouletier-Dilling, Pablo Bosh, Alan R. Davis, Jessica A. Shafer, Steven L. Stice, Zbigniew Gugala, Francis H. Gannon, and Elizabeth A. Olmsted-Davis. American Society of Gene Therapy 8th Annual Meeting, St. Louis Missouri 2005.
3. BMP2 Induced Bone Formation Follows Similar Cellular Events in the Presence and Absence of an Immune System. Christine M. Fouletier-Dilling, Zawaunyka Lazard, Jessica A. Shafer, Francis H. Gannon, Alan R. Davis and Elizabeth A. Olmsted-Davis. American Society of Gene Therapy 9th Annual Meeting, Baltimore MD 2006.

Manuscripts:

1. Christine Fouletier-Dilling, Pablo Bosh, Alan R. Davis, Jessica Shafer, Steven Stice, Zbigniew Gugala, Francis H. Gannon, and Elizabeth A. Olmsted-Davis (2005). A Novel Compound Enables

High-Level Adenovirus Transduction in the Absence of an Adenovirus-Specific Receptor. Human Gene Therapy 16(11): 1287-1298.

2. Malavosklish Bikram, Christine Fouletier-Dilling, John A, Hipp, Francis Gannon, Alan R. Davis, Elizabeth A. Olmsted-Davis, and Jennifer L. West. Endochondral Bone Formation from Hydrogel Carriers Loaded with BMP2-Transduced Cells. (Annals of Biomedical Engineering, In Press 2007).
3. C. Fouletier-Dilling, F. Gannon, E.A. Olmsted-Davis, Z. Lazard, M. Heggeness, J.A. Shafer, J.A. Hipp, and A.R. Davis. Efficient and Rapid Osteoinduction in an Immune Competent Host. (Human Gene Therapy, In revision).

Conclusions:

We conclude that the peripheral blood mononuclear cells can be transduced to express BMP2, using the chimeric adenovirus vector Ad5F35, along with the polyamine, GeneJammer®. However, this level of induction coupled to the significant reduction in BMP2 expression from the hydrogel encapsulated cells, is not sufficient to produce endochondral bone. We propose the use of mesenchymal stem cells as a potential alternative. Bone marrow mesenchymal stem cells have previously been shown to be versatile in an autologous setting. Further, these cells have been shown to somewhat suppress normal graft versus host responses. Since these cells are routinely manufactured for clinical use, they are an ideal source of cells for this type of therapy. They are readily transduced and our preliminary data suggest they are viable after hydrogel encapsulation.

We have demonstrated the ability of the BMP2 transduced cells to induce spine fusion in Nod/SCID mice, and have validated that the bone induction mechanism in this model, works similarly in immune competent mice. Finally we have demonstrated the ability to encapsulate the BMP2 transduced cells in a hydrogel material, and still maintain their viability and efficient secretion of BMP2. Further, delivery of the hydrogel encapsulated cells led to targeted bone formation, and vertebral fusion when implanted in a spine setting. These are the first steps in developing a safe and efficacious noninvasive gene therapy for the tissue engineering of bone.

However, for this system to become a reality, we must determine the minimal number of transduced cells required for spine fusion when delivered through this targeted method. Using this information we must next reduce the volume of polymer used for encapsulation to better fit the spatial restrictions found in the spine, and finally we must move towards using the polymer encapsulation system which is photo-polymerized in place rather than preformed structures that must be surgically implanted. We must perform more replicates to identify to develop a time frame for fusion that will provide a ≥ 90% success rate. To aid in these goals we propose to improve both the secretion of BMP2 through re-engineering the BMP2 protein to remove a region known to have strong binding to glycoprotein's on the cell. Previous work in the literature has shown removal of such sites greatly increases the diffusion of secreted proteins. Further, we will introduce cellular binding sites both on the external and internal surfaces to aid in recruitment of the stem cells to site of new bone formation. Finally we have proposed to add in a regulated promoter system to the expression of BMP2 and demonstrate *in vivo* using a novel imaging methodology sensitive enough to potentially track handfuls of cells to confirm both the localized and regulated expression of BMP2.

Completion of this project would significantly advance the current state of gene therapy in this field by eliminating the search for an optimal osteoprogenitor cell and scaffolding. But even more importantly, it would offer a non-invasive alternative to current treatments for degenerative spine disorders. Posterolateral spine fusion, which normally results in 500-1000 cc of blood loss as well as a 5 to 7 day hospital stay and a recovery period of up to a year, could be performed on an outpatient basis with this minimally invasive procedure, without concern over undue morbidity. This technology would benefit a broad age range of patients, and greatly reduce treatment costs as well as loss work time. Our proposed method has the potential to improve the safety of current spine surgery techniques and would offer an alterative to patients who require spine fusion but are not candidates for major surgery.

References:

Olmsted-Davis, E.A., Gugala, Z., Gannon, F. H., Yotnda, P., McAlhany, R.E., Lindsey, R.W., and Davis, A.R. Use of a chimeric adenovirus vector enhances BMP2 production and bone formation. Hum Gene Ther 13:1337-1347; 2002.

Gugala, Z., Olmsted-Davis, E.A., Gannon, F.H., Lindsey, R.W. and Davis, A.R. Osteoinduction by Ex Vivo Adenovirus-Mediated BMP2 Delivery Is Independent of Cell Type. Gene Ther 10(16):1289-1296; 2003.
Fouletier-Dilling, C., Bosh, P. Davis, A.R., Shafer, J.A., Stice, S. Gugala, Z., Gannon, F.H. and Olmsted-Davis, E.A. A Novel Compound Enables High-Level Adenovirus Transduction in the Absence of an Adenovirus-Specific Receptor. Hum Gene Ther 16(11): 1287-1298; 2005.
Thies, R.S., Bauduy, M., Ashton, B.A., Kurtzberg, L., Wozney, J.M., and Rosen, V. Recombinant human bone morphogenetic protein-2 induces osteoblastic differentiation in W-20-17 stromal cells. Endo 130, 1318-1324; 1992.
Olmsted, E.A., Blum, J.S., Rill, D., Yotnda, P., Gugala, Z., Lindsey, R.W., and Davis, A.R. Adenovirus-mediated BMP2 expression in human bone marrow stromal cells. J Cell Biochem 82:11-21; 2001
Blum JS, Li RH, Mikos AG, Barry MA. An optimized method for the chemiluminescent detection of alkaline phosphatase levels during osteodifferentiation by bone morphogenetic protein 2. J Cell Biochem; 80: 532-537; 2001.
Malavosklish Bikram, Christine Fouletier-Dilling, John A, Hipp, Francis Gannon, Alan R. Davis, Elizabeth A. Olmsted-Davis, and Jennifer L. West. Endochondral Bone Formation from Hydrogel Carriers Loaded with BMP2-Transduced Cells. Ann Biomed Eng, In Press 2007, see appendix.
Cruise GM, Scharp DS, Hubbell JA. Characterization of permeability and network structure of interfacially photopolymerized poly(ethylene glycol) diacrylate hydrogels. Biomaterials 19: 1287-1294; 1998.
DeLong SA, Moon JJ, West JL. Covalently immobilized gradients of bFGF on hydrogel scaffolds for directed cell migration. Biomaterials 26: 3227-3234; 2005.
Yang Y, Haecker SE, Su Q, and Wilson JM. Immunology of gene therapy with adenoviral vectors in mouse skeletal muscle. Hum. Mol. Genet. 5, 1703-1712; 1996.
Olmsted-Davis EA, Gannon FH, Ozen M, Ittmann MM, Gugala Z, Hipp JA, Moran KM, Fouletier-Dilling C, Schmura-Martin S, Lindsey RW, Heggeness MH, Brenner MK and A. R. Davis. Hypoxic Adipocytes Pattern Early Heterotopic Bone Formation Am J Path 170:620-632; 2007.
Shafer JA, Davis AR, Gannon FH, Fouletier-Dilling C, Lazard Z, Moran K, Gugala Z, Ozen M, Ittman MM, Heggeness MH, and EA Olmsted-Davis. Bone Tissue Engineering: A Model for Delineating the Early Events in Endochondral Bone Formation. (Tissue Engineering, In Press 2007, see appendix).
Alden TD, Pittman DD, Hankins GR, Beres EJ, Engh JA, Das S, Hudson SB, Kerns KM, Kallmes DF, and Helm GA. In vivo endochondral bone formation using a bone morphogenic protein 2 adenoviral vector. Hum Gene Ther: 1999: 10:2245-2253; 1999.
Okubo Y., Bessho K, Fujimura K, Iizuka T, and Miyatake S. Osteoinduction by bone morphogenetic protein-2 via adenoviral vector under transient immunosuppression. Biochem. Biophys. Res. Commun. 267, 382-387; 2000.
Sonobe J, Bessho K, Kaihara S, Okubo Y, and Iizuka T. Bone induction by BMP2 expressing adenoviral vector in rats under treatment with FK506. J. Musculoskeletal Res. 6, 23-29; 2002.
Kaihara S, Bessho K, Okubo Y, Sonobe J, Kawai M, and Iizuka T. Simple and effective osteoinduction gene therapy by local injection of a bone morphogenetic protein-2 expressing recombinant adenoviral vector and FK506 mixture in rats. Gene Ther. 11, 439-447; 2004.
Koh JT, Ge C, Zhao M, Wang Z, Krebsbach PH, Zhao Z, and Franceschi RT. Use of a stringent dimerizer-regulated gene expression system for controlled BMP2 delivery. Mol.Thera. 14, 684-691; 2006.
Koehler DR, Sajjan U, Chow YH, Martin B, Kent G, Transwell AK, McKerlie C, Forstner JF, and Hu J. Protection of Cftr knockout mice from acute lung infection by a helper-dependent adenoviral vector expressing Cftr in airway epithelia. Proc. Natl. Acad. Sci. USA. 100, 15364-15369; 2003.

Appendices:

1. Malavosklish Bikram, Christine Fouletier-Dilling, John A, Hipp, Francis Gannon, Alan R. Davis, Elizabeth A. Olmsted-Davis, and Jennifer L. West. Endochondral Bone Formation from Hydrogel Carriers Loaded with BMP2-Transduced Cells. (Annals of Biomedical Engineering, In Press 2007).
2. C. Fouletier-Dilling, F. Gannon, E.A. Olmsted-Davis, Z. Lazard, M. Heggeness, J.A. Shafer, J.A. Hipp, and A.R. Davis. Efficient and Rapid Osteoinduction in an Immune Competent Host. (Human Gene Therapy, In revision).
3. Shafer JA, Davis AR, Gannon FH, Fouletier-Dilling C, Lazard Z, Moran K, Gugala Z, Ozen M, Ittman MM, Heggeness MH, and EA Olmsted-Davis (2007) Bone Tissue Engineering: A Model

for Delineating the Early Events in Endochondral Bone Formation. (Tissue Engineering, In Press, see appendix).

Annals of Biomedical Engineering (© 2007)
DOI: 10.1007/s10439-007-9263-4

Endochondral Bone Formation from Hydrogel Carriers Loaded with BMP2-transduced Cells

MALAVOSKLISH BIKRAM,[1] CHRISTINE FOULETIER-DILLING,[2] JOHN A. HIPP,[3] FRANCIS GANNON,[4] ALAN R. DAVIS,[2,3,5] ELIZABETH A. OLMSTED-DAVIS,[2,3,5] and JENNIFER L. WEST[6]

[1]Department of Pharmacological and Pharmaceutical Sciences, University of Houston, 1441 Moursund Street, Houston, TX 77030, USA; [2]Center for Cell and Gene Therapy, Baylor College of Medicine, Houston, TX 77030, USA; [3]Department of Orthopaedic Surgery, Baylor College of Medicine, Houston, TX 77030, USA; [4]Department of Pathology, Baylor College of Medicine, Houston, TX 77005, USA; [5]Department of Pediatrics, Baylor College of Medicine, Houston, TX 77030, USA; and [6]Department of Bioengineering, Rice University, 6100 Main St. MS 144, Houston, TX 77005, USA

(*Received 23 July 2006; accepted 22 January 2007*)

Abstract—The success of *ex vivo* viral gene therapy systems for promoting bone formation could be improved through the development of systems to spatially localize gene expression. Towards this goal, we have encapsulated adenovirus-transduced human diploid fetal lung fibroblasts (MRC-5) expressing bone morphogenetic protein-type 2 (BMP-2) within non-degradable poly(ethylene glycol)-diacrylate (PEG-DA) hydrogels and implanted these intramuscularly to promote endochondral bone formation. To optimize BMP-2 secretion, the molecular weight of the polymers and cell densities were varied. Polymers with molecular weights of 6, 10, and 20 kDa were used to prepare hydrogels containing 1, 5, or 10 million transduced cells. The results showed that 10 million transduced fibroblasts that was the maximum number of cells feasible for encapsulation within PEG-DA 10 and 20 kDa hydrogels produced the highest amount of secreted BMP-2 protein. Encapsulation of MRC-5 and transduced fibroblasts resulted in 71 and 58% cell viability, respectively. The bioactivity of secreted BMP-2 protein from the hydrogels was confirmed with an alkaline phosphatase assay. Micro-CT of the lower limb muscles of NOD/SCID mice following implantation with hydrogels showed 39.5 ± 25.0 mm^3 mineralized tissue and 31.8 ± 7.8 mm^3 for the cell-injected mice, and the bone was localized to the hydrogel surfaces. Histology revealed bone as well as cartilage for both hydrogel implanted and cell-injected animals.

Keywords—Gene therapy, Adenovirus, Bone, Hydrogel, Cell encapsulation, Biomaterials, Bone morphogenetic protein, Tissue engineering, Tissue repair.

INTRODUCTION

There is an overwhelming need to develop safe and efficacious systems for bone regeneration for the treatment of fractures, osteoporosis, tumor resection, spinal arthrodesis, maxillofacial surgery, and implant fixation.[4,12,14,26,28,30] In many of these cases, there are large defects that remain relatively unrepaired. Therefore, bone regeneration is needed in order to restore the structure and function to the bone. Current treatments for these defects include autografts, allografts, and xenografts. However, one of the major limitations of bone regeneration using these types of treatment is the source of graft material. The benchmark for most orthopedic applications is autologous bone graft obtained from the patient's iliac crest, which is not only limited but requires an additional surgical procedure.[1,47] Thus, allogeneic and xenogeneic bone grafts have been developed but issues related to immunogenicity, disease transmission, immunological rejection, and unfavorable biomechanical properties have limited their use.[10,24,25,45]

Therefore, in an effort to overcome the hurdles associated with bone graft materials, research has focused on the induction of bone with proteins such as bone morphogenetic proteins (BMPs). These cytokine proteins have been shown to induce the formation of new cartilage and bone tissues as well as to act as potent morphogens in pattern formation and development of the embryonic skeleton.[18,19,23,27,41,44] As a result, BMP-2 protein was commercially introduced as a bone graft substitute for spinal fusion and was subsequently applied to a collagen sponge as the protein carrier.[16] However, the use of a collagen sponge reduces the protein's bioavailability, so that large amounts of protein are required to produce a clinical response.[17] Therefore, gene therapy may be an alternative to direct protein delivery.

Presently, there have been several promising studies utilizing viral vectors encoding BMP-2 for promoting heterotopic bone formation.[29,48,49] These studies

Address correspondence to Jennifer L. West, 6100 Main St. MS 144, Houston, TX 77005, USA. Electronic mail: jwest@rice.edu

include the use of retroviruses such as lentiviruses,[37] adeno-associated viruses (AAV),[13] and adenoviruses.[35] For example, using a chimeric adenovirus, Ad5F35-BMP2, containing the cDNA for human BMP-2, injection of *ex vivo* transduced cells expressing high levels of BMP-2 has been shown to induce endochondral bone formation.[15,31] The recombinant chimeric adenoviral BMP-2 vector was constructed from adenovirus type 5 (Ad5) containing a fiber gene from adenovirus type 35 (Ad35), which facilitates entry into cells in a coxsackie-adenovirus receptor (CAR) independent fashion. However, the localization of BMP-2-transduced cells at a delivery site needs to be improved in order to circumvent uncontrolled gene expression in undesirable places such as vital organs and blood vessels. An alternative to direct administration of *ex vivo* transduced cells is the encapsulation of cells within a protective barrier that can restrict cell migration from an injected site and in doing so effectively localize gene expression. Currently, there are many types of materials that can be used for cell encapsulation including silk fibroin hydrogels,[11] oligo(poly(ethylene glycol) fumarate) (OPF) hydrogels,[38] sodium alginate hydrogels,[2] hydroxypropylmethylcellulose hydrogels,[40] and poly(ethylene glycol)-diacrylate (PEG-DA) hydrogels.[46] Hubbell *et al.* has previously shown that pancreatic islets of Langerhans encapsulated within PEG-DA hydrogels were able to allow the rapid diffusion of nutrients and insulin. Moreover, they demonstrated that encapsulation within the PEG-DA hydrogels provided immunoprotection since the hydrogels were not permeable to antibodies or complement proteins and did not interact with inflammatory cells.[6,7,22]

PEG-DA hydrogels are hydrophilic, polymeric networks that imbibe large quantities of water without dissolution and in doing so impart the physical characteristics of soft tissues. Moreover, the pores or mesh sizes of the hydrogel can be controlled by varying the molecular weight of the PEG-DA polymers so as to mediate the diffusion of gases, nutrients, and metabolites throughout the network.[32] In addition, these hydrogels can be photopolymerized in any conformation with the use of photoinitiators using visible or long wavelength ultraviolet (UV) light. Also, PEG-DA hydrogels have been widely used for tissue engineering applications such as in the development of biocompatible barriers to prevent thrombosis and restenosis[20,21] and for cell encsapsulation.[6,7,22,34]

Therefore, the objective in this paper is to encapsulate adenovirus-transduced cells expressing BMP-2 within non-degradable PEG-DA hydrogels for endochondral bone formation. Our central hypothesis is that encapsulation of cells expressing BMP-2 will lead to spatial control of gene expression that will limit bone formation to a desired area. Thus, we have encapsulated human diploid fetal lung fibroblasts (MRC-5), which have been transduced *ex vivo* with the adenovirus, Ad5F35BMP2, within non-degradable PEG-DA hydrogels. The molecular weight of the PEG-DA polymers as well as the cell densities within the hydrogels will be varied so as to optimize both BMP-2 protein secretion from the hydrogels and the mechanical properties of the hydrogels.

MATERIALS AND METHODS

Cell Culture Maintenance

Human diploid fetal lung fibroblasts (MRC-5) were obtained from American Type Culture Collection (ATCC; Manassas, VA). The cells were propagated in Eagle's Minimum Essential Media (EMEM; ATCC) supplemented with 10% fetal bovine serum (FBS; BioWhittaker, Walkerrsville, MD), 1000 U/L penicillin, 100 mg/L streptomycin, and 0.25 μg/ml amphotericin B (Sigma; St. Louis, MO), and grown in a humidified incubator at 37°C and 5% CO_2.

Fibroblast Transduction with Adenoviral Vectors

MRC-5 cells were transduced by replacing the media from the cultured cells with fresh EMEM supplemented with 10% FBS and the antibiotic–antimycotic. Ad5F35BMP2 adenoviral vectors at a previously optimized concentration of 2500 viral particles per cell were then added to the flask, which was incubated overnight prior to use.[31] The transduced cells were then rinsed with sterile phosphate buffered saline (PBS), trypsinized, and counted with a hemacytometer.[15]

Hydrogel Preparation

The molecular weight of the PEG-DA polymers and hence the mesh size of the hydrogels can affect the diffusion of gases and nutrients throughout the scaffold as well as efficient diffusion of BMP-2 protein from the hydrogels. Additionally, the molecular weight of the polymers can also influence the mechanical properties of the hydrogels. Thus, in order to determine the optimum PEG-DA hydrogel for cell encapsulation and hence gene expression, hydrogels of varying molecular weight were prepared. PEG-DA (6000, 10,000, 20,000 Da) was synthesized by reaction of PEG (Fluka, Milwaukee, WI) with acryloyl chloride as previously described.[9] The dried polymers were then dissolved in 10 ml of ultrapure water and purified by dialysis (MWCO 3500 Da; Fisher

Scientific, Pittsburg, PA) against deionized water for 3 days. The purified polymers were then lyophilized and stored at −20 °C. Polymer solutions were sterilized via filtration (0.2 μm filter; Gelman Sciences, Ann Arbor, MI) prior to use. Hydrogel disks (11.5 mm (d) × 0.5 mm (h)) were photopolymerized by combining 0.1 g/ml PEG-DA (10% w/v) with 1.5% (v/v) triethanolamine/HEPES buffered saline (HBS, pH 7.4), 37 mM 1-vinyl-2-pyrrolidinone, 10 mM eosin Y, and MRC-5 or MRC-5 cells transduced with Ad5F35BMP-2 viral vectors for hydrogels with cells for a final concentration of 1, 5, or 10 million cells/disk, which was the maximum number of cells that were feasible for encapsulation. The pre-polymer solution was formulated with and without cells as described above to a final volume of 150 μl, which was then pipetted into the wells of a 48-well cell culture dish that was exposed to visible light for 2 min. The hydrogels were then immediately transferred to 150 mm × 25 mm cell culture dishes (Corning Inc., Corning, NY) to which 35 ml cell culture media was added. Control cells were seeded in tissue culture flasks (Fisher Scientific; Pittsburg, PA) that were pre-treated with a 1% (w/v) gelatin solution (Sigma, St. Louis, MO).

Hydrogel Characterization

PEG-DA hydrogels prepared from varying molecular weight precursors were fabricated as described above. The hydrogels were then dried in a vacuum oven for 1 week, after which the dry weights were recorded. To determine the swelling ratios (swelling ratio = W_s/W_d where W_s and W_d are the weight of water in the swollen gel after equlibrium and the dry weight of the gel, respectively), the hydrogels were reswollen in PBS and the swollen weights were recorded.[50] The water content, molecular weight between crosslinks (M_c), and the mesh sizes of the prepared hydrogels were then determined as previously described.[5,8] The compressive moduli of the different hydrogels with and without transduced fibroblasts were determined using an Instron® 3342 (Canton, MA) mechanical tester. Briefly, the hydrogel precursors were formulated with and without 10 million transduced fibroblasts as described above. The solutions were then placed in a rectangular glass mold (~1.4 mm thickness) and exposed to visible light for 2 min. The faceplate was removed and a cork borer was used to cut out 11.5 mm diameter disks that corresponded to a final volume of 150 μl. The disks were then transferred to cell culture plates to which 35 ml of complete media was added and the plates were incubated overnight. Prior to analysis, the hydrogels were dabbed with a Kimwipe to remove excess surface media and placed between two parallel platens mounted on the Instron® mechanical tester. The compressive modulus of the hydrogels was determined from the slope of the calculated stress (Pa) versus strain curves using a 10 N load cell at a crosshead speed of 1 mm/min.

ELISA for BMP-2

BMP-2 levels were measured with a Quantikine® BMP-2 immunoassay kit (R & D Systems Inc.; Minneapolis, MN) as per manufacturer's instructions. Transduced and non-transduced cells were encapsulated and maintained in 35 ml of media as described above. Control cells were seeded at a density of 1, 5, and 10 million cells per flask and also maintained in 35 ml of media as described above. Samples of 1.0 ml of the conditioned media from both the cultured flasks and hydrogel disks were then taken at 1, 3, 5, 7, 9, and 15 days followed by media change and the samples were then assayed for secreted BMP-2 protein. Levels of BMP-2 protein were normalized to total protein content determined with a BCA™ protein assay kit (Pierce; Rockford, IL) and reported as pg BMP-2/mg protein. The PEG-DA hydrogels with encapsulated transduced fibroblasts that produced the highest amounts of secreted BMP-2 protein compared with their plated counterparts as well as the hydrogels with best mechanical properties were then selected as the optimal molecular weight for further analysis.

Cell Viability

Viability of the MRC-5 and transduced fibroblasts encapsulated within the optimized PEG-DA (10 kDa) hydrogels were determined with a LIVE/DEAD® Viability/Cytotoxicity kit (Molecular Probes; Eugene, OR). Briefly, hydrogel disks with either 10 million MRC-5 or transduced fibroblasts were formulated and photopolymerized in 48-well cell culture plates as described above. The hydrogels were then transferred to cell culture dishes to which 35 ml of media was added. On days 1 and 7, the media was removed and the hydrogels were transferred to 6-well plates. The disks were washed with sterile tissue culture grade PBS three times for 10 min each. The fluorophore solution was then prepared by adding 20 μl ethidium homodimer (2 mM) and 5 μl calcein AM (4 mM) to 10 ml PBS. The resulting solution was vortexed and 2 ml was then added to each well containing the hydrogels. The plate was incubated for 45 min at 37 °C after which the hydrogels were washed as previously described and the fluorescence of the live and dead cells were analyzed using a Zeiss LSM 510 confocal microscope (Thornwood, NY) with LSM 5 Image Browser software (Version 1.0). Briefly, three sections of each of the

hydrogel were viewed and within each section, three independent areas of the section were analyzed in which all fluorescently labeled cells within the view were taken into account. The amount of fluorescently labeled live and dead cells was reported as a percent of the total cells counted.

Alkaline Phosphatase Activity

Conditioned media from the optimized PEG-DA (10 kDa) hydrogel constructs with 10 million transduced fibroblasts as well as the plated controls were used to assess the ability of the secreted BMP-2 to stimulate alkaline phosphatase activity in W20-17 cells.[31] W20-17 cells are bone marrow stromal cells that were originally isolated from murine bone marrow by Thies *et al.*,[39] and further demonstrated that these cells respond to BMP-2 by up-regulation of the alkaline phosphatase activity. Briefly, W20-17 cells at a cell density of 5×10^4 cells/well were seeded in 24-well plates. After 24 h, the cell culture media was replaced and 200 μl of conditioned media was added to the wells of the plates that were then incubated for 3 days. The cellular alkaline phosphatase was extracted by three freeze–thaw cycles in 100 μl/cm^2 of 25 mM Tris–HCl (pH 8.0) with 0.5% Triton X-100. After extraction, 100 μl of CSPD® Ready-to-use solution with Sapphire II enhancer (Tropix, Inc., Bedford, MA) was added to the samples. The alkaline phosphatase activity was then measured by chemiluminescence in which the output from each sample was integrated for 10 s after a 2 s delay by a luminometer (TD-20/20, Turner Designs, Sunnyvale, CA).

Western Blot Detection

Conditioned media from the optimized PEG-DA (10 kDa) hydrogels with 10 million transduced fibroblasts were precipitated by addition of five volumes of cold acetone and the resulting solution was stored overnight at −20 °C.[31] The proteins were pelleted by centrifugation for 10 min at 4000 rpm, resuspended in sample buffer (0.5 M Tris–HCl, pH 6.8, 10% (w/v) sodium dodecyl sulfate, 25% glycerol, 0.5% (w/v) bromophenol blue, and 5% (v/v) β-mercaptoethanol, and heated at 95 °C for 4 min. The samples were cooled on ice and the proteins were separated on a Tris–HCl 4–15% Ready gel (Bio-rad; Hercules, CA) under denaturing conditions and transferred to a supported nitrocellulose membrane (Bio-rad; Hercules, CA). Purified recombinant BMP-2 protein (Research Diagnostics, Inc.; Flanders, NJ) was used as the positive control. BMP-2 protein was detected with an Opti-4CN substrate (Bio-rad; Hercules, CA) kit with an anti-BMP-2 monoclonal antibody (Genetics Institute; Cambridge, MA) and a secondary anti-mouse IgG antibody conjugated with horseradish peroxidase (Bio-rad; Hercules, CA).

In vivo Formation of Endochondral Bone

To facilitate implantation into the muscle, hydrogel beads were employed rather then disks. PEG-DA (10 kDa) hydrogel solution with 10 million transduced fibroblasts were formulated as previously described. Aliquots of 25 μl hydrogel solution were pipetted along surgical suture (CP Medical, Portland, OR) on the surface of a Teflon® sheet (Boedeker Plastics; Shiner, TX) to form 6 hydrogel microbeads, which represented a single sample having a total volume of 150 μl (Fig. 6). The hydrogels were photopolymerized and added to cell culture medium prior to implantation the same day. Female NOD/SCID mice (8–12 weeks old; Charles River Laboratories; Wilmington, MA) were placed five per cage and fed with an *ad libitum* diet and tap water in a 12 h day/night cycle according to Baylor College of Medicine Institutional Animal Care and Use Committee (IACUC) protocols. Prior to surgery, the animals were separated into groups of three and each hind leg of the mouse was shaved and cleansed with alcohol and then a skin incision was made to reveal the muscles of the upper long bone. Blunt dissection of the muscles of both hind legs created pockets for the hydrogel constructs. The PEG-DA (10 kDa) hydrogel beads (6 beads with total volume = 150 μl) containing 10 million transduced fibroblasts were then inserted into the quadricep muscles of each of the two hind legs of the mouse. Control hydrogels were prepared with MRC-5 cells transduced with the Ad5F35-HM4 empty cassette viral vector and these control hydrogels were implanted into each of the two hind legs of the designated control animals. The muscles of the animals were then sutured and the skin was stapled. The control animals were injected intramuscularly into each of the two hind legs of the mouse with either 10 million transduced fibroblasts or 10 million MRC-5 cells transduced with the empty Ad5F35-HM4 viral vector. Two weeks after implantation, one mouse was sacrificed and the hydrogels were removed, washed with PBS and analyzed for cell viability as described above. After 3 weeks, the remaining mice were sacrificed and both lower limbs were removed and fixed in formaldehyde solution (VWR; Sugar Land; TX). The overlying skin of each of the lower limbs of the formaldehyde preserved NOD/SCID mice were removed and scanned at 14 μm resolution with a commercial micro-CT system (GE Locus SP, GE Heathcare, London, Ontario). Three-dimensional reconstructions of the lower limb bones and any mineralized tissue in the surrounding muscle

were created at 29 μm resolution to visualize endochondral mineralized tissues. A volume of interest was defined for each specimen, and a threshold was chosen to exclude any non-mineralized tissue. The total volume of endochondral bone was then measured (eXplore MicroView, v. 2.0, GE Healthcare, London, Ontario) and the femurs and tibias of the animals were not taken into account for the measurements of mineralized tissue in the muscles of the animals. The formaldehyde fixed lower limbs of the NOD/SCID mice were then decalcified in EDTA, embedded in paraffin, and sectioned at a thickness of 5 μm. The sections were stained with hematoxylin and eosin and observed under light microscopy.

Statistics

Statistical analysis was performed with Graph-Pad Prism® version 3.02 software using one-way ANOVA with Tukey's *post-hoc* test for p-values ≤ 0.05. Data represented with error bars indicates sample group mean $\pm$ standard deviation of the mean (σ).

RESULTS

Characterization of PEG-DA Hydrogels

The 6, 10, and 20 kDa hydrogels were characterized with respect to swelling ratios and water content as determined from the dried and swollen hydrogel weights for a sample size of five ($n = 5$). The swelling ratio for the 6, 10, and 20 kDa hydrogels was found to be 8 ± 0.7, 10 ± 0.4, and 16 ± 0.2, respectively. The water content of the hydrogels was 89 ± 0.7, 91 ± 0.3, and $94 \pm 0.1\%$ for the 6, 10, and 20 kDa, respectively. In addition, the molecular weight between crosslinks, M_c, of the hydrogels was 617 ± 98, 780 ± 54, 1556 ± 24 g/mol for the 6, 10, and 20 kDa PEG-DA hydrogels, respectively, in which the hydrogels had mesh sizes of 34 ± 3, 39 ± 2, and 65 ± 1 Å, respectively.

In Vitro Optimization of BMP-2 Expression

In addition to optimizing the molecular weight of the PEG-DA hydrogels, different cell densities were encapsulated within the hydrogels to investigate optimum loading and gene expression. As can be seen from the ELISA data for a sample size of five ($n = 5$) for each group, encapsulation of 1 million cells within any of the hydrogels resulted in ~20-fold reduction in detected BMP-2 protein compared with the plated controls ($p < 0.001$) (Fig. 1a) and the expression was biphasic over the 15-day period with highest protein detected (~600 pg/ml) on day 5. In contrast, BMP-2 protein detected for 5 and 10 million encapsulated cells was found to be ~4600 and ~7000 pg/ml, respectively up to day 7 regardless of the molecular weights of the polymers in which peak BMP-2 protein

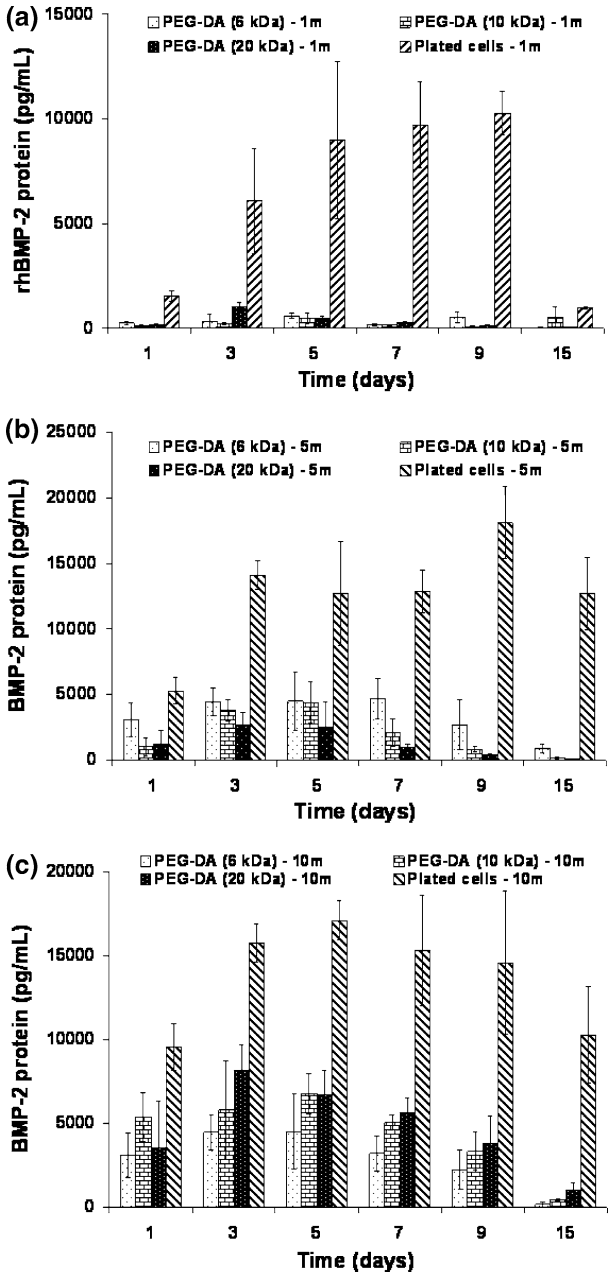

FIGURE 1. (a) Evaluation of BMP-2 protein secretion from 1 million adenovirus transduced MRC-5 cells (tMRC-5) encapsulated within PEG-DA (6, 10, 20 kDa) hydrogels with ELISA assay. (b) Evaluation of BMP-2 secretion from 5 million adenovirus transduced MRC-5 cells (tMRC-5) encapsulated within PEG-DA (6, 10, 20 kDa) hydrogels with ELISA assay. (c) Evaluation of BMP-2 secretion from 10 million adenovirus transduced MRC-5 cells (tMRC-5) encapsulated within PEG-DA (6, 10, 20 kDa) hydrogels with ELISA assay. Negative hydrogel and plated controls were less than 100 pg/ml BMP-2 detected. Data reported as mean ± SD, $n = 5$.

secretion occurred between days 3–7 for the 5 million cells within 6 kDa hydrogels and day 3 for the 10 million cells within the 20 kDa hydrogels (Fig. 1b and c).

Mechanical Testing of PEG-DA Hydrogels

To determine the compressive moduli of the PEG-DA hydrogels after encapsulation with transduced fibroblasts, we performed compressive testing with the PEG-DA hydrogels of various molecular weights containing a cell concentration of 10 million transduced fibroblasts for a sample size of five ($n = 5$). The compressive modulus of the PEG-DA hydrogel only was 454 ± 63, 395 ± 55, and 155 ± 19 kPa for the 6, 10, and 20 kDa hydrogels, respectively (Fig. 2). The maximum compressive strength was found to be 0.231 ± 0.19, 0.220 ± 0.063, and 0.076 ± 0.042 kN for the 6, 10, and 20 kDa hydrogels, respectively. Subsequent encapsulation of the hydrogels with 10 million transduced fibroblasts resulted in a significant decrease in compressive modulus of the hydrogels to 153 ± 93 kPa ($p < 0.001$), 236 ± 48 kPa ($p < 0.01$), and 90 ± 10 kPa ($p < 0.05$) for PEG-DA 6, 10, and 20 kDa, respectively. The maximum compressive strength was found to be 0.011 ± 0.003, 0.259 ± 0.206, and 0.009 ± 0.001 kN for the 6, 10, and 20 kDa hydrogels, respectively. In addition, even though there was no difference in compressive modulus for the 6 and 10 kDa PEG-DA hydrogels containing fibroblasts, there was a significant decrease in compressive modulus of the encapsulated 20 kDa hydrogels in comparison with both the 6 and 10 kDa hydrogels ($p < 0.001$).

Viability of Encapsulated Cells

The viability of 10 million non-transduced and transduced fibroblasts was determined following encapsulation of cells within the PEG-DA 10 kDa hydrogels after 1 and 7 days via staining with calcein AM and ethidium homodimer, which causes live cells to fluoresce green and dead cells to fluoresce red. The data showed that encapsulation of cells after 24 h resulted in 71 ± 9% viable non-transduced fibroblasts, whereas PEG-DA hydrogels with transduced fibroblasts had 58 ± 7% viable cells. However, even though there was a decrease in cell viability following encapsulation, the cell viability after 7 days in culture was maintained at 69 ± 8% viable for non-transduced fibroblasts and 60 ± 14% viable for transduced fibroblasts, respectively. The sample size for all data collected was five ($n = 5$).

Characterization of Secreted BMP-2

The Western blot showed that only the plated transduced cells (Fig. 3a, lanes 5–8) and hydrogels containing cells transduced with the Ad5F35BMP2 vector (Fig. 3a, lanes 10–17) produced detectable amounts of BMP-2 protein. In contrast, no BMP-2 protein was detected from the control hydrogel only (Fig. 3a, lane 2) or from the conditioned medium from non-transduced cells (Fig. 3a, lanes 3 & 4). In addition, an alkaline phosphatase assay was performed with the cultured hydrogel media to investigate the biological activity of secreted BMP-2 protein, since BMP-2 has been shown to induce alkaline phosphatase activity in W20-17 cells.[39] The alkaline phosphatase assay showed that conditioned media from the encapsulated

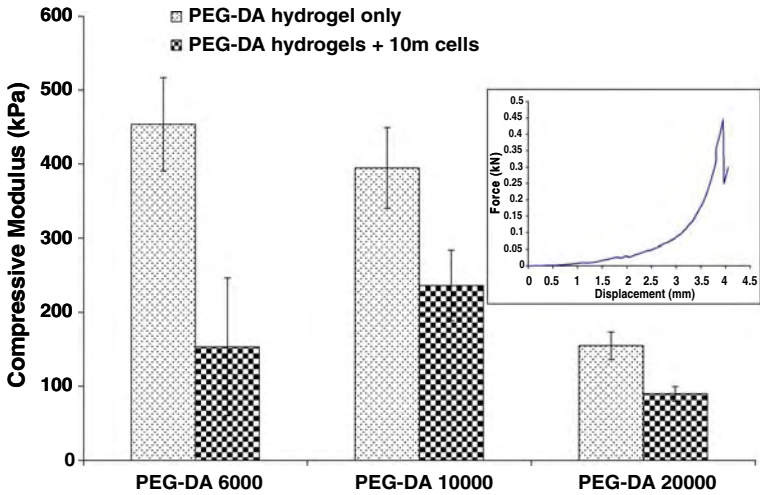

FIGURE 2. Compressive modulus for prepared PEG-DA hydrogels of varying molecular weights with and without 10 million encapsulated transduced fibroblasts after 24 h. Inset shows representative load versus displacement curve for the raw data. Data reported as mean ± SD, $n = 5$.

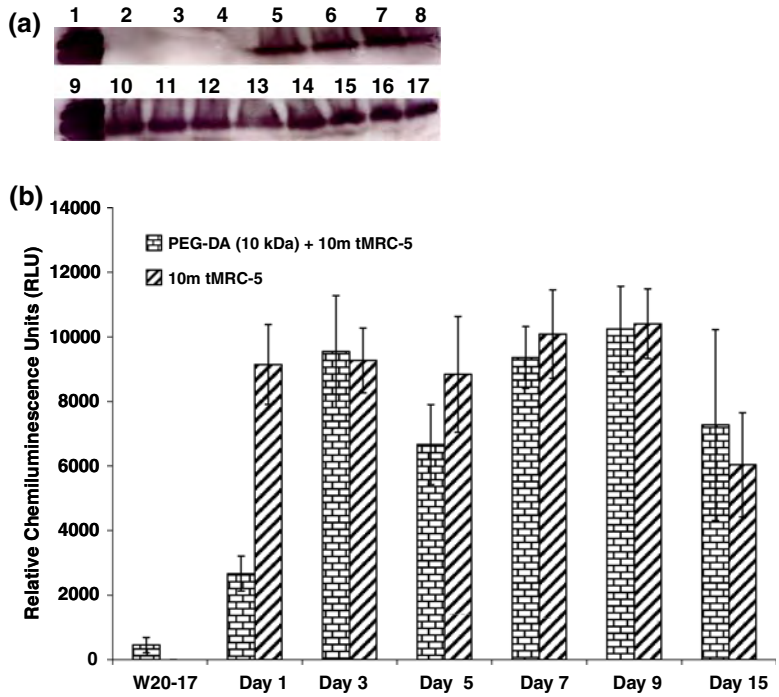

FIGURE 3. Western blot analysis for the detection of secreted BMP-2 protein. (a) Human recombinant BMP2 (lane 1), conditioned medium from PEG-DA (10 kDa) hydrogels only (lane 2), conditioned medium from 10 million MRC-5 cells encapsulated within PEG-DA (10 kDa) hydrogels (lanes 3 and 4), conditioned medium from 10 million transduced fibroblasts control (lanes 5–8), human recombinant BMP-2 (lane 9), conditioned medium containing secreted BMP-2 protein from 10 million transduced fibroblasts encapsulated within PEG-DA (10 kDa) hydrogels (lanes 10–17). (b) Alkaline phosphatase activity in W20-17 cells without the addition of conditioned medium (W20-17) and after addition of conditioned media from PEG-DA (10 kDa) hydrogels with 10 million transduced fibroblasts and control plated transduced fibroblasts (Days 1–15). Data reported as mean ± SD, $n = 5$.

transduced fibroblasts contained active BMP-2 protein, which produced high levels of alkaline phosphatase activity in W20-17 cells that was comparable to the levels of alkaline phosphatase activity obtained from the medium collected from the control plated transduced fibroblasts (Fig. 3b).

Endochondral Bone Formation

To evaluate endochondral bone formation, PEG-DA (10 kDa) hydrogels containing a total of 10 million transduced fibroblasts were implanted intra-muscularly in each hind limb of three NOD/SCID mice per group ($n = 6$), and microCT was used to measure the volume of bone formed after 3 weeks. The mean amount of mineralized tissue in the muscle of the mice was 31.8 ± 7.8 mm^3 for mice injected with transduced fibroblasts only, 39.5 ± 25.0 mm^3 for mice implanted with the PEG-DA hydrogels encapsulated with transduced fibroblasts, respectively ($p = 0.47$), and no bone was detected in any of the control animals (0.0 mm^3). More importantly, the mineralized tissue that was formed in the muscle of animals implanted with the hydrogels was found to be localized to the hydrogel surfaces. Representative images are shown in Fig. 4. Moreover, there was no endochondral bone detected in the mice that were administered control cells transduced with the Ad5F35-HM4 control empty cassette vector either as a cell suspension or in hydrogel constructs. In addition, calcein AM/ethidium homodimer staining of transduced fibroblasts within the implanted hydrogel constructs showed that $68 \pm 19\%$ of the cells were still viable 2 weeks after surgical implantation. Histological analysis confirmed the presence of bone as well as cartilage for both groups of animals implanted with the hydrogels and those receiving transduced fibroblasts only. In contrast, there was no bone and/or cartilage observed for either animals injected with *ex vivo* transduced Ad5F35-HM4 cells or for the animals that were implanted with PEG-DA hydrogels containing *ex vivo* transduced Ad5F35-HM4 cells. Representative images for each group are shown in Fig. 5.

DISCUSSION

In this study, we have demonstrated that adenovirus-transduced BMP-2 expressing fibroblasts can be localized within PEG-DA hydrogels, which allowed

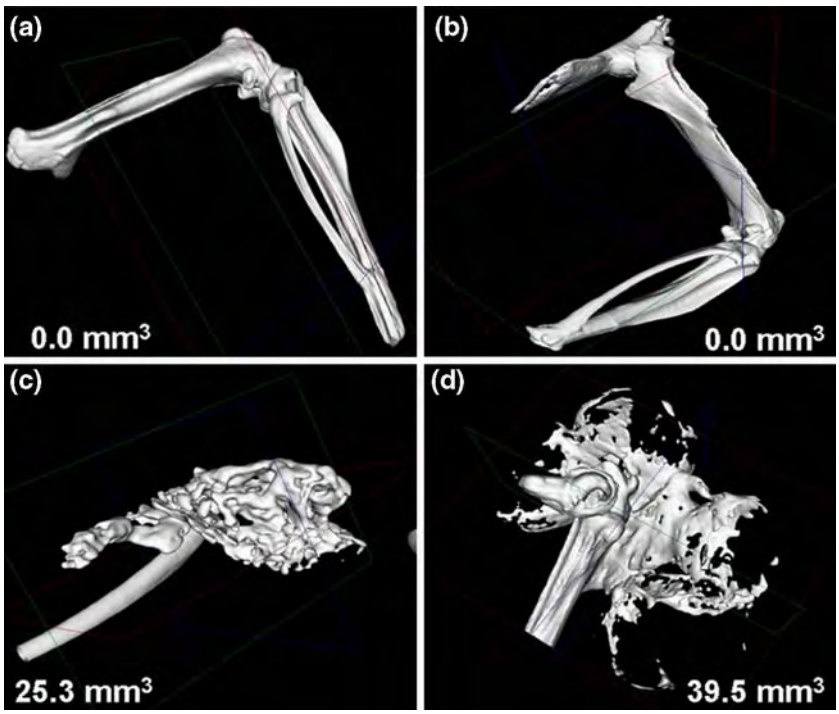

FIGURE 4. Micro-CT analysis of endochondral bone formation at 3 weeks. (a) Representative image of control 10 million MRC-5 cells transduced with HM4-1 adenovirus, (b) representative image of control PEG-DA (10 kDa) hydrogels with 10 million MRC-5 cells transduced with HM4-1 adenovirus, (c) representative image of bone formation from 10 million transduced fibroblasts expressing BMP-2 administered via intramuscular (i.m.) injection, and (d) representative image of bone formation from PEG-DA (10 kDa) constructs with 10 million transduced fibroblasts expressing BMP-2 following surgical implantation. Measurements for the femur and tibia shown in panels were not included in any of the volume calculations and the values of mineralized tissues shown in figure are only for the depicted image. Data reported as mean ± SD, $n = 6$.

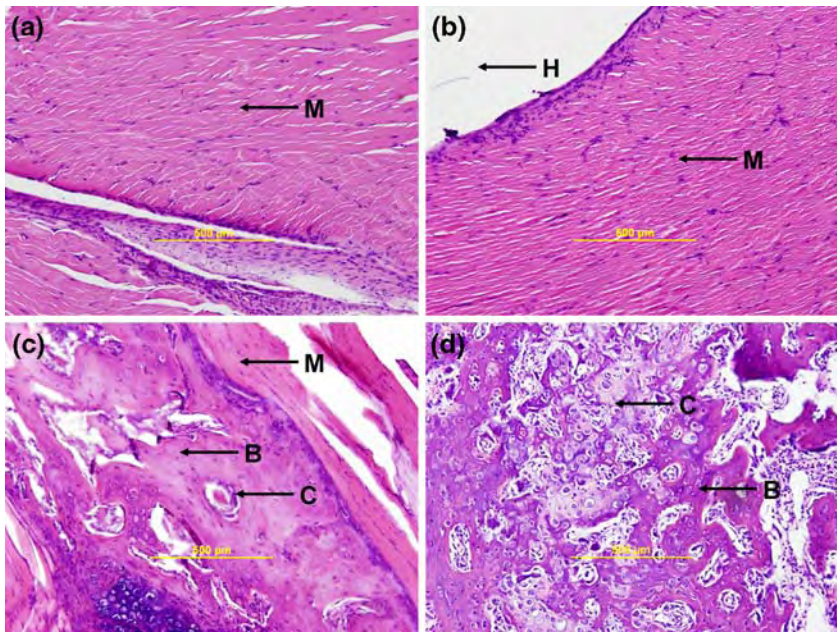

FIGURE 5. Histological evaluation of endochondral bone formation at 3 weeks. (a) 10 million MRC-5 cells transduced with HM4-1 adenovirus, (b) PEG-DA (10 kDa) hydrogels with 10 million MRC-5 cells transduced with HM4-1 adenovirus, (c) 10 million transduced fibroblasts expressing BMP-2, (d) PEG-DA (10 kDa) hydrogels with 10 million transduced fibroblasts expressing BMP-2 where M, H, B, C represents muscle, hydrogel, bone, and cartilage, respectively.

the diffusion of sufficient amounts of BMP-2 protein from the cell-seeded hydrogels to induce bone formation *in vivo*. The data from the ELISA assays suggested that cell densities within the hydrogels are very important for BMP-2 production by the transduced cells, suggesting that maybe cell–cell contact is an important consideration. Investigation of cell densities and BMP-2 production for this specific cell line on tissue culture plates of varying sizes showed that the same number of cells plated on different flasks of varying sizes produced significantly different gene expression (data not shown). Thus, even though specific cell–cell contact measurements were not made, this data suggests that cell densities for this particular cell line in a 3D polymeric network that would increase cell–cell distances may affect gene expression and hence suggest that maybe cell–cell contact is an important consideration. This observation will be further investigated in future studies. The molecular weight of the hydrogel precursor polymer also plays an important role, impacting both diffusion and mechanical properties. Prior studies have shown that the molecular weights of PEG precursors were directly proportional to the hydrogel's permeability to oligonucleotides and proteins.[43] However, even though diffusion of BMP-2 [MW 26 kDa] protein from the hydrogels may be impeded by the mesh sizes of the polymeric network, the localized encapsulation of high cell densities that constitutively express BMP-2 protein can be utilized to produce bone *in vivo*.

The compressive moduli of the PEG-DA hydrogels of varying molecular weights were determined in order to select the hydrogel with the best mechanical properties following cell encapsulation. The data showed that the compressive moduli of the PEG-DA hydrogels only decreased with increasing molecular weight, which was probably due to an increase in the molecular weight of the hydrogel crosslinks, M_c, and hence an increase in mesh size of the hydrogels resulting in a less rigid structure (Fig. 2). Subsequent encapsulation of cells resulted in a significant decrease in compressive moduli of the hydrogels, which was due to the formation of a composite material. In addition, the significant decrease in compressive modulus for the cell-encapsulated 20 kDa hydrogels in comparison with 6 and 10 kDa cell-encapsulated hydrogels was probably due to the increase in M_c (1556 ± 24 g/mol) and mesh size of (65 ± 1 Å) of these hydrogels as well as to the formation of a composite material, which resulted in very soft hydrogels. Our concern for the integrity of the cell encapsulated hydrogels following implantation into the hindlimb muscles of the animals led us to select the PEG-DA (10 kDa) hydrogels for further studies because of their better mechanical properties.

The BMP-2 protein secreted from the cell-seeded PEG-DA hydrogels was characterized with Western blot analysis, which confirmed that the mature form of the BMP-2 protein from the hydrogels was the same as the mature form of BMP-2 protein secreted from the plated transduced fibroblasts. Also, no BMP-2 protein was detected in any of the negative controls, which were not transduced with the Ad5F35BMP2 viral vector. In addition, the data from the alkaline phosphatase assay indicated that the secreted BMP-2 protein from the hydrogels was biologically active, since the media from the cultured hydrogels were able to stimulate alkaline phosphatase activity in W20-17 cells. The similar levels of alkaline phosphatase activity that was observed for the plated control as well as for the conditioned media suggested that a saturation limit at very high BMP-2 concentrations was achieved due to the sensitivity of the chemiluminescence substrate.[3]

For surgical implantation, hydrogels were formed as microbeads (Fig. 6) to allow localized deployment of BMP-2 production in complex geometries. An ELISA assay was performed with conditioned media from the microbeads, which indicated that the shape of the hydrogels could be successfully modified from large disks to small beads without any change in BMP-2 secretion (data not shown). The data from the microCT analysis, which showed the formation of bone in the muscle tissue following implantation of the PEG-DA hydrogel beads indicated that the transduced cells within the hydrogels were able to produce sufficient levels of BMP-2 protein, despite lower BMP-2

FIGURE 6. PEG-DA (10 kDa) hydrogel microbeads synthesized on surgical suture for *in vivo* implantation into NOD/SCID mice. Scale measure depicted represents mm increments.

secretion from the encapsulated cells. Therefore, the micro-CT data suggest that lower amounts of BMP-2 protein expressed over time may be adequate for bone formation. Moreover, the formation of bone that was found to be localized to the hydrogel construct suggests that this may be a unique method of spatially controlling gene expression to only a desired area. This spatial control of gene expression is extremely important for the expression of BMP-2 since uncontrolled bone formation in vital organs could lead to deleterious effects. Tantamount to this is that the formation of bone localized to the tiny hydrogel surface will be less likely to hinder the quality of bone formed within a desired area. Specifically, in spinal fusions the standard treatments are quite invasive and involves decortication of the traverse processes of the vertebrae followed by insertion of bone grafting materials either free or within cages.[33,42] In addition, the process is augmented with pedicle screw instrumentation or intervertebral joint screw-fixation, which is used to provide mechanical stability during the fusion process but in doing so occupies valuable surface area that could be utilized to enhance bone fusion.[36] Thus, the use of these tiny hydrogel constructs represents a significant improvement over the current spinal hardware, in that it utilizes much less surface area in comparison with joint screw-fixation in which placement of the hydrogels next to the defect [not within the defect] and periosteum may be sufficient to induce strong bone formation despite deposition of some bone onto the hydrogel surface. In addition, the data obtained from the stained sections of the muscle tissue corroborated the presence of bone formed in the muscle and the sections also showed the presence of cartilage in both the hydrogel-implanted animals and the animals injected with the transduced fibroblasts. Thus, the presence of cartilage in the muscles shows that bone formation may be occurring via an endochondral pathway. Moreover, the successful use of several microbead constructs in producing similar levels of mineralized tissue compared to the cell injected animals instead of one large hydrogel disk for the localization of BMP-2 protein expression suggests that smaller beads may improve the diffusion of gases and nutrients throughout the hydrogels as well as BMP-2 diffusion by decreasing the diffusional distances within the hydrogels. This observation is supported by the experimental cell viability study for hydrogel beads implanted into the hindlimb muscles of the animals in which we found that there was a higher fraction of live to dead cells retrieved from the implanted hydrogels in comparison with cultured cell encapsulated hydrogel disks. Thus, the sum of the smaller parts may be more effective than the whole and this observation can be used to improve the delivery of BMP-2 protein.

CONCLUSION

In summary, we have shown that encapsulation of adenovirus-transduced cells expressing BMP-2 within non-degradable PEG-DA hydrogel carriers can be used to spatially control the production and the release of BMP-2 protein. In addition, these PEG-DA hydrogels can facilitate the encapsulation of high cell densities that can produce sufficient amounts of BMP-2 protein to elicit bone formation *in vivo*, even though lower amounts of BMP-2 protein was detected from the hydrogel carriers in comparison to the same number of plated transduced fibroblasts. Thus, these results illustrate the benefits of localized gene therapy, which can significantly limit unwanted side effects and may have suitable applications for many orthopedic procedures such as spinal fusion.

ACKNOWLEDGEMENTS

We thank James J. Moon, Melissa K. McHale, Jessica A. Shafer and Rachel E. Whitmire for technical assistance. This work was supported by Department of Defense award W81XWH-04-1-0068.

REFERENCES

[1]Banwart, J. C., M. A. Asher, and R. S. Hassanein. Iliac crest bone graft harvest donor site morbidity. A statistical evaluation. *Spine* 20:1055–1060, 1995.

[2]Barralet, J. E., L. Wang, M. Lawson, J. T. Triffitt, P. R. Cooper, and R. M. Shelton. Comparison of bone marrow cell growth on 2D and 3D alginate hydrogels. *J. Mater. Sci. Mater. Med.* 16:515–519, 2005.

[3]Blum, J. S., R. H. Li, A. G. Mikos, and M. A. Barry. An optimized method for the chemiluminescent detection of alkaline phosphatase levels during osteodifferentiation by bone morphogenetic protein 2. *J. Cell. Biochem.* 80:532–537, 2001.

[4]Buser, D., W. Martin, and U. C. Belser. Optimizing esthetics for implant restorations in the anterior maxilla: Anatomic and surgical considerations. *Int. J. Oral Maxillofac. Implants* 19(Suppl):43–61, 2004.

[5]Canal, T. and N. A. Peppas. Correlation between mesh size and equilibrium degree of swelling of polymeric networks. *J. Biomed. Mater. Res.* 23:1183–1193, 1989.

[6]Cruise, G. M., O. D. Hegre, F. V. Lamberti, S. R. Hager, R. Hill, D. S. Scharp, and J. A. Hubbell. In vitro and in vivo performance of porcine islets encapsulated in interfacially photopolymerized poly(ethylene glycol) diacrylate membranes. *Cell Transplant.* 8:293–306, 1999.

[7]Cruise, G. M., O. D. Hegre, D. S. Scharp, and J. A. Hubbell. A sensitivity study of the key parameters in the interfacial photopolymerization of poly(ethylene glycol) diacrylate upon porcine islets. *Biotechnol. Bioeng.* 57:655–665, 1998.

[8]Cruise, G. M., D. S. Scharp, and J. A. Hubbell. Characterization of permeability and network structure of

interfacially photopolymerized poly(ethylene glycol) diacrylate hydrogels. *Biomaterials* 19:1287–1294, 1998.
[9]DeLong, S. A., J. J. Moon, and J. L. West. Covalently immobilized gradients of bFGF on hydrogel scaffolds for directed cell migration. *Biomaterials* 26:3227–3234, 2005.
[10]Ferrara J. L. and G. Yanik. Acute graft versus host disease: Pathophysiology, risk factors, and prevention strategies. *Clin. Adv. Hematol. Oncol.* 3:415–419, 428, 2005.
[11]Fini, M., A. Motta, P. Torricelli, G. Giavaresi, N. Nicoli Aldini, M. Tschon, R. Giardino, and C. Migliaresi. The healing of confined critical size cancellous defects in the presence of silk fibroin hydrogel. *Biomaterials* 26:3527–3536, 2005.
[12]Franceschi, R. T. Biological approaches to bone regeneration by gene therapy. *J. Dent. Res.* 84:1093–1103, 2005.
[13]Gafni, Y., G. Pelled, Y. Zilberman, G. Turgeman, F. Apparailly, H. Yotvat, E. Galun, Z. Gazit, C. Jorgensen, and D. Gazit. Gene therapy platform for bone regeneration using an exogenously regulated, AAV-2-based gene expression system. *Mol. Ther.* 9:587–595, 2004.
[14]Gass, M. and B. Dawson-Hughes. Preventing osteoporosis-related fractures: An overview. *Am. J. Med.* 119:S3–S11, 2006.
[15]Gugala, Z., E. A. Olmsted-Davis, F. H. Gannon, R. W. Lindsey, and A. R. Davis. Osteoinduction by ex vivo adenovirus-mediated BMP2 delivery is independent of cell type. *Gene Ther.* 10:1289–1296, 2003.
[16]Haid R. W. Jr., C. L. Branch Jr., J. T. Alexander, and J. K. Burkus. Posterior lumbar interbody fusion using recombinant human bone morphogenetic protein type 2 with cylindrical interbody cages. *Spine J.* 4:527–538; discussion 38–39, 2004.
[17]Hecht, B. P., J. S. Fischgrund, H. N. Herkowitz, L. Penman, J. M. Toth, and A. Shirkhoda. The use of recombinant human bone morphogenetic protein 2 (rhBMP-2) to promote spinal fusion in a nonhuman primate anterior interbody fusion model. *Spine* 24:629–636, 1999.
[18]Hedberg, E. L., H. C. Kroese-Deutman, C. K. Shih, R. S. Crowther, D. H. Carney, A. G. Mikos, and J. A. Jansen. Effect of varied release kinetics of the osteogenic thrombin peptide TP508 from biodegradable, polymeric scaffolds on bone formation in vivo. *J. Biomed. Mater. Res. A* 72:343–353, 2005.
[19]Hedberg, E. L., C. K. Shih, J. J. Lemoine, M. D. Timmer, M. A. Liebschner, J. A. Jansen, and A. G. Mikos. In vitro degradation of porous poly(propylene fumarate)/poly(DL-lactic-co-glycolic acid) composite scaffolds. *Biomaterials* 26:3215–3225, 2005.
[20]Hill-West, J. L., S. M. Chowdhury, M. J. Slepian, and J. A. Hubbell. Inhibition of thrombosis and intimal thickening by in situ photopolymerization of thin hydrogel barriers. *Proc. Natl. Acad. Sci. USA* 91:5967–5971, 1994.
[21]Hill-West, J. L. and J. A. Hubbell. Separation of the arterial wall from blood contact using hydrogel barriers reduces intimal thickening after balloon injury in the rat: The roles of medial and luminal factors in arterial healing. *Proc. Natl. Acad. Sci. USA* 93:13188–13193, 1996.
[22]Hill, R. S., G. M. Cruise, S. R. Hager, F. V. Lamberti, X. Yu, C. L. Garufis, Y. Yu, K. E. Mundwiler, J. F. Cole, J. A. Hubbell, O. D. Hegre, and D. W. Scharp. Immunoisolation of adult porcine islets for the treatment of diabetes mellitus. The use of photopolymerizable polyethylene glycol in the conformal coating of mass-isolated porcine islets. *Ann. N.Y. Acad. Sci.* 831:332–343, 1997.
[23]Jansen, J. A., J. W. Vehof, P. Q. Ruhe, H. Kroeze-Deutman, Y. Kuboki, H. Takita, E. L. Hedberg, and A. G. Mikos. Growth factor-loaded scaffolds for bone engineering. *J. Control Release* 101:127–136, 2005.
[24]Khan, S. N., F. P. Cammisa Jr., H. S. Sandhu, A. D. Diwan, F. P. Girardi, and J. M. Lane. The biology of bone grafting. *J. Am. Acad. Orthop. Surg.* 13:77–86, 2005.
[25]Kobayashi, T., G. Harb, R. V. Rajotte, G. S. Korbutt, A. G. Mallett, H. Arefanian, D. Mok, and G. R. Rayat. Immune mechanisms associated with the rejection of encapsulated neonatal porcine islet xenografts. *Xenotransplantation* 13:547–559, 2006.
[26]Lewandrowski, K. U., A. C. Hecht, T. F. DeLaney, P. A. Chapman, F. J. Hornicek, and F. X. Pedlow. Anterior spinal arthrodesis with structural cortical allografts and instrumentation for spine tumor surgery. *Spine* 29:1150–1158, 2004: discussion 9.
[27]Lyons, K. M., R. W. Pelton, and B. L. Hogan. Organogenesis and pattern formation in the mouse: RNA distribution patterns suggest a role for bone morphogenetic protein-2A (BMP-2A). *Development* 109:833–844, 1990.
[28]Marx, R. E.. Clinical application of bone biology to mandibular and maxillary reconstruction. *Clin. Plast. Surg.* 21:377–392, 1994.
[29]Musgrave, D. S., P. Bosch, S. Ghivizzani, P. D. Robbins, C. H. Evans, and J. Huard. Adenovirus-mediated direct gene therapy with bone morphogenetic protein-2 produces bone. *Bone* 24:541–547, 1999.
[30]Narayan, P., R. W. Haid, B. R. Subach, C. H. Comey, and G. E. Rodts. Effect of spinal disease on successful arthrodesis in lumbar pedicle screw fixation. *J. Neurosurg.* 97:277–280, 2002.
[31]Olmsted-Davis, E. A., Z. Gugala, F. H. Gannon, P. Yotnda, R. E. McAlhany, R. W. Lindsey, and A. R. Davis. Use of a chimeric adenovirus vector enhances BMP2 production and bone formation. *Hum. Gene Ther.* 13:1337–1347, 2002.
[32]Pathak, C. P., A. S. Sawhney, and J. A. Hubbell. Rapid photopolymerization of immunoprotective gels in contact with cells and tissue. *J. Am. Chem. Soc.* 114:8311–8312, 1992.
[33]Sandhu H. S. Anterior lumbar interbody fusion with osteoinductive growth factors. *Clin. Orthop. Relat. Res.* 56–60, 2000.
[34]Sawhney, A. S., C. P. Pathak, and J. A. Hubbell. Interfacial photopolymerization of poly(ethylene glycol)-based hydrogels upon alginate-poly(l-lysine) microcapsules for enhanced biocompatibility. *Biomaterials* 14:1008–1016, 1993.
[35]Sonobe, J., Y. Okubo, S. Kaihara, S. Miyatake, and K. Bessho. Osteoinduction by bone morphogenetic protein 2-expressing adenoviral vector: Application of biomaterial to mask the host immune response. *Hum. Gene Ther.* 15:659–668, 2004.
[36]Steffen, T., A. Tsantrizos, I. Fruth, and M. Aebi. Cages: Designs and concepts. *Eur. Spine J.* 9(Suppl 1):S89–S94, 2000.
[37]Sugiyama, O., D. S. An, S. P. K. Kung, B. T. Feeley, S. Gamradt, Q. L. Liu, I. S. Y. Chen, and J. R. Lieberman. Lentivirus-mediated gene transfer induces long-term transgene expression of BMP-2 in vitro and new bone formation in vivo. *Mol. Ther.* 11:390–398, 2005.
[38]Temenoff, J. S., H. Park, E. Jabbari, T. L. Sheffield, R. G. LeBaron, C. G. Ambrose, and A. G. Mikos. In vitro osteogenic differentiation of marrow stromal cells

encapsulated in biodegradable hydrogels. *J. Biomed. Mater. Res. A* 70:235–244, 2004.

[39]Thies, R. S., M. Bauduy, B. A. Ashton, L. Kurtzberg, J. M. Wozney, and V. Rosen. Recombinant human bone morphogenetic protein-2 induces osteoblastic differentiation in W-20-17 stromal cells. *Endocrinology* 130:1318–1324, 1992.

[40]Trojani, C., P. Weiss, J. F. Michiels, C. Vinatier, J. Guicheux, G. Daculsi, P. Gaudray, G. F. Carle, and N. Rochet. Three-dimensional culture and differentiation of human osteogenic cells in an injectable hydroxypropylmethylcellulose hydrogel. *Biomaterials* 26:5509–5517, 2005.

[41]Wang, E. A., V. Rosen, J. S. D'Alessandro, M. Bauduy, P. Cordes, T. Harada, D. I. Israel, R. M. Hewick, K. M. Kerns, and P. LaPan, et al... Recombinant human bone morphogenetic protein induces bone formation. *Proc. Natl. Acad. Sci. USA* 87:2220–2224, 1990.

[42]Weiner, B. K., and R. D. Fraser. Spine update lumbar interbody cages. *Spine* 23:634–640, 1998.

[43]West, J. L. and J. A. Hubbell. Photopolymerized hydrogel materials for drug delivery applications. *React. Polym.* 25:139–147, 1995.

[44]Wozney, J. M., V. Rosen, A. J. Celeste, L. M. Mitsock, M. J. Whitters, R. W. Kriz, R. M. Hewick, and E. A. Wang. Novel regulators of bone formation: Molecular clones and activities. *Science* 242:1528–1534, 1988.

[45]Xiao, Y. F., J. Y. Min, and J. P. Morgan. Immunosuppression and xenotransplantation of cells for cardiac repair. *Ann. Thorac. Surg.* 77:737–744, 2004.

[46]Yang, F., C. G. Williams, D. A. Wang, H. Lee, P. N. Manson, and J. Elisseeff. The effect of incorporating RGD adhesive peptide in polyethylene glycol diacrylate hydrogel on osteogenesis of bone marrow stromal cells. *Biomaterials* 26:5991–5998, 2005.

[47]Younger, E. M. and M. W. Chapman. Morbidity at bone graft donor sites. *J. Orthop. Trauma* 3:192–195, 1989.

[48]Zhao, M., Z. Zhao, J. T. Koh, T. Jin, and R. T. Franceschi. Combinatorial gene therapy for bone regeneration: Cooperative interactions between adenovirus vectors expressing bone morphogenetic proteins 2, 4, and 7. *J. Cell. Biochem.* 95:1–16, 2005.

[49]Zhu, W., B. A. Rawlins, O. Boachie-Adjei, E. R. Myers, J. Arimizu, E. Choi, J. R. Lieberman, R. G. Crystal, and C. Hidaka. Combined bone morphogenetic protein-2 and -7 gene transfer enhances osteoblastic differentiation and spine fusion in a rodent model. *J. Bone Miner. Res.* 19:2021–2032, 2004.

[50]Zhung, X.-Z. and R.-X. Zhuo. Synthesis and characterization of a novel thermosensitive gel with fast response. *Colloid Polym. Sci.* 277:1079–1082, 1999.

Efficient and Rapid Osteoinduction in an Immune Competent Host

CHRISTINE M. FOULETIER-DILLING[1], FRANCIS H. GANNON[1,3,4], ELIZABETH A. OLMSTED-DAVIS[1,2,3], ZAWAUNYKA LAZARD[1], MICHAEL H. HEGGENESS[3], JESSICA A. SHAFER[1,2], JOHN A. HIPP[3] and ALAN R. DAVIS[1,2,3]

[1]Center for Cell and Gene Therapy, Departments of [2]Pediatrics, [3]Orthopedic Surgery and [4]Pathology, Baylor College of Medicine, Houston, TX 77030

Running Title: Osteoinduction in an Immune Competent Host

Corresponding author: Dr. Alan R. Davis, Departments of Pediatrics, Baylor College of Medicine, Houston, TX 77030
Phone: (713) 798-1253
E-mail: ardavis@bcm.tmc.edu

ABSTRACT

Osteoinductive systems to induce targeted rapid bone formation hold clinical promise but development of technologies for clinical use that must be tested in animal models is often a difficult challenge. We previously demonstrated that implantation of human cells transduced with an Ad5F35BMP2 to express high levels of BMP2 and bone is rapidly formed at targeted sites. Inclusion of human cells in this model precluded us from testing this system in an immune competent animal model, thus limiting the information about the efficacy of this approach. Here, for the first time we demonstrate the similarity between BMP2 induced endochondral bone formation in a system using human cells in an immune incompetent mouse and a murine cell based BMP2-gene therapy system in immune competent animals. In both cases the delivery cells are rapidly cleared within five days, and in neither case do they appear to contribute to any of the structures forming in the tissues. Endochondral bone formation progressed through a highly ordered series of stages that were both morphologically and temporally indistinguishable between the two models. Even long term analysis of the heterotopic bone demonstrated similar bone volumes over and the eventual remodeling to form similar structures. The results suggest that the rapid nature of BMP2 to induce bone formation overrides contributions from either immune status or the nature of delivery cells.

OVERVIEW SUMMARY

The rapid osteoinductive nature of BMP2 makes this an ideal candidate for use in cell based gene therapy approaches, since long term expression is not required. Progression through endochondral bone formation to vascularized bone occurs even in the presence of substantial clearing of the transduced cells. In these systems the transduced cells are not required to contribute to the final bone structures, thus potential alteration of cellular function through viral transduction is not a concern. However, translation into the clinical has been slowed by difficulty in developing a human system that can be readily tested in animal models. If human cells are utilized, the choice of animal models becomes limited to immune compromised animals. Here we compared endochondral bone formation in two such gene therapy systems with consistent BMP2 expression to determine the impact varying cell type, and immune background have on efficacy.

Mary Ann Liebert, Inc., 140 Huguenot Street, New Rochelle, NY 10801

INTRODUCTION

The ability to induce bone formation via gene therapy is a desirable goal for a wide range of clinical conditions affecting the skeleton. Thus there are numerous studies seeking to develop both viral and non-viral based gene therapy systems which can introduce genes encoding osteogenic factors that can lead to rapid bone formation. These systems vary widely in the osteoinductive component employed, delivery strategies, and efficacy.

One of the best studied families of osteoinductive proteins are the bone morphogenetic proteins (BMPs). The original members of this family were identified from bone matrix by their ability to induce “de novo” bone formation in skeletal muscle (Urist *et al*, 1965; Wozney *et al*, 1988). Since the time of this original finding, recombinant BMP2 protein has been introduced into the clinic for the enhancement of spine fusion. BMP2 is often used in conjunction with, or as an alternative to, bone graft materials. However, there are difficulties with delivery of the recombinant protein. It is extremely labile and must be combined with a collagen carrier in order to maintain a high enough concentration locally to induce bone formation (Bonadio *et al*, 1999). Recent reports describe significant acute inflammation associated with this treatment, which led to detrimental side effects in many cases (Alden *et al*, 1999; Christ et *al*, 1997, Molinier-Freukel *et al*, 2002).

The use of cell and gene therapy presents an alternative strategy for BMP delivery. Several studies have attempted to directly administer the BMP2 gene via viral vectors, with limited success (Musgrave *et al*, 1999). In all cases, this

Mary Ann Liebert, Inc., 140 Huguenot Street, New Rochelle, NY 10801

system yielded little to no bone formation leaving investigators to speculate on whether additional osteoinductive components are necessary for endochondral bone formation. One of the most studied additions to this system was inclusion of an osteoprogenitor or mesenchymal stem cell as the delivery cell for the BMP2 (Lieberman 1998; Gazit *et al*, 1999; Lee *et al*, 2002; Niyibizi *et al*, 2004). However, the results of this work are somewhat conflicting, in that most studies reported no engraftment of the cells into the endochondral bone, yet, it is widely believed that the cells are necessary for coordinating bone formation.

Recently, Weiss *et al*, 2006 suggested the inclusion of vascular endothelial growth factor, in combination with the BMPs as a means of enhancing the reaction. However, our recent studies show that the transduction efficiency of the delivery cells for optimal BMP2 production is the key parameter in determining the extent of bone formation (Olmsted *et al*, 2001, Olmsted-Davis *et al*, 2002). We demonstrated that efficient transduction of cells to express BMP2 could induce rapid endochondral bone formation (Gugala *et al*, 2003) and was independent of cell type transduced. But interpretation of this work and translation into the clinic has been complicated by the fact the murine model was immune compromised, and thus may be providing a “unique” environment for the virally transduced delivery cells to survive and function. The requirement to use human cells and an immune compromised animal, comes from the restriction of the chimeric virus to human cells, with most murine cells completely lacking its receptor (Mallam *et al*, 2004; Fouletier-Dilling *et al*, 2005).

To circumvent this issue we developed a cell based gene therapy system in which autologous murine cells could be readily transduced to express BMP2 which resulted in rapid endochondral bone formation when delivered to normal mice (Fouletier-Dilling *et al*, 2005). This system employs a polyamine compound known as GeneJammer® which provides a novel entry route for the virus, thus bypassing the need for a specific receptor. We have shown this to be effective at transducing a variety of animal cells as well (Bosch *et al*, 2006).

Here we present a detailed comparison of the two gene therapy models for their ability for long term survival of the transduced cells *in vivo* for BMP2 production, to recapitulate all the stages of endochondral bone formation, and retain the newly formed bone at steady state levels, long term at a targeted location. In both approaches, we observed rapid endochondral bone formation that appears to be independent of immune background. We have demonstrated that the BMP2 production is sufficient in both systems to induce the entire endochondral bone formation cascade as a result of the injected, transduced cells. This bone production proceeds from new vessel formation with associated inflammation, to rapid cell expansion and chondrogenesis, within 4-5 days of induction. Mineralized bone formation was observed in the tissues, independent of the model, within seven days of induction. Within two weeks of the initial induction the bone formation appeared to plateau, then significantly decrease to a steady state level. Comparison of the heterotopic bones at two and four weeks suggested that it had remodeled into a well mineralized exterior with a hollow interior reminiscent of skeletal bone.

MATERIALS AND METHODS

Cell culture: Cell lines: A murine osteoblast cell line (MC3T3-E1) and a human fibroblast cell line (MRC5) were obtained from American Type Culture Collection, propagated in αMEM and DMEM media respectively. This cell is unable to induce bone formation before transduction. The cell lines were supplemented with 10% fetal bovine serum (Hyclone, Logan, UT), 100 units/ml penicillin, 100 µg/ml streptomycin, and 0.25 µg/ml amphotericin B (Life Technologies Inc., Gaithersburg, MD). A murine stromal cell line (W20-17) (a gift from Genetics Institute, Cambridge, MA) was propagated as described by Thies *et al*, 1992. Briefly, the cells were grown in DMEM supplemented as described above and cultured at a subconfluent density in order to maintain the phenotype. All cell types were grown at 37°C and 5% CO_2 in humidified air.

Transduction of cells with adenovirus in the presence of GeneJammer® Adenoviruses: Replication defective E1-E3 deleted first generation human type 5 adenovirus (Ad5) and/or modified forms in which the normal fiber protein has been substituted for the human adenovirus type 35 fiber (Ad5F35) were constructed to contain cDNAs for BMP2 in the E1 region of the virus (Olmsted *et al.*, 2001). The virus particles (vp) to plaque forming units (pfu) ratio are: 55, 76, 200 and 111 for Ad5BMP2, Ad5F35BMP2, Ad5-empty and Ad5F35HM4 respectively, and all viruses were shown to be negative for replication competent adenovirus.

Cell transduction: MC3T3 cells (1 x 10^6) were transduced with Ad5BMP2 at a virus concentration of 5000 vp/cell with 1.2% GeneJammer®. This is a critical procedure for the production of bone in the C57BL/6 mice as MC3T3 cells lack the receptor for Ad5, coxsackievirus-adenovirus receptor (CAR) and therefore GeneJammer® is used to efficiently transduce these cells (Fouletier-Dilling *et al*, 2005). The concentration used of the polyamine compound was previously determined (Fouletier-Dilling *et al*, 2005). Briefly, 15μl of GeneJammer® or PBS was added to 500μl of αMEM medium without supplements and incubated for 10 minutes at room temperature. The virus was then added at indicated concentrations and the mixture further incubated for 10 minutes at room temperature. This virus-GeneJammer® mixture was added to approximately 1 x 10^6 cells along with 750 μl of αMEM supplemented with 10% FBS and antibiotics/antimycotics. The cells were incubated at 37°C for 4 hours and then the mixture was diluted with 3 ml of fresh media containing FBS. MRC5 cells were transduced as previously described (Davis *et al*, 2000) with Ad5F35BMP2 at at virus concentration of 2500vp/cell.

Quantification of BMP2: BMP2 protein was measured in culture supernatant taken from MC3T3 cells 72 hours after transduction with varying concentrations of Ad5BMP2 in the presence of GeneJammer®. Similarly, BMP2 protein was measured in culture supernatant taken from MRC5 cells 72 hours after transduction with varying concentrations of Ad5F35BMP2. Briefly, 10^6 cells were transduced as described above and culture supernatant collected and

assayed using a Quantikine BMP2 Immunoassay from R&D Systems (DBP200, R&D Systems Inc., Minneapolis, MN).

Alkaline phosphatase assay: W20-17 cells were assayed for alkaline phosphatase activity three days after addition of either, Ad5BMP2, Ad5-empty, Ad5F35BMP2, Ad5F35HM4 or medium alone by a chemiluminescent procedure (Olmsted *et al*, 2001). Cellular alkaline phosphatase was extracted by three freeze-thaw cycles in 100 $\mu l/cm^2$ of 25 mM Tris-HCl, pH 8.0 and 0.5% Triton X-100 and the activity was then measured by addition of CSPD® Ready-to-use with Sapphire II enhancer (Tropix, Inc., Bedford, MA) to the samples. The light output from each sample was integrated for 10 seconds after a 2 second delay by the luminometer (TD-20/20, Turner Designs, Sunnyvale, CA). Alkaline phosphatase levels were recorded in relative luminescence units (RLU) and normalized to protein content with the BCA assay using bovine serum albumin to derive a standard curve. Data are presented as percent induction above unstimulated basal control cells. Statistical analysis was performed as described previously. Briefly all data were taken in triplicate and reported as mean and standard deviation. A Student's t test with 95% confidence interval ($p<0.05$) was done between the untreated control and each experimental condition.

Heterotopic bone assay: MC3T3 cells were transduced in the presence of GeneJammer® with Ad5BMP2 (5000 vp/cell) or an Ad5-empty (5000 vp/cell) which is a control adenovirus type 5 vector that lacks a transgene in the E1

deleted region. Briefly, cells were removed by trypsin, resuspended at a concentration of 5 x 10^6 cells/100 µl PBS, and then delivered through intramuscular injection into the hind limb quadriceps muscle of C57BL/6 mice (3 animals per group). MRC5 cells were transduced with Ad5F35BMP2 (2500vp/cell) or Ad5F35HM4 which is a control adenovirus lacking a transgene cassette and then injected into the hind limb quadriceps muscle of NOD/SCID mice (n=6). Animals were euthanized after injection of the transduced cells, at daily intervals for the first week, then weekly intervals (2-4 weeks) for long term studies. At appropriate times, hind limbs were harvested, and placed in formalin. All animal studies were performed in accordance with standards of the Baylor College of Medicine, Department of Comparative Medicine after review and approval of the protocol by the Institutional Animal Care and Use Committee (IACUC).

Histological analysis and staining analysis: Mouse hind limbs were formalin fixed, decalcified, divided in half longitudinally to expose the internal tissues, then both halves of the tissue embedded into a single paraffin block. The tissues were oriented so that the internal areas were exposed to the outside of the paraffin block, allowing for the tissue to be sectioned from the inside out. Serial sections (5 µm) were prepared that encompassed the whole hind limb reactive site (approximately 10-15 sections per tissue specimen depending on the type of transduced cells the tissue received). The reactive area within the tissues was consistently larger in samples undergoing bone formation than in adjacent control

tissues. We then performed Hematoxylin and Eosin staining on every 5th slide to locate the center region containing either our delivery cells or the newly forming endochondral bone. Once this site was located, serial unstained slides were used for immunohistochemical staining. All tissue images reported in this manuscript were within the central region of the reaction, and representative of the other sections found in the tissues. Immunohistochemistry was performed with a Homo-Mouse™ Poly-HRP IHC detection kit (ImmunoVision Technologies, Daly City, CA), according to the manufacturer's instructions for the following antibodies: Hexon antibody (Clontech Laboratories, catalogue number S3049) and human mitochondria (Chemicon International catalogue number MAB 1273). All sections were analyzed with light microscopy.

Micro-computed tomography (CT): Specimens isolated at 2, 3, and 4 weeks were scanned with a micro-CT system (Explore Locus SP, General Electric, London, Ontario) at 14 μ resolution. Bone density was determined with a density calibration phantom. Three-dimensional reconstructions of the region injected with BMP2 producing cells were generated to identify regions of heterotopic ossification. The volume of heterotopic mineralized tissue was then calculated with the use of the quantitative bone analysis software provided with the micro-CT system. For this analysis, any tissue with a density greater than 0.26 g/cc of hydroxyapatite was considered mineralized tissue. The total volume of heterotopic mineralized tissue was measured for the right and left hind limb, and

the difference in values between the C57BL/6 and the NOD/SCID mice was assessed by standard *t*-test analysis.

Mary Ann Liebert, Inc., 140 Huguenot Street, New Rochelle, NY 10801

RESULTS

BMP2 expression and activity

For comparison, the two cell-based gene therapy systems were evaluated for their ability to secrete BMP2, so that in future analysis both systems would be producing equivalent amounts of BMP2. Thus, BMP2 expression was measured by quantifying the amount of protein secreted into the culture supernatant after transduction of the cells with the respective adenoviruses at varying multiplicity of infections (MOIs). Culture supernatants were collected 72 hours after initial transduction and BMP2 was quantified by an enzyme-linked immunosorbent assay (ELISA). MOIs were adjusted so that the expression level of BMP2 between the MC3T3 cells transduced by Ad5BMP2 and MRC5 cells transduced by Ad5F35BMP2 were the same (Figure 1A). Based on these findings, all other subsequent studies were done using these doses so as to have comparable expression of BMP2.

We next determined the functional activity of BMP2 protein using a W20-17 cell-based assay (Thies *et al*, 1992) which measures the induction of alkaline phosphatase in response to active BMP2. In this assay, the murine bone marrow cell line W20-17 was exposed to culture supernatant from the MC3T3 cells or MRC5 cells that had been transduced respectively with Ad5BMP2 at a concentration of 5000vp/cell or Ad5F35BMP2 at a concentration of 2500vp/cell. Culture supernatants from MC3T3 and MRC5 cells transduced with control viruses were also included to verify that the W20-17 response was specific to BMP2. Cell lysates were assayed for alkaline phosphatase activity approximately

three days after addition of the tentative BMP2 containing supernatant. In all cases in which cells were transduced with AdBMP2 viruses, the cells secreted active BMP2, with no significant differences (*p* value is 0.6985) (Figure 1B), whereas supernatants from cells transduced with control viruses did not induce alkaline phosphatase activity.

Delivery cells are not longer present by day 6

With establishment of the transduction criteria essential for each system to make equivalent active BMP2, these transduced cells were then tested for their engraftment potential in the corresponding mouse models. The Ad5BMP2 model was developed to efficiently transduce the C57BL/6 autologous cells for induction of bone in an immune competent setting (Fouletier-Dilling *et al*, 2005), we next measured the engraftment of these cells into the site of bone formation and compared this to the Ad5F35BMP2 transduced human cells delivered to immune incompetent NOD/SCID mice. Even though the MC3T3 cells are considered to be “osteoblastic”, no bone formation was ever observed using non-transduced cells or those cells transduced with control vector. Since both cell types possess adenovirus antigens as a result of the transduction using first-generation adenoviral vectors, we were interested in determining if the human cells would have similar survival rates in NOD/SCID mice which lack the lymphocytic arm of the immune system, as compared to the cells delivered to wild type mice.

The cells were tracked by two different systems. In the NOD/SCID (immune incompetent) model, the human cells were detected by immunohistochemical staining for the expression of a protein specific to human mitochondria. We observed positive staining for the human cells in tissues isolated from 1-5 days after induction (Figure 2A), but were completely absent by day 6 after their initial injection into the muscle. In the C57BL/6 (immune competent) model, we looked for the expression of the hexon protein, the largest and most abundant of the structural proteins in the icosahedral adenoviral capsid, by immunohistochemistry as a means of locating the transduced cells. As seen in Figure 2B, transduced cells were still present at day 6 after induction, but had not engrafted into any of tissue structures associated with the newly forming bone. Although the original report that first generation adenovirus vectors elicted production of virus neutralizing antibodies against capsid antigens was presented over a decade ago (Yang *et al*, 1996), the study presented here directly shows the production of a capsid viral antigen *in vivo.* By 7 days post-induction, the transduced cells were completely absent in all tissue sections encompassing the reaction site. These results demonstrate that the transduced cells are cleared prior to bone formation. However, in all cases the cells did not appear to be associated with any of the newly forming cartilage and bone. Interestingly, the cells were cleared at the same rate in both systems, seemingly independent of the immune status of the animal.

Stage by stage comparison of bone formation in immune-competent and immune-deficient

We have recently characterized through immunohistochemical phenotyping and cell tracking, the initial stages of endochondral bone formation in the NOD/SCID model (Olmsted-Davis *et al*, 2007; Shafer *et al*, 2007). These stages are extremely reproducible and include the appearance of brown adipocytes on days 1-2, new vessels on days 3-4, cartilage on days 4-6, and bone on days 6-8. These previous studies have linked the early mesenchymal precursors for chondrocytes and osteoblasts to be of a myelo-monocytic origin (Shafer *et al*, 2007).

Here we compared these stages of endochondral bone formation between the two mouse models given that both systems are capable of producing equivalent functional BMP2, as well as with control mice that received cells transduced with an empty cassette vector. The emphasis is to detect any differences in the progression of endochondral bone formation including temporal changes that may be resulting from the difference in immunological backgrounds of the animals. Figure 3 shows resultant photomicrographs from the immune-competent model (C57BL/6), the immune-incompetent model (NOD/SCID) and the control section at days 2, 4, 6 and 7. The images are representative of the reaction within the tissues for each of the days. As can be seen in Figure 3, day 2, the sections look similar with both the delivery cells and visible inflammation present in the tissues regardless of whether the cells were expressing BMP2. However, by four days after the initial injection, the experimental sections for both

models no longer match the control sections. The tissues receiving the cells transduced to express BMP2, showed a significant increase in the number of cells within the tissues. Our previous studies have shown these to be a myelo-monocytic precursor both migrating into the tissues as well as proliferating, to form the new cartilage (Shafer *et al*, 2007). Alternatively, the inflammatory response is essentially gone by day 4 in the control sections. Both the transduced cells as well as the host-derived cells are greatly reduced in volume compared to the previous days (see Figure 3) and these results confirm earlier data showing the disappearance of the delivery cells in both systems (Figure 2). The cartilage is well established and similar in the experimental sections in both models at day 6, however the control section demonstrates a complete absence of both inflammatory cells and the injected cells. By day 7 newly formed bone is observed in both models that received the BMP2 transduced cells, suggesting that the presence of a complete immune system did not reduce the rapid nature of the endochondral bone formation previously reported in the immune competent model.

Long term bone expression

While the endochondral bone formation during the first 7 days was histologically similar in both systems, we wanted to compare long term bone formation, and/or retention. Figure 4 represents the Hematoxylin and Eosin stained photomicrographs taken of tissues isolated from the immune-incompetent model (NOD/SCID) and immune-competent (C57BL/6) 2 weeks, 3

weeks and 4 weeks after injection of the BMP2 producing cells. The histological analysis of the sections are dramatically different from a 2 week time point to the 4 week time point but remains similar between the two systems. As expected the bone appears to be remodeling into a more hollow structure, but surprisingly, a large amount of fat cells are appearing over time in the central compartment or presumptive marrow cavity of this tissue.

Microcomputed tomographic analysis was performed on tissues (*n*=6) isolated 2, 3 and 4 weeks after induction of bone formation to compare total bone volume between the two model systems (Figure 5A). The results show similar bone volume at all time periods with no significant difference between the two systems, however there was a significant decrease in the overall bone volume in both systems when samples were compared temporally (Figure 5A). The bone volume peaked at two weeks and decreased significantly by 4 weeks in both models (Figure 5A). Heterotopic bone is apparent in all samples, regardless of the model. Three dimensional reconstruction of heterotopic bone from representative NOD/SCID and C57BL/6 (Figure 5B) tissue samples are shown. Two dimensional cross-sectional analysis of the three dimensional reconstruction show thicker bone that is less well mineralized in both NOD/SCID and C57BL/6 at two weeks which becomes much thinner and more well mineralized by four weeks. This change in overall bone volume may reflect both the remodeling of the presumptive marrow cavity as well as the lack of weight bearing forces on the heterotopic bone.

DISCUSSION

The study presented here provides a detailed comparison between two different gene therapy models to produce rapid bone formation at a directed site. Both systems employ the efficient but transient expression of BMP2 through a cell based gene therapy approach, and appears to produce localized bone capable of remodeling into a mature structure. Interestingly, both the immune compromised (NOD/SCID) and an immune competent (C57BL/6) models yielded identical temporal, morphologic and volumetric measurements of the bone formation. In all cases transient expression of BMP2 within the tissues led to rapid endochondral bone formation in which mineralized bone was detected by 7 days after induction.

Previous studies delivering BMP2 through a cell based gene therapy approach in which the cells were transduced with first generation adenoviral vectors demonstrated bone formation only in immune compromised animals (Alden *et al*, 1999). Similar results were observed by Okubo *et al*, 2000 and Sonobe *et al*, 2002 who observed endochondral bone formation only in immunosuppressed rats but not in immune-competent animals. In more recent studies, Sonobe *et al* 2004, used collagen as a biomaterial to mask the host immune response and suggested this was a requirement for bone formation in immune-competent animals. In other studies investigators attempted to mask severe inflammatory responses by inclusion of immunosuppressant's such as FK506 or Cyclosporin A (Kaihara *et al*, 2004; Okubo *et al*, 2000).

Here we compare endochondral bone formation in both immune compromised and immune competent mice and demonstrate the equivalent nature of these systems. Our data suggests that immunogenicity and clearance of the adenovirus transduced cells does not interfere with the osteoinductive nature of BMP2. Using set parameters to obtain equivalent functional BMP2 production in the two systems, we injected the MRC5 into the NOD/SCID animals and the MC3T3 cells into the C57BL/6 mice. We then compared the temporal formation of bone and morphologic features in the two different models. The bone formation was essentially the same in each of the models.

Thus this cell based BMP2 gene therapy system has several unique properties which set it apart from other cell and gene therapies. First, long-term expression of the transgene is not a requirement, as evidenced by the significant endochondral bone formation, even with rapid clearing of the BMP2 transduced delivery cells. The ability of BMP2 to induce endochondral bone formation through a trigger-type mechanism has also been demonstrated by others (Koh *et al*, 2006). This property provides significant advantages over other gene therapy targets which require long term persistence of the transgene and have limited ability for readministration. Even the helper dependent adenovirus with its lessened immunogenicity has not solved the problem (Koehler *et al*, 2003).

Another issue in these gene therapy systems is the fate of the cells used to introduce the BMP2 into the local micro-environment. In our cell-based gene therapy systems, the adenovirus transduced cells serve only to produce BMP2 and are not part of the bone that is created, which is derived entirely from the

host. Thus the adenovirus transduction and eventual clearing does not affect the final bone production. We demonstrate here that the transduced cells completely cleared within 7 days of injection regardless of whether the mouse has a complete immune system. These findings are consistent with recent studies by Dragoo *et al*, 2005 in which the authors found that inclusion of stem cells isolated from human adipose tissues as delivery cells for the BMP2, did not contribute to the newly forming bone. Similarly, Engstrand *et al*, 2000 have demonstrated that delivery of retrovirally transduced W20-17 cells led to significant bone formation but that the transduced cells themselves were rapidly cleared last less than one week postimplantation.

Alternatively others developing cell based gene therapy approaches in different models have found that the cells do contribute to the newly forming bone. Lee *et al*, in 2001, demonstrated that muscle-derived cells and the bone marrow stromal cells could still contribute to the newly forming bone even though they functioned as delivery cells. Moutsatsos *et al*, 2001 used the C3H10T1/2 mesenchymal stem cell line engineered to express high levels of BMP2 protein and showed that these cells were able to contribute both to the bone healing, beyond recruitment of host derived cells. Perhaps the lack of viral transduction of these cells aided in their ability to undergo osteogenesis and contributes to bone. Recently Gamradt *et al*, 2006 suggested that mesenchymal stem cells transduced with first generation adenovirus vectors could also contribute to the newly forming bone as functional osteoblasts. Interestingly, in these studies, the authors tagged the BMP2 with a Myc epitope thus the authors tracked the

secreted BMP2 rather than the delivery cells themselves. Although the cells were delivered in a collagen sponge that perhaps protected the delivery cells to some extent, the authors could demonstrate the presence of the tagged BMP2 protein up to 2 weeks after delivery. It is unclear whether the tag may have stabilized the protein or whether in their system the delivery cells actually undergo osteogenesis.

However, here we present data that demonstrates the ability of BMP2 to rapidly form bone without requiring a specific delivery cell. Thus the choice of delivery cells can be based on other factors than those associated with bone formation. This finding greatly enhances the versatility of the system, in that one can select a cell type based on manufacturing properties as well as versatility to the general population. The ability to develop a single qualified cell type that could be used universally in the population would greatly reduce the cost and time associated with this therapy, thus allowing for more widespread applications.

ACKNOWLEDGMENTS

This work was funded in part by the Army Grant DAMD W81XWH-04-1-0068 and by the National Institutes of Health Grant 5RO1 EB005173-02

REFERENCES

ALDEN T.D., PITTMAN D.D, HANKINS G.R, BERES E.J, ENGH J.A, DAS S, HUDSON S.B, KERNS K.M, KALLMES D.F, and HELM G.A. (1999). In vivo endochondral bone formation using a bone morphogenic protein 2 adenoviral vector. Human Gene Therapy. **10**:2245-2253.

BONADIO, J., SMILEY, E., PATIL, P., and GOLDSTEIN, S. (1999). Localized, direct plasmid gene delivery in vivo: prolonged therapy results in reproducible tissue regeneration. Nat. Med. **5**, 753-759.

BOSCH, P., FOULETIER-DILLING, C., OLMSTED-DAVIS, E.A., DAVIS, A.R., and STICE, S.L. (2006). Efficient adenoviral-mediated gene delivery into porcine mesenchymal stem cells. Mol.Reprod. Dev. **73**, 1393-1403.

CHRIST, M., LUSKY, M., STOECKEL, F., DREYER, D., DIETERLE, A., MICHOU, A.I., PAVIRANI, A., and MEHTALI, M. (1997). Gene therapy with recombinant adenovirus vectors: evaluation of the host immune response. Immunol.Lett. **57**, 19-25.

DAVIS, A.R., WIVEL, N.A., PALLADINO, J.T., TAO, L., and WILSON, J.M. (2000). Construction of adenoviral vectors. Methods Mol.Bio. **135**,1219-1230.

DRAGOO, J.L., LIEBERMAN, J.R., LEE, R.S., DEUGARTE, D.A., LEE, Y., ZUK, P.A., HEDRICK, M.H., and BENHAIM., P. (2005). Tissue-engineered bone from BMP2-transduced stem cells derived from human fat. Plastic Reconstr. Surg. **115**, 1665-1673.

ENGSTRAND, T., DALUISKI, A., BAHAMONDE, M.E., MELHUS, H., and LYONS, K.M. (2000). Transient production of bone morphogenetic protein 2 by allogeneic transplanted transduced cells induces bone formation. Hum. Gene Thera. **11**, 205-211.

FOULETIER-DILLING, C.M., BOSCH, P., DAVIS, A.R., SHAFER, J.A., STICE, S.L., GUGALA, Z., GANNON, F.H., and OLMSTED-DAVIS, E.A. (2005). Novel compound enables high-level adenovirus transduction in the absence of an adenovirus specific receptor. Hum.Gene Thera. **16**, 1287-1297.

GAMRADT, S.C., ABE, N., BHAMONDE, M.E., LEE, Y-P., NELSON, S.D., LYONS, K.M., and LIBERMAN, J.R. (2006). Tracking expression of virally mediated BMP2 in gene therapy for bone repair. Clinical Orthop. and Related Res. **450**, 238-245.

GAZIT, D., TURGEMAN, G., KELLEY, P., WANG, E., JALENAK, M., ZILBERMAN, Y., and MOUTSATSOS, I. (1999). Engineered pluripotent mesenchymal cells integrate and differentiate in regenerating bone: a novel cell-mediated gene therapy. The journal of Gene Med. **1**, 121-133.

GUGALA, Z., OLMSTED-DAVIS, E.A., GANNON, F.H., LINDSEY, R.W., and DAVIS, A.R. (2003). Osteoinduction by ex-vivo adenovirus-mediated BMP2 delivery is independent of cell type. Gene Ther. **10**, 1289-1296.

KAIHARA, S., BESSHO, K., OKUBO, Y., SONOBE, J., KAWAI, M., and IIZUKA, T. (2004). Simple and effective osteoinduction gene therapy by local injection of a bone morphogenetic protein-2 expressing recombinant adenoviral vector and FK506 mixture in rats. Gene Ther. **11**, 439-447.

KOEHLER, D.R., SAJJAN, U., CHOW, Y.H., MARTIN, B., KENT, G., TRANSWELL, A.K., McKERLIE, C., FORSTNER, J.F., and HU, J. (2003). Protection of Cftr knockout mice from acute lung infection by a helper-dependent adenoviral vector expressing Cftr in airway epithelia. Proc. Natl. Acad. Sci. USA. **100**, 15364-15369

KOH, J.T, GE, C., ZHAO, M., WANG, Z., KREBSBACH, P.H., ZHAO, Z., and FRANCESCHI, R.T. (2006). Use of a stringent dimerizer-regulated gene expression system for controlled BMP2 delivery. Mol.Thera. **14**, 684-691

LEE, J.Y., MUSGRAVE, D., PELINKOVIC, D., FUKUSHIMA, K., CUMMINS, J., USAS, A., ROBBINS, P., FU, F.H., and HUARD, J. (2001). Effect of bone morphogenetic protein-2 expressing muscle-derived cells on healing of critical-sized bone defects in mice. J. of Bone and Joint Surg. **83**, 1032-1039.

LEE, J.Y., PENG, H., USAS, A., MUSGRAVE, D., CUMMINS, J., PELINKOVIC, D., JANKOWSKI, R., ZIRAN, B., ROBBINS, P., and HUARD, J. (2002). Enhancement of bone healing based on ex-vivo gene therapy using human muscle-derived cells expressing bone morphogenetic protein 2. Hum. Gene Ther. **13**, 1201-1211.

LIBERMAN, J.R., LE, L.Q., WU, L., FINERMAN, G.A., BERK, A., WITTE, O.N., and STEVENSON, S. (1998). Regional gene therapy with a BMP-2-producing murine stromal cell line induces heterotopic and orthotopic bone formation in rodents. J. Orthop.Res. **16**, 330-339.

MALLAM, J.N., HURWITZ, M.Y., MAHONEY, T., CHEVEZ-BARRIOS, P., and HURWITZ, R.L. (2004). Efficient gene transfer into retinal cells using adenoviral vectors: dependence on receptor expression. Invest. Ophthalmol. Vis. Sci. **45**, 1680-1687.

MOLINIER-FRENKEL, V., LENGAGNE, R., GADEN, F., HONG, S.S., CHOPPIN, J., GAHERY-SEGARD, H., BOULANGER, P., and GUILLET, J.G. (2002). Adenovirus hexon protein is a potent adjuvant for activation of a cellular immune response. J. Virology **76**, 127-135.

MOUTSATSOS, I.K., TURGEMAN, G., ZHOU, S., KURKALLI, B.G., PELLED, G., TZUR, L., KELLEY, P., STUMM, N., MI, S., MULLER, R., ZILBERMAN, Y.,

and GAZIT, D. (2001). Exogenously regulated stem cell-mediated gene therapy for bone regeneration. Mol.Therap. **3**, 449-451.

MUSGRAVE, D.S., BOSCH, P., GHIVIZZANI, P.D., ROBBINS, P.D., EVANS, C.H., and HUARD, J. (1999). Adenovirus-mediated direct gene therapy with bone morphogenic protein-2 produces bone. Bone **24**, 541-547.

NIYIBIZI, C., WANG, S., MI, Z., and ROBBINS, P.D. (2004). The fate of mesenchymal stem cells transplanted into immunocompetent neonatal mice: implications for skeletal gene therapy via stem cells. Mol.Ther. **9**, 955-963.

OKUBO, Y., BESSHO, K., FUJIMURA, K., IIZUKA, T., and MIYATAKE, S. (2000). Osteoinduction by bone morphogenetic protein-2 via adenoviral vector under transient immunosuppression. Biochem. Biophys. Res. Commun. **267**, 382-387.

OLMSTED, E.A., BLUM, J.S., RILL, D., YOTNDA, P., GUGALA, Z., LINDSEY, R.W., and DAVIS, A.R. (2001). Adenovirus-mediated BMP2 expression in human bone marrow stromal cells. J. Cell Biochem. **82**, 11-21.

OLMSTED-DAVIS, E.A., GUGALA, Z., GANNON, F.H., YOTNDA, P., MCALHANY, R.E., LINDSEY, R.W., and DAVIS, A.R. (2002). Use of a chimeric adenovirus vector enhances BMP2 production and bone formation. Hum. Gene Thera. **13**, 1337-1347.

OLMSTED-DAVIS, E.A., GANNON, F.H., OZEN, M., ITTMANN, M.M., GUGALA, Z., HIPP, J.A., MORAN, K.M., FOULETIER-DILLING, C.M., SCHUMARA-MARTIN, S., LINDSEY, R.W., HEGGENESS, M. H., BRENNER, M.K., and DAVIS, A.R. (2007). Hypoxic adipocytes pattern early heterotopic bone formation. American Journal of Pathology **170,** 1-13.

SHAFER, J., DAVIS, A.R., GANNON, F.H., FOULETIER-DILLING, C.M., LAZARD, Z., MORAN, K., GUGALA, Z., OZEN, M., ITTMANN, M., HEGGENESS, M. H., and OLMSTED-DAVIS, E.A. (2007). Oxygen Tension Directs Chondrogenic Differentiation of Myelo-Monocytic (In Press)

SONOBE, J., BESSHO, K., KAIHARA, S., OKUBO, Y., and IIZUKA, T. (2002). Bone induction by BMP2 expressing adenoviral vector in rats under treatment with FK506. J. of Musculoskeletal Res. **6**, 23-29.

SONOBE, J., OKUBO, Y., KAIHARA, S., MIYATAKE, S., and BESSHO, K. (2004). Osteoinduction by bone morphogenetic protein 2-expressiong adenoviral vector: Application of biomaterial to mask the host immune response. Hum. Gene Thera. **15**, 659-668.

THIES, R.S., BAUDUY, M., ASHTON, B.A., KURTZBERG, L., WOZNEY, J.M., and ROSEN, V. (1992). Recombinant human bone morphogenetic protein-2 induces osteoblastic differentiation in W-20-17 stromal cells. Endocrinology **130**, 1318-1324.

URIST, M.R. (1965). Bone: Formation by autoinduction. Science **150**, 893-899.

WEISS, K.R., COOPER, G.M., JADLOWIEC, J.A., McGOUGH, R.L., and HUARD, J. (2006). VEGF and BMP expression in mouse osteosarcoma cells. Clin. Orthop. Relat. Res. **450,**111-117.

WOZNEY, J.M., ROSEN, V., CELESTE, A.J., MITSOCK, L.M., WHITTERS, M.J., KRIZ, R., HEWICK, R., and WANG, E.A. (1988). Novel regulators of bone formation: molecular clones and activities. Science **242**, 1528-1534.

YANG, Y., HAECKER, S.E., SU, Q., and WILSON, J.M. (1996). Immunology of gene therapy with adenoviral vectors in mouse skeletal muscle. Hum. Mol. Genet. **5**, 1703-1712.

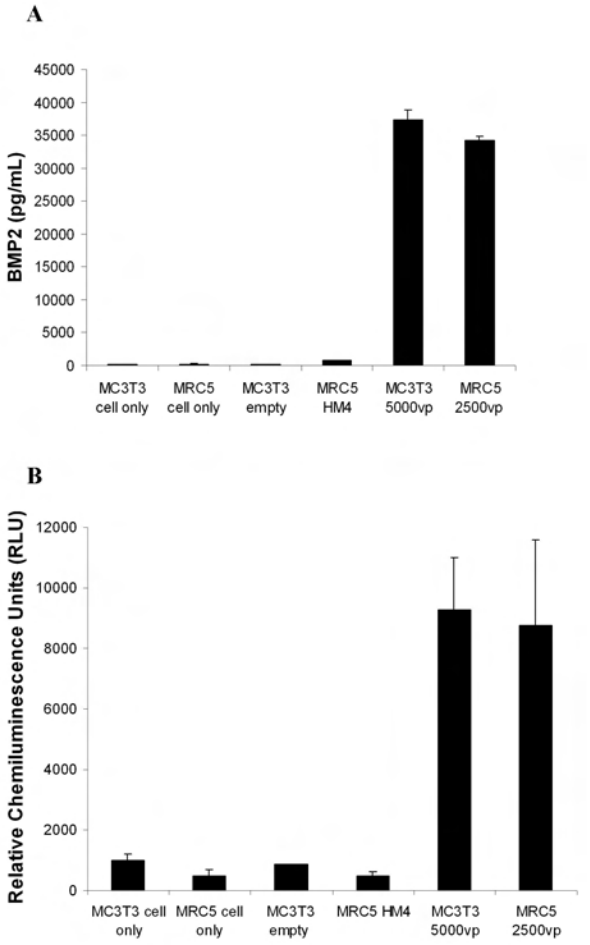
A
BMP2 (pg/mL)
45000
40000
35000
30000
25000
20000
15000
10000
5000
0
MC3T3 cell only
MRC5 cell only
MC3T3 empty
MRC5 HM4
MC3T3 5000vp
MRC5 2500vp
B
Relative Chemiluminescence Units (RLU)
12000
10000
8000
6000
4000
2000
0
MC3T3 cell only
MRC5 cell only
MC3T3 empty
MRC5 HM4
MC3T3 5000vp
MRC5 2500vp

Figure 1

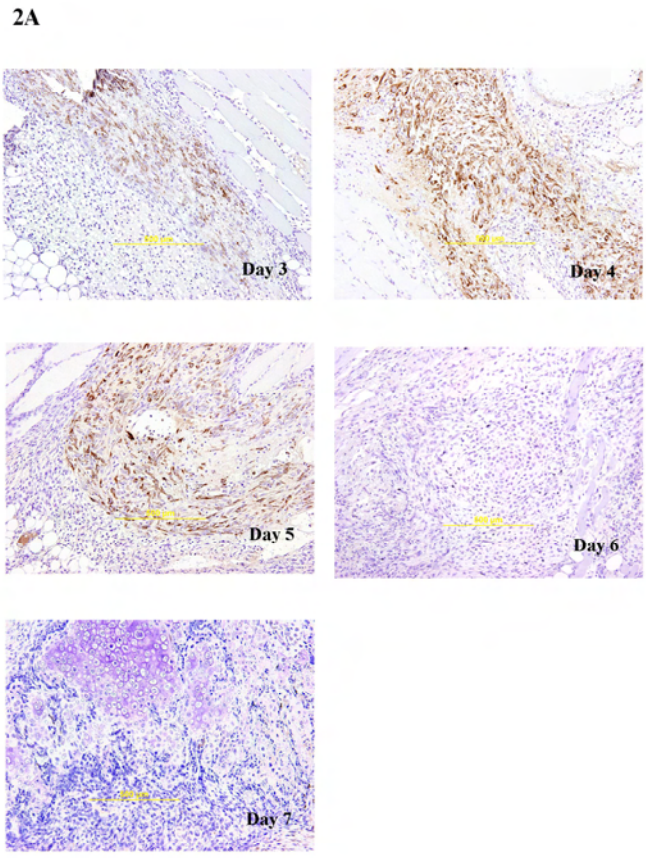
2A
Day 3
Day 4
Day 5
Day 6
Day 7

2B

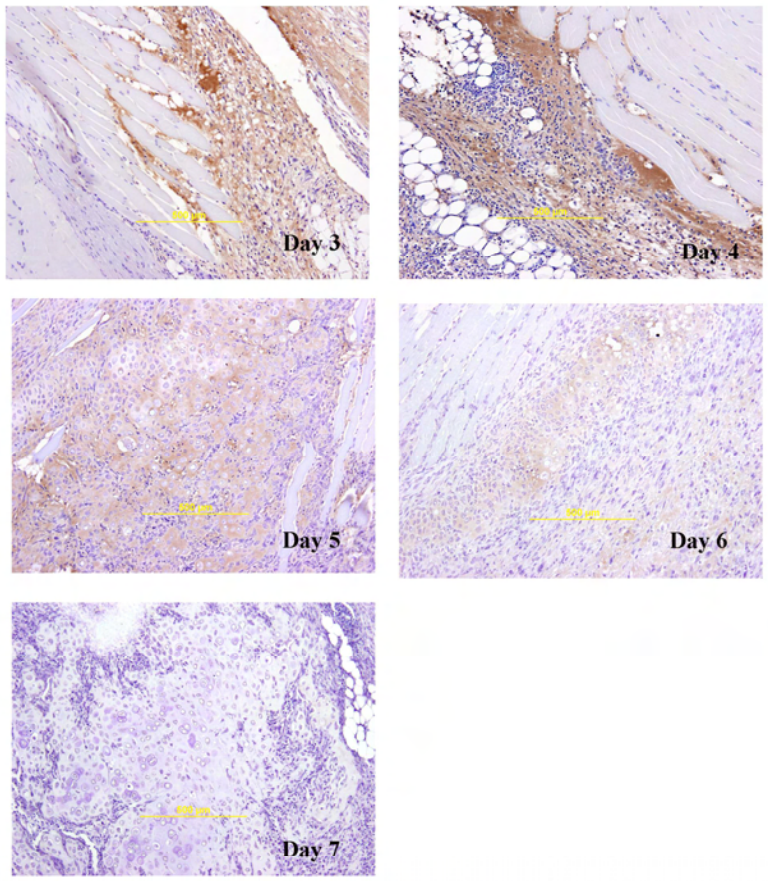

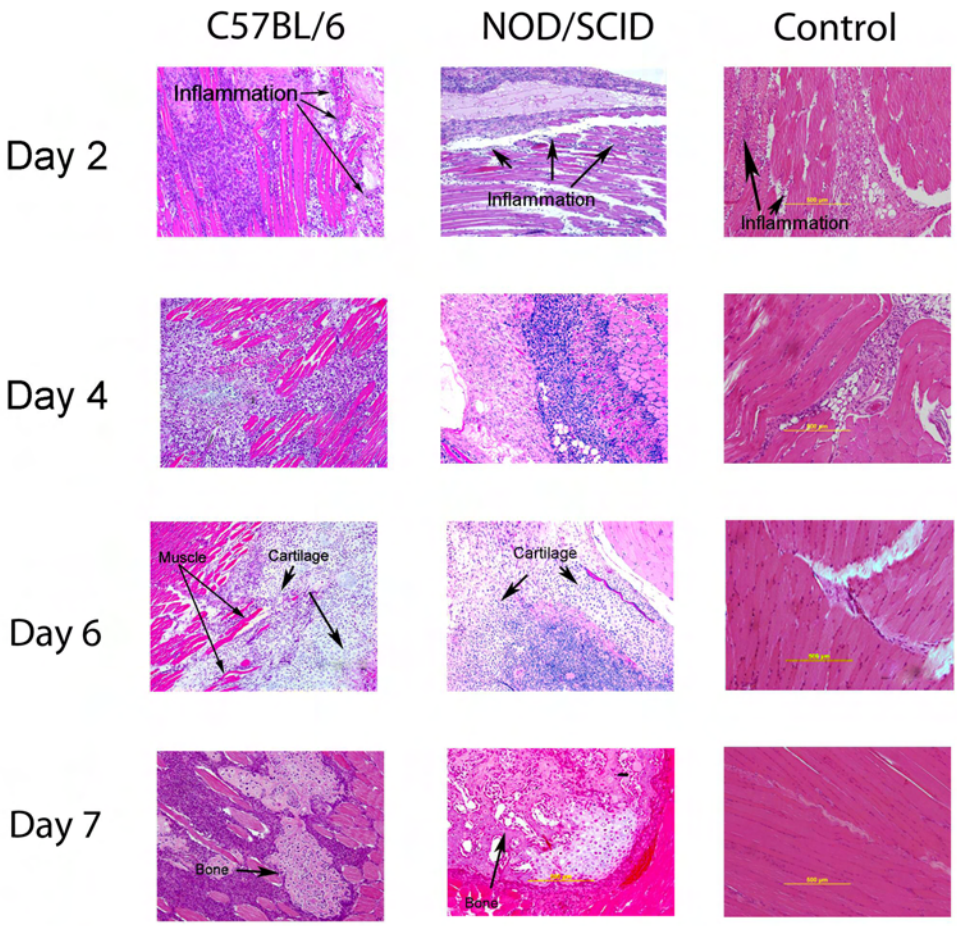
C57BL/6
NOD/SCID
Control
Day 2
Inflammation
Inflammation
Inflammation
Day 4
Day 6
Muscle
Cartilage
Cartilage
Day 7
Bone
Bone

Figure 3

Figure 4

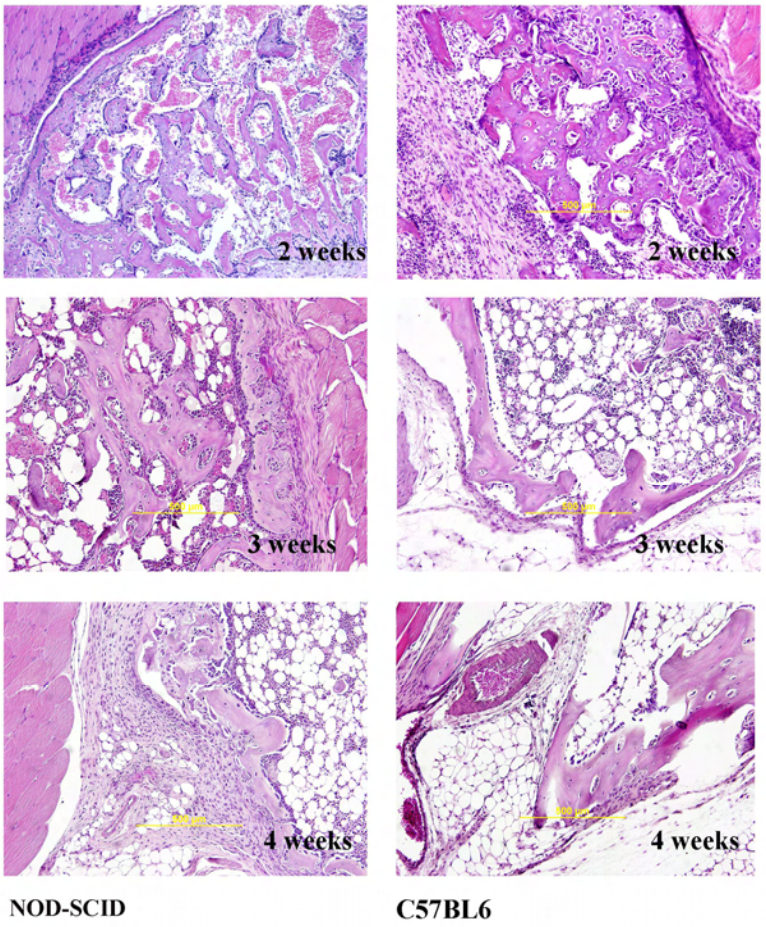

5A

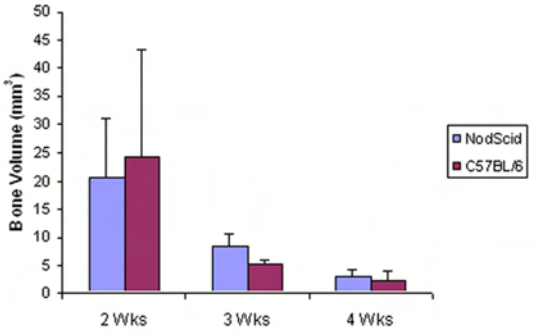
Bone Volume (mm³)
50
45
40
35
30
25
20
15
10
5
0
2 Wks
3 Wks
4 Wks
NodScid
C57BL/6

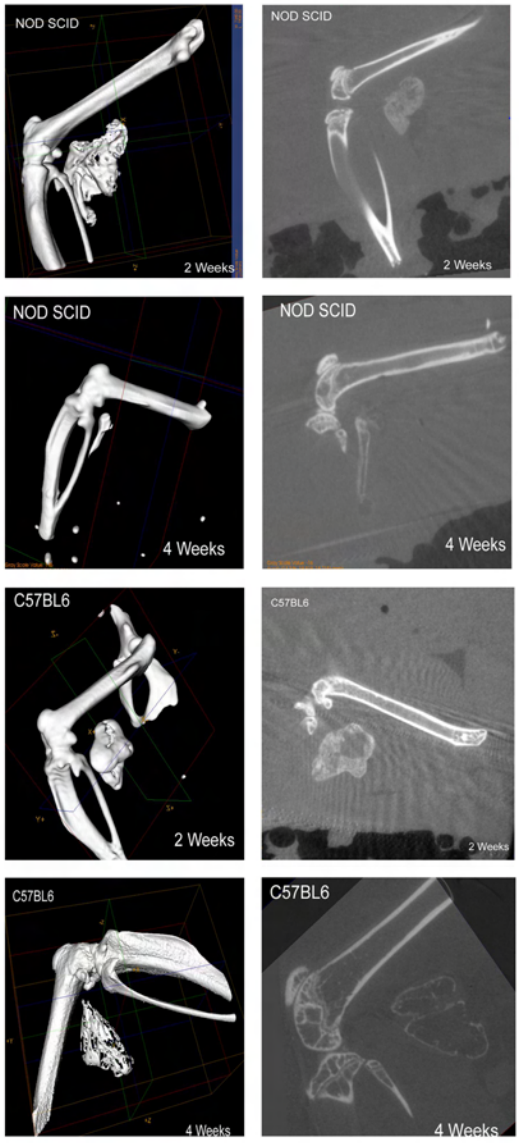
NOD SCID
2 Weeks
NOD SCID
2 Weeks
NOD SCID
4 Weeks
NOD SCID
4 Weeks
C57BL6
2 Weeks
C57BL6
2 Weeks
C57BL6
4 Weeks
C57BL6
4 Weeks

5B

Figure 1: Quantification of BMP2 *in vitro* (**A**) and activity of BMP2 (**B**). **(A)** The quantity of BMP2 was measured in culture supernatant taken from MC3T3 cells transduced with Ad5BMP2 (5000vp/cell) and MRC5 cells transduced with Ad5F35BMP2 (2500vp/cell) using the Quantikine assay (R&D systems). The concentration of BMP2 was extrapolated from a standard curve based on known concentrations of recombinant BMP2. BMP2 concentrations in the supernatant are reported as picograms per milliliter, $n = 3$. $p>0.5$ (Student t test). **(B)** BMP2 activity was measured in culture supernatant taken from MC3T3 cells transduced with Ad5BMP2 (5000vp/cell) and MRC5 cells transduced with Ad5F35BMP2 (2500vp/cell) by determining the increase in alkaline phosphatase activity in W20-17 cells 72h after exposure. Alkaline phosphatase activity is depicted as average relative chemiluminescence units (RLU), where $n=3$. Columns and error bars represent means $\pm$ standard deviation, respectively, for $n=3$ experiments $p>0.5$ (Student t test).

Figure 2: Immunohistochemistry for human mitochondria **(A)** and hexon **(B)** proteins. **(A)** Staining for human mitochondria on NOD/SCID sections from day 3 to 7 demonstrates positivity within the transduced cells from days 3-5 while the sections from days 6-7 are negative indicating absence of the delivery cells. **(B)** Low power photomicrographs of slides stained for hexon taken from days 3-7. Positivity is noted within the transduced cells from days 3 to 5 while the sections from day 6 are weakly positive and day 7 is negative indicating the absence of the delivery cells. (Immunohistochemistry, magnification 40.5X)

Figure 3: Photomicrographs from the first week in both experimental (NOD/SCID and C57Bl/6) and control animals. Day 2, an inflammatory infiltrate is observed in both experimental and control animals; Day 4 the experimental sections for both models no longer match the control sections. The experimental sections showed a significant increase in the number of cells within the tissues while cell numbers appear greatly reduced in volume in the control section; Days 6-7 show an orderly maturation of the cartilage component with progression to bone in both experimental sections while cell numbers in the control section steadily decline.
(Hematoxylin and Eosin, 10.5X)

Figure 4: Long term analysis of bone formation (2-4 weeks)
NOD/SCID sections (left column) demonstrates well-formed bone with osteoblastic and osteoclastic activity that results in a presumptive marrow cavity by 4 weeks (bottom left image). C57/BL6 sections (right column) follow an identical patterning and remodeling that also results in a presumptive marrow cavity. (Hematoxylin and Eosin, magnification 100X)

Figure 5: Micro CT analysis of long term bone formation

Graphical representation of the heterotopic bone volumes measured by MicroCT **(A)**. The bone volumes in both systems remain relatively similar and both systems show a significant decrease in overall bone volume from 2 to 4 weeks. **(B)**Three dimensional and two dimensional reconstructions MicroCT image of the bone formed at 2 weeks and 4 weeks by post injection with BMP2 in NOD/SCID and C57BL6/ animals.

Oxygen Tension Directs Chondrogenic Differentiation of Myelo-Monocytic Progenitors During Endochondral Bone Formation

Jessica Shafer[b*], Alan R. Davis[a, b, c*], Francis H. Gannon[c,d], Christine M. Fouletier-Dilling[a], ZaWaunyka Lazard[a], Kevin Moran[c], Zbigniew Gugala[e], Mustafa Ozen[d], Michael Ittmann[d], Michael H. Heggeness[c], and Elizabeth Olmsted-Davis[a, b, c]

[a]Center for Cell and Gene Therapy, Departments of [b]Pediatrics, [c]Orthopedic Surgery, and [d]Pathology, Baylor College of Medicine, Houston, TX 77030; [e]Department of Rehabilitation and Orthopedic Surgery, University of Texas Medical Branch, Galveston TX 77555

Correspondence: Elizabeth A. Olmsted-Davis, One Baylor Plaza, BCMN505, Houston TX 77030, USA. Telephone: 713-798-1253; Fax: 713-798-1230; e-mail: edavis@bcm.tmc.edu

*Both authors contributed equally to this work

Key words: monocytes, vascular smooth muscle cells, chondrogenesis, endochondral bone formation, hypoxia

Abstract: Synthesis of bone requires both essential progenitors to form the various structures and the correct microenvironment for their differentiation. To identify these factors we have utilized a system which exploits bone morphogenetic protein's ability to rapidly induce endochondral bone formation. One of the earliest events observed was the influx and proliferation of fibroblastic cells that express both vascular smooth muscle cell markers, smooth muscle α actin (SMA), smooth muscle myosin heavy chain (SMMHC) as well as the monocytic marker CD68. The expression of these factors was lost by days 4-5, coincident with the upregulation of *Sox9* and the appearance of chondrocytes. Studies with a Cre/lox system, in which a myeloid-specific promoter driving Cre recombinase, can irreversibly unblock expression of β-galactosidase only in cells of myeloid origin, showed specific activity in the newly formed chondrocytes. These results suggest that early chondrocyte progenitors are of myeloid origin. Simultaneous with this recruitment we determined that a numbers of these cells were in a hypoxic state, indicative of low oxygen environment. The cells in the hypoxic regions were undergoing chondrogenesis, whereas cells in adjacent normoxic regions appeared to be assembling into new vessels, suggesting the oxygen microenvironment is critical for establishment of the cartilage.

INTRODUCTION

Bone tissue engineering holds great promise for the repair of nonunion fractures and large segmental defects (1). Yet, the bone tissues that have been generated to date typically fail in their applications because they are not properly perfused and are mainly compromised of mature osteoblasts, thus they are incapable of engrafting and providing any true regenerative functions (1). Ideally, one would like to produce well vascularized, structurally sound, implantable bone that contains marrow with pluripotent repopulating stem cells that would efficiently engraft into the skeletal bone. However, assembling such a complex structure is a significant engineering challenge.

Bone morphogenetic protein 2 (BMP 2) was identified more than a decade ago, for its ability to elicit bone formation at heterotopic sites (2) (3) (4). Since this initial finding, BMP2 has been shown to be involved in limb patterning and development of the embryonic skeleton (5). Further BMP2 contributes to the developing vasculature (for review see (6)) and plays a key a role in neuronal differentiation (for reviews see (7) and (8)). The data suggests that this factor is capable of inducing a number of different phenotypes in the developing embryo.

This protein has also been shown to function as a potent differentiation factor capable of inducing both osteogenesis and chondrogenesis in adult mesenchymal progenitors (for review see (9)). Interestingly, in one study, the phenotypic determinant was not BMP2, although it was essential for these processes, but rather the oxygen microenvironment (10).

The data collectively suggest that in a specific microenvironment, BMP2 is capable of inducing the differentiation of progenitors to form several of the tissues associated with endochondral bone. Thus we exploited a model of rapid *de novo* bone formation previously developed in the laboratory (11) (12), to identify the early

progenitors and to define the relationship between phenotypic fate and the oxygen microenviroment.

MATERIALS AND METHODS

Transduction of cells for BMP2 production: MRC-5 or MC3T3E-1 cells were purchased from American Type Culture Collection (Manassas, VA) and maintained according to their specifications. Adenoviruses were propagated and transductions performed as previously described (14). Briefly, MRC-5 cells were transduced at a multiplicity of 2500 virus particles per cell (vp/cell) with either Ad5F35BMP2 or Ad5F35HM4. For transduction of MC3T3E-1 cells, Ad5BMP2 or Ad5Empty (5000 vp/cell) was adsorbed in 1.2% GeneJammer® Transfection Reagent (Stratagene, La Jolla, CA) as previously described (13). The particle to PFU ratio for Ad5BMP2 and Ad5Empty was and respectively. The virus particles (vp) to plaque forming units (pfu) ratio are: 55, 76, 200 and 111 for Ad5BMP2, Ad5F35BMP2, Ad5-empty and Ad5F35HM4 respectively, and all viruses were shown to be negative for replication competent adenovirus.

Characterization of myeloid-restricted β-galactosidase expression:

LysM-Cre mice were then bred to R26R mice (Jackson Laboratory, Bar Harbor, Maine) and resulting heterozygous offspring LysM-Cre/R26R were analyzed for myeloid restricted β-galactosidase activity. Both peripheral blood leukocytes, and whole bone marrow were stained using the Mouse Lineage Panel (BD Biosciences, San Diego, CA) followed by strepavidin-PE for detection. Analysis of β-galactosidase activity in hematopoietic cells was performed as previously reported (15). Results showed β-galactosidase activity in monocytes and granulocytes (7.6% and 5.6%, respectively); it

was virtually absent in lymphocyte populations (0.25% T cells and 1.8% B cells). The monocyte-specific expression of β-galactosidase activity observed was as expected and in agreement with the original report of Clausen *et al* (16).

Injections: Virus-transduced cells were removed by trypsin, washed, and resuspended at a concentration of 5 x 10^6 cells per 100 µl PBS, 50 ul of which was injected into the hind limb quadriceps muscle of the mice (2 animals per group). At specified testing intervals, the animals were euthanized, the hind limbs were removed, and the muscle tissue was fixed in 10% neutral buffered formalin. For studies using the LysM-Cre/R26R, the C57BL/6 derived cell line MC3T3-E1 was transduced with Ad5BMP2 or Ad5empty and used to induce bone formation. In studies performed using NOD/SCID mice, we used the human fibroblast line MRC-5 which was transduced with either Ad5F35BMP2 or Ad5F35HM4.

Detection of hypoxia: Oxygen gradients in muscle tissue were measured with the Hypoxyprobe™-1 Kit (Chemicon) according to the manufacturer's directions. Briefly, 4 groups of mice (n=2 each) were injected with cells transduced to express BMP2, as described above. On days 2, 3, 4 and 5 after injection of BMP2-producing cells, a group received Hypoxyprobe™-1 at a dose of 60 mg/kg body weight approximately 2 hours before isolation of the tissues. The extracted tissues were placed immediately into cold formalin and processed later as described below. Hypoxyprobe™-1 protein adducts were detected in hypoxic cells with a monoclonal antibody to Hypoxyprobe™-1.

Detection of β-galactosidase activity in tissues: Muscle tissue surrounding the injection site was excised and quick frozen, for sectioning with a cryostat (Shandon-Thermo, Walden Maine). Tissue sections (3-5 µm each) were then fixed for 15 min in

0.5% glutaraldehyde in PBS, washed in PBS, and then moved to staining media that contained 1 mg/ml X-gal as described (17) for two hours.

Histology: Decalcified, paraffin-embedded (5 µm) sections of hind limb quadriceps muscle were deparaffinized in xylene, rehydrated, and treated for 5 minutes with 0.3% triton X 100, and then incubated for 10 minutes at 37°C with Digest-All-1 (Zymed Laboratories, San Francisco, CA), followed by a 15 minute treatment with Peroxide Block (Innogenex, San Ramon, CA). At each step, sections were washed with PBS containing 0.05% Tween 20. For routine histology, sections were stained with hematoxylin and eosin.

Immunohistochemistry: The type of procedure used for immunohistochemistry varied with the antibody used. All incubations were performed at room temperature. For mouse monoclonal and rabbit polyclonal antibodies, a PowerVision Homo-Mouse IHC kit (ImmunoVision Technologies, Daly City, CA) was used according to the manufacturer's instructions. For goat polyclonal antibodies, sections were treated after peroxide blocking with 1.5% horse serum in Tris- buffered saline (TBS) for 30 minutes followed by incubation with primary antibody. After washing, the sections were treated with horse anti-goat biotinylated secondary antibody in 1.5% horse serum in TBS for 30 minutes, followed by a 10 minute incubation with avidin-HRP and 2-10 minute incubation with DAB (Vectorlabs, Burlingame, CA). In double antibody labeling experiments, sections were incubated simultaneously with both primary antibodies, making certain that they were from rabbit and mouse. An antibody against mouse IgG conjugated to Alex fluor 488 and one against rabbit IgG conjugated to Alexa fluor 647 were used for detection. The primary antibodies were anti-alpha smooth muscle actin (Sigma), anti-VWF (Chemicon), anti-smooth muscle myosin heavy chain (Biomedical Technologies), anti-

Sox9 (Santa Cruz Biotechnology, Inc, Santa Cruz, CA), anti-CD68 (Serotec, Raleigh, NC), anti-β-galactosidase antibody (Abcam, Cambridge, MA) and anti-Ki-67 (Dako).

Microscopy and imaging: For bright-field imaging, tissue sections were counterstained with hematoxylin, dehydrated through a graded series of ethanol and cleared with NeoClear (EM Science, Gibbstown, NJ,). For fluorescence imaging, sections were mounted with a SlowFade Anti-fade kit (Molecular Probes, Eugene, OR) and counter-stained with DAPI. Slides were viewed with an Olympus BX41 microscope equipped with a reflected fluorescence system and a DP70 digital camera with DPcontroller/manager software.

RESULTS

BMP2 Induced Endochondral Bone Formation:

Tissues containing the site of BMP2 induced bone formation were isolated daily over 7 days. The observed histologic stages leading to bone formation (Fig. 1, n=10) were reproducible, with putative host derived progenitors rapidly appearing within the tissues within 3-4 days after injection of BMP2-producing cells (Fig. 1A). This happens almost simultaneously with the appearance and assembly of new vessels within the region (Fig 1B). This observation was confirmed by the appeance of replicating endothelial cells, a hallmark of new vessel formation (18) (Fig 1C). Cartilage is first observed 5 days after induction with BMP2 (not shown) and mineralized bone, which had not yet formed marrow, by 7 days (Fig 1D). Marrow formation is observed in 14 days (not shown).

We did not observe contribution of our transduced delivery cells, as determined by staining for adenovirus hexon (Figure 1A) to any of the structures at any phase of bone formation and have previously demonstrated that these cells are rapidly cleared

from the tissue in as little as 5 days (12) (Dilling in preparation). Thus their only contribution to bone formation appears to be production of the BMP2 (12).

Origin of tentative progenitors:

Previous reports have suggested that chondrocytic progenitors possess several vascular smooth muscle cell markers (19),(20) (21) and may be an early vascular smooth muscle cell (22) (23). We chose to determine if these cells were rapidly expanding vascular smooth muscle cells. Using an antibody against smooth muscle alpha actin (SMA, green), a protein associated with vascular smooth muscle cells, and one against Ki-67 (red) as markers for proliferation, we tested this prediction in tissue collected on days 2, 3, 4, and 5 after injection of BMP2-producing cells. VSMCs were present in the tissue on days 2, 3 and 4 as determined by SMA positivity (green), and the majority of these cells were replicating (yellow) (Figs. 2A-C). By day 5, which marks the first appearance of cartilage in our model, the VSMC replication was complete (Fig. 2D); although some of the cells were still replicating (red), none expressed SMA.

Although the data suggest that these progenitors may be of vascular smooth muscle cell origin, these cells did not possess markers of vascular smooth muscle cell progenitors (data not shown), thus we questioned whether these cells could be more similar to a progenitor population described in the literature which possessed both myeliod and vascular cell markers (24), (25). Kuwana and colleagues (26) had previously demonstrated the presence of a myelo-mesenchymal progenitor capable of forming chondrocytes. Thus we next chose to determine if these host-derived progenitors were of myelo-monocytic origin. We immunostained muscle sections (DAPI, Fig. 3A) for SMA (green, Fig. 3B) and CD68, (red, Fig.3C) a myeloid specific marker, in tissues isolated 4 days after induction of bone formation. The results demonstrate a significant overlapping expression of these two markers, with simultaneous loss of both

markers during chondrogenesis (Fig.3A). These results suggest a monocytic origin for the $CD68^+$ SMA^+ progenitors. Interestingly, fully differentiated SMA^+ VSMCs surrounding established vessels within the tissues did not stain positively for CD68 (data not shown).

To further determine the chondrogenic potential of these myelomonocytic progenitors *in vivo* we relied on the Cre/*loxP* DNA recombination system (27) (28) (29) (30) which conditionally targets monocyte and granulocytes. The *LysM* locus in mice is exclusively active in hematopoietic cells of the myelomonocytic lineage, being expressed moderately in committed myeloid progenitors, and highly in mature macrophages and neutrophils (16). Thus, mice possessing myeloid specific β-galactosidase activity were injected with either Ad5BMP2- or Ad5empty-transduced cells and tissues isolated 5 days after the initial injection. We also performed these experiments in the R26R mouse strain, as a negative control for the β-galactosidase analysis. Frozen tissues were sectioned and stained for β-galactosidase activity. As can be seen in Fig. 4C, significant positive staining (blue color) was observed in cells at the site of new cartilage formation. The R26R control tissues completely lacked β-galactosidase activity altogether (Fig. 4D). To further confirm this finding, we immunostained similar tissues that had been formalin fixed and paraffin embedded, using an anti-β-galactosidase antibody. The results in Figure 4A-B show positive staining (brown color) for β-galactosidase activity in cells in both the tentative perichondrium and newly forming cartilage. These results suggest that chondrocytes are derived from a myelomonocytic progenitor.

Differentiation of chondrocytes:

Tissue analysis after immunostaining with the VSMC phenotypic markers demonstrated a unique pattern in the later stages of ossification (days 4-6), during which

time cartilage is beginning to form. On day 5, cells possessing the characteristic morphology of chondrocytes were readily apparent (Fig. 5A, B) together with newly formed cartilage (Alcian blue stain). Although the monocytic progenitors and chondrocytes formed distinct populations, higher-power images (Fig. 5B) revealed what appeared to be SMA^+ cells that were assuming a more rounded appearance and showed variable loss of SMA expression (Fig. 5B, brown color), suggesting that chondrocytic differentiation follows a loss of SMA expression. Analysis of serial sections from these day-5 tissues showed a similar pattern of SMMHC (Fig. 5C, brown color) and SMA (Fig. 5D) expression, with loss occurring in cells that appeared to be undergoing chondrogenesis coincident with the expression of *Sox9* (31) (32) (Fig. 5E).

Oxygen state within the muscle and newly formed vessels and cartilage

We observed a consistent cellular architecture within the day-5 tissues in which newly forming vessels were observed adjacent to the perichondrium. As shown in Figure 6A, endothelial cells (brown) appeared to be localized adjacent to the monocytic progenitors but opposite the newly formed cartilage. Since chondrogenic differentiation of stem cells has been shown to require low oxygen levels (33) we hypothesized that the oxygen state within localized regions of the target tissue may be inducing the monocytic progenitors to begin chondrogenesis. This idea is consistent with a recent report by Robins *et al* ,(34) which demonstrated the transcriptional activation of *Sox9* in mesenchymal stem cells after exposure to hypoxic conditions. To test this prediction, we measured hypoxia in the tissue sections using a system that was designed to detect protein adducts of reductively activated pimonidazole,(35) a characteristic product of hypoxic cells. As can be seen in Figure 6B,C, chondrocytes were clearly hypoxic (brown staining), while tissues bordering the perichondrium containing the new vessels retained normal oxygen tension (Fig. 6B). Animals injected with the empty control vector,

Ad5F35HM4, showed no staining for hypoxia (Fig. 6D). Together, these findings suggest that local oxygen tension may direct the differentiation of monocytic progenitors to become either chondrocytes in low oxygen or assemble into new vessels in regions of normoxia.

DISCUSSION

Using a murine model of endochondral bone formation, we have attempted to identify the origin and phenotype of the progenitors that form the cartilage with emphasis on potential environmental cues that may direct their differentiation to the chondrogenic lineage. We chose to study this process using a model of *de novo* bone formation, based on the unique ability of BMP2 to induce all stages of endochondral bone formation (36). In our model, human fibroblasts are transduced to express and deliver bone morphogenetic protein 2 (BMP2) into the quadriceps muscle of NOD/SCID mice (11) (12) (13). Detailed analysis of the cellular and tissue changes near the injection site suggests that delivery of the BMP2 expressing cells can within hours recruit progenitors of myeloid origin from the circulation to this area for the establishment of cartilage and bone.

The model used in our studies is one of heterotopic ossification, however, since BMPs are incorporated into bone matrix (37), it may resemble normal bone repair where an initial injury leads to release of the stored BMP, followed by an inflammatory process at the site of injury and fracture hematoma. However, without critical dissection and comparison of these two processes, we cannot draw any conclusions about the physiological nature of our model. Rather, here we utilized the rapid nature of the bone formation to identify potential progenitors, and key factors involved in their differentiation. In this model, complex oxygen gradients can be readily established, and multiple progenitors either recruited or expanded, at a level of complexity not easily reproduced

ex vivo. Thus it provides us with a system to study the capacity of various progenitors to form the structures of cartilage and bone, and uncover micro-environmental factors that are essential to this process. By identification of the differentiation capacity and appropriate environmental cues to induce these progenitors to undergo chondrogenesis, we can begin to harness their potential for tissue engineering.

Although much evidence exists demonstrating the presence of a mesenchymal stem cell capable of undergoing differentiation to either the cartilage or bone lineage (33) (38) the origin of this cell has led to significant controversy with evidence being presented for muscle satellite cells (39), bone marrow stem cells (15) (40), as well as other types of stem cells (41) . Certainly bone marrow-derived cells have been show to differentiate into cartilage (33), however, little was known about their phenotype. In studies by Demer et al (23), vascular smooth muscle progenitors were shown to be capable of expressing several proteins associated with functional chondrocytes. Additionally, in studies by El-Maadawy *et al*,(19) using mice lacking matrix Gla protein the authors showed the differentiation of a progenitor expressing SMA and SMMHC to chondrocytes in the arteries. However, it is unclear whether these findings are general or specific to the vascular environment. Here we present evidence, in a different model, of a similar chondrocyte progenitor possessing the same vascular smooth muscle cell markers. Within 3 days after induction of bone formation by BMP2, the majority of host cells infiltrating the muscle fibers and actively proliferating expressed SMA as well as SMMHC. Interestingly, we also observe simultaneous new vessel formation, suggesting that these processes may in some way be linked.

However, we extended this knowledge by identifying key markers which are not expressed on vascular smooth muscle cells. Here we demonstrate the presence of the monocytic marker CD68 on these progenitors, which is not found on fully differentiated vascular smooth muscle cells found associated with vessels (data not shown). Jabs *et*

al (42) isolated a population of progenitors that co-expressed both SMA and the monocyte/macrophage marker CD68 (ED-1) (43) from tissues undergoing repair which had associated inflammation. Interestingly, pericytes have been similarly described (44), in that they are specialized vascular smooth muscle cells that often migrate away from vessels for tissue repair and the differentiation of peripheral blood mononuclear cells to fibroblasts has been previously observed(45).

We further confirmed the myeloid origin of these cells, by using a cre/lox system designed to determine if indeed the differentiated target originated from a such a progenitor. In these experiments, mice expressed cre recombinase using the *LysM* gene promoter, which is exclusively active in hematopoietic cells of the myelomonocytic lineage, being expressed moderately in committed myeloid progenitors, and highly in mature macrophages and neutrophils (16). These mice also possessed a *LacZ* gene which is silenced by an intervening DNA sequence flanked by lox P sites that separates the promoter from the transcriptional start site. Thus only cells of myeloid origin that express cre recombinase will have the intervening sequence removed, and β-galactosidase activity. Further, since this involves a DNA rearrangement, once β-galactosidase is active it cannot be terminated upon differentiation of the cells. The results clearly demonstrate that the chondrocytic progenitor is of myeloid origin. This finding suggests a tentative mechanism for the recruitment of stem cells for repair of damaged tissues. However, Cunningham *et al*, (46) demonstrated more than a decade ago, the ability of BMP2 to function as a chemoattractant for monocytes. Thus BMP2 may play a role in both recruitment and differentiation of these cells.

Although no one has previously demonstrated a myeloid origin for chondrocytes, there is much evidence that supports the existence of a mesenchymal progenitor which possesses monocytic markers (45) (47) (48). Recently, Camargo *et al*, demonstrated a similar myelomonocytic population of cells was capable of specifically recruiting and

contributing to muscle repair. In these studies the authors also use the LysM Cre/R26R murine model except they induced muscle injury rather than bone formation (47). The authors suggested this population may be mesenchymal stem cells.

The stimulus that triggers these progenitors to selectively differentiate to chondrocytes is not entirely clear, but may involve a shift in oxygen tension. This hypothesis is supported by several studies demonstrating that mesenchymal stem cells can be induced to differentiate in environments of low oxygen tension.(33, 49) Indeed, both progenitors in the tentative perichondrial region and newly forming $Sox9^{+}$ chondrocytes were in a hypoxic state, while the monocytic progenitors bordering the tentative perichondrium, and surrounding the newly forming vessels were normoxic (Fig 6). Thus, the hypoxic cellular response in progenitors most distal to the endothelial cells could induce chondrocytic differentiation, while the newly assembled vessels would restore normoxia to the tissues, thus defining the border of cartilage. The close proximity of new vessel formation to the boundaries of chondrocyte maturation perhaps implicates a coupling of these two processes. If correct, this model of monocyte differentiation (Fig 7) would suggest a novel regulatory role for oxygen tension in patterning the newly forming cartilage.

It is has been suggested that pericytes or VSMCs not associated with vessels may also be derived from myelo-monocytic precursors and perhaps function as vascular progenitors in angiogenesis (44) (50). It is intriguing to speculate that these progenitors in the presence of low oxygen and BMP2 undergo chondrogenic differentiation, but when exposed to factors expressed by replicating endothelial cells (i.e. VEGFs), and normoxia terminally differentiate to mature VSMCs (Figure 7). Thus the microenvironment could effectively dictate the terminal phenotypic fate of these cells, and thus elegantly coordinate the replacement or repair of complex organs such as bone, in an adult organism. The identification of this novel stem cell population, and the

critical role that the microenvironment plays in its differentation state is the first step in being able to recruit, expand and potentially harness its potential for tissue engineering.

ACKNOWLEDGEMENTS

We wish to thank John Gilbert for critical reading of the manuscript as well as Malcolm Brenner for helpful discussion and suggestions. We wish to thank Eleanor Davis for her help labeling slides. This work was supported by grants from the Department of Defense to ARD and EAO-D and in part by a grant from The Methodist Hospital (MH).

LEGENDS TO FIGURES

Figure 1. Events occuring after injection of BMP2-producing cells Sections prepared from tissue taken on days 1-7 days were analyzed . (A) Sections were stained with an antibody against adenovirus hexon; black arrows, hexon positive and red arrows, hexon negative cells (B) Representative tissue section taken 4 days after induction with BMP2; the first appearance of tentative “new” vessels leaking red blood cells (arrows). H & E stain. (C) A section ,3 days post-injection, was stained with an antibody against VWF (green color), and simultaneously stained with an antibody against Ki-67 (red color). Yellow cells (arrows) are replicating endothelial cells. (D). Heterotopic bone (B) and cartilage (C) formed 7 days after injection with the BMP2-producing cells.

Figure 2. Replication of VSMCs after injection of BMP2-producing cells. Sections were prepared from tissue obtained (A) 2 days (B) 3 days, (C) 4 days, and (D) 5 days postinjection of cells. Sections were stained with an antibody against SMA (green) and simultaneously stained with an antibody against Ki-67 (red). Yellow cells (arrows) are replicating VSMCs.

Figure 3. Co-expression of monocytic and vascular markers on the putative chondro-progenitor cells. Tissue sections were taken from animals 5 days after injection of BMP2-producing cells. Sections were stained with an antibody against CD-68 (ED-1), (red color, B) and simultaneously stained with an antibody against SMA (green color, C). DAPI (A) stains all cells in the section.

Figure 4. Myelomonocytic cells are precursors to chondrocytes. Bone formation was induced and tissues isolated from both LysM-Cre/RXR26 (n=4) and R26R (n=4) mice 5 days after injection of cells transduced with either Ad5BMP2 of Ad5HM4. The myelomonocytic marker â-galactosidase was detected by immunostaining with an anti-â-galactosidase antibody (brown color) in the LysM-Cre/R26R but completely absent in the R26R parental strain (A and B, respectively). In addition frozen sections from either LysM-Cre/R26R or R26R mice (C and D, respectively) were assayed for â-galactosidase enzymatic activity.

Figure 5. Chondrogenesis during “de novo” bone formation. (A, B) Sections taken at 5 days postinjection of BMP2 were stained with an antibody against SMA and counterstained with Alcian blue as well as hematoxylin. Four-day serial sections were also stained with antibodies against SMA (C, brown color), SMMHC (D, brown color), and Sox9 (E, brown color).

Figure 6. Areas of hypoxia in the chondrogeneic phase of *de novo* bone formation. Tissue sections were isolated from mice 5 days after induction with Ad5F35BMP2-transduced cells. Two hours prior to harvesting the tissues, the mice were injected with pimonidazole for the detection of hypoxia. (A) Section stained with an antibody against VWF (brown color), arrows denote discrete

areas of chondrogenesis and vessel formation. (B and C) Sections stained with Hypoxyprobe™-1Mab1, which specifically reacts with the pimonidazole after it is bound in hypoxic cells. Positive cells are brown. (D) Control animals. Sections were counterstained with hematoxylin.

Figure 7. Potenial model for monocytic involvement in bone and vessel formation. A myelomonocytic cell $CD68^+$ SMA^+ differentiates to either a pre-chondrocyte (Sox 9^+) or vascular smooth muscle cell depending upon the oxygen tension in the microenvironment.

REFERENCES

1. Rose, F.R., and Oreffo, R.O. Bone tissue engineering: hope vs hype. Biochem Biophys Res Commun 292, 1, 2002.
2. Urist, M.R. Bone: formation by autoinduction. Science 150, 893, 1965.
3. Urist, M.R., Nakagawa, M., Nakata, N., and Nogami, H. Experimental myositis ossificans: cartilage and bone formation in muscle in response to a diffusible bone matrix-derived morphogen. Arch Pathol Lab Med 102, 312, 1978.
4. Wozney, J.M. Engineering new bone with bone morphogenic proteins. Ann Endocrinol (Paris) 67, 180, 2006.
5. Wan, M., and Cao, X. BMP signaling in skeletal development. Biochem Biophys Res Commun 328, 651, 2005.
6. Moser, M., and Patterson, C. Bone morphogenetic proteins and vascular differentiation: BMPing up vasculogenesis. Thromb Haemost 94, 713, 2005.
7. Rohrer, H. The role of bone morphogenetic proteins in sympathetic neuron development. Drug News Perspect 16, 589, 2003.
8. Cayuso, J., and Marti, E. Morphogens in motion: growth control of the neural tube. J Neurobiol 64, 376, 2005.
9. Hoffmann, A., and Gross, G. BMP signaling pathways in cartilage and bone formation. Crit Rev Eukaryot Gene Expr 11, 23, 2001.
10. Salim, A., Nacamuli, R.P., Morgan, E.F., Giaccia, A.J., and Longaker, M.T. Transient changes in oxygen tension inhibit osteogenic differentiation and Runx2 expression in osteoblasts. J Biol Chem 279, 40007, 2004.
11. Olmsted-Davis, E.A., Gugala, Z., Gannon, F.H., Yotnda, P., McAlhany, R.E., Lindsey, R.W., and Davis, A.R. Use of a chimeric adenovirus vector enhances BMP2 production and bone formation. Hum Gene Ther 13, 1337, 2002.
12. Gugala, Z., Olmsted-Davis, E.A., Gannon, F.H., Lindsey, R.W., and Davis, A.R. Osteoinduction by ex vivo adenovirus-mediated BMP2 delivery is independent of cell type. Gene Ther 10, 1289, 2003.
13. Fouletier-Dilling, C.M., Bosch, P., Davis, A.R., Shafer, J.A., Stice, S.L., Gugala, Z., Gannon, F.H., and Olmsted-Davis, E.A. Novel compound enables high-level adenovirus transduction in the absence of an adenovirus-specific receptor. Hum Gene Ther 16, 1287, 2005.
14. Davis, A.R., Wivel, N.A., Palladino, J.L., Tao, L., and Wilson, J.M. Construction of adenoviral vectors. Mol Biotechnol 18, 63, 2001.
15. Olmsted-Davis, E.A., Gugala, Z., Camargo, F., Gannon, F.H., Jackson, K., Kienstra, K.A., Shine, H.D., Lindsey, R.W., Hirschi, K.K., Goodell, M.A., Brenner, M.K., and Davis, A.R. Primitive adult hematopoietic stem cells can function as osteoblast precursors. Proc Natl Acad Sci U S A 100, 15877, 2003.
16. Clausen, B.E., Burkhardt, C., Reith, W., Renkawitz, R., and Forster, I. Conditional gene targeting in macrophages and granulocytes using LysMcre mice. Transgenic Res 8, 265, 1999.

17. Nolan, G.P., Fiering, S., Nicolas, J.F., and Herzenberg, L.A. Fluorescence-activated cell analysis and sorting of viable mammalian cells based on beta-D-galactosidase activity after transduction of Escherichia coli lacZ. Proc Natl Acad Sci U S A 85, 2603, 1988.
18. Sheu, W.H., Ou, H.C., Chou, F.P., Lin, T.M., and Yang, C.H. Rosiglitazone inhibits endothelial proliferation and angiogenesis. Life Sci 78, 1520, 2006.
19. El-Maadawy, S., Kaartinen, M.T., Schinke, T., Murshed, M., Karsenty, G., and McKee, M.D. Cartilage formation and calcification in arteries of mice lacking matrix Gla protein. Connect Tissue Res 44 Suppl 1, 272, 2003.
20. Luo, G., Ducy, P., McKee, M.D., Pinero, G.J., Loyer, E., Behringer, R.R., and Karsenty, G. Spontaneous calcification of arteries and cartilage in mice lacking matrix GLA protein. Nature 386, 78, 1997.
21. Bobryshev, Y.V. Transdifferentiation of smooth muscle cells into chondrocytes in atherosclerotic arteries in situ: implications for diffuse intimal calcification. J Pathol 205, 641, 2005.
22. Tintut, Y., Alfonso, Z., Saini, T., Radcliff, K., Watson, K., Bostrom, K., and Demer, L.L. Multilineage potential of cells from the artery wall. Circulation 108, 2505, 2003.
23. Abedin, M., Tintut, Y., and Demer, L.L. Mesenchymal stem cells and the artery wall. Circ Res 95, 671, 2004.
24. Hewitson, T.D., Wu, H.L., and Becker, G.J. Interstitial myofibroblasts in experimental renal infection and scarring. Am J Nephrol 15, 411, 1995.
25. Frid, M.G., Brunetti, J.A., Burke, D.L., Carpenter, T.C., Davie, N.J., and Stenmark, K.R. Circulating mononuclear cells with a dual, macrophage-fibroblast phenotype contribute robustly to hypoxia-induced pulmonary adventitial remodeling. Chest 128, 583S, 2005.
26. Kuwana, M., Okazaki, Y., Kodama, H., Izumi, K., Yasuoka, H., Ogawa, Y., Kawakami, Y., and Ikeda, Y. Human circulating CD14+ monocytes as a source of progenitors that exhibit mesenchymal cell differentiation. J Leukoc Biol 74, 833, 2003.
27. Kuhn, R., and Schwenk, F. Advances in gene targeting methods. Curr Opin Immunol 9, 183, 1997.
28. Rajewsky, K. Clonal selection and learning in the antibody system. Nature 381, 751, 1996.
29. Alberts, B.J.L., J; Raff, M.; Roberts, K. and Walter, P. Molecular Biology of the Cell. Garland Science, New York, New York, 2002.
30. Kinner, B., Gerstenfeld, L.C., Einhorn, T.A., and Spector, M. Expression of smooth muscle actin in connective tissue cells participating in fracture healing in a murine model. Bone 30, 738, 2002.
31. Sekiya, I., Tsuji, K., Koopman, P., Watanabe, H., Yamada, Y., Shinomiya, K., Nifuji, A., and Noda, M. SOX9 enhances aggrecan gene promoter/enhancer activity and is up-regulated by retinoic acid in a cartilage-derived cell line, TC6. J Biol Chem 275, 10738, 2000.
32. Akiyama, H., Chaboissier, M.C., Martin, J.F., Schedl, A., and de Crombrugghe, B. The transcription factor Sox9 has essential roles in successive

steps of the chondrocyte differentiation pathway and is required for expression of Sox5 and Sox6. Genes Dev 16, 2813, 2002.
33. Pittenger, M.F., Mackay, A.M., Beck, S.C., Jaiswal, R.K., Douglas, R., Mosca, J.D., Moorman, M.A., Simonetti, D.W., Craig, S., and Marshak, D.R. Multilineage potential of adult human mesenchymal stem cells. Science 284, 143, 1999.
34. Robins, J.C., Akeno, N., Mukherjee, A., Dalal, R.R., Aronow, B.J., Koopman, P., and Clemens, T.L. Hypoxia induces chondrocyte-specific gene expression in mesenchymal cells in association with transcriptional activation of Sox9. Bone, 2005.
35. Varghese, A.J., Gulyas, S., and Mohindra, J.K. Hypoxia-dependent reduction of 1-(2-nitro-1-imidazolyl)-3-methoxy-2-propanol by Chinese hamster ovary cells and KHT tumor cells in vitro and in vivo. Cancer Res 36, 3761, 1976.
36. Cao, X., and Chen, D. The BMP signaling and in vivo bone formation. Gene 357, 1, 2005.
37. Pietrzak, W.S., Woodell-May, J., and McDonald, N. Assay of bone morphogenetic protein-2, -4, and -7 in human demineralized bone matrix. J Craniofac Surg 17, 84, 2006.
38. Backesjo, C.M., Li, Y., Lindgren, U., and Haldosen, L.A. Activation of Sirt1 decreases adipocyte formation during osteoblast differentiation of mesenchymal stem cells. J Bone Miner Res 21, 993, 2006.
39. Cao, B., and Huard, J. Muscle-derived stem cells. Cell Cycle 3, 104, 2004.
40. Dominici, M., Pritchard, C., Garlits, J.E., Hofmann, T.J., Persons, D.A., and Horwitz, E.M. Hematopoietic cells and osteoblasts are derived from a common marrow progenitor after bone marrow transplantation. Proc Natl Acad Sci U S A 101, 11761, 2004.
41. Verfaillie, C.M. Multipotent adult progenitor cells: an update. Novartis Found Symp 265, 55, 2005.
42. Jabs, A., Moncada, G.A., Nichols, C.E., Waller, E.K., and Wilcox, J.N. Peripheral blood mononuclear cells acquire myofibroblast characteristics in granulation tissue. J Vasc Res 42, 174, 2005.
43. Holness, C.L., and Simmons, D.L. Molecular cloning of CD68, a human macrophage marker related to lysosomal glycoproteins. Blood 81, 1607, 1993.
44. De Palma, M., Venneri, M.A., Galli, R., Sergi Sergi, L., Politi, L.S., Sampaolesi, M., and Naldini, L. Tie2 identifies a hematopoietic lineage of proangiogenic monocytes required for tumor vessel formation and a mesenchymal population of pericyte progenitors. Cancer Cell 8, 211, 2005.
45. Postlethwaite, A.E., Shigemitsu, H., and Kanangat, S. Cellular origins of fibroblasts: possible implications for organ fibrosis in systemic sclerosis. Curr Opin Rheumatol 16, 733, 2004.
46. Cunningham, N.S., Paralkar, V., and Reddi, A.H. Osteogenin and recombinant bone morphogenetic protein 2B are chemotactic for human monocytes and stimulate transforming growth factor beta 1 mRNA expression. Proc Natl Acad Sci U S A 89, 11740, 1992.

47. Camargo, F.D., Green, R., Capetanaki, Y., Jackson, K.A., and Goodell, M.A. Single hematopoietic stem cells generate skeletal muscle through myeloid intermediates. Nat Med 9, 1520, 2003.
48. Camargo, F.D., Chambers, S.M., and Goodell, M.A. Stem cell plasticity: from transdifferentiation to macrophage fusion. Cell Prolif 37, 55, 2004.
49. Schipani, E. Hypoxia and HIF-1alpha in chondrogenesis. Ann N Y Acad Sci 1068, 66, 2006.
50. Salnikov, A.V., Roswall, P., Sundberg, C., Gardner, H., Heldin, N.E., and Rubin, K. Inhibition of TGF-beta modulates macrophages and vessel maturation in parallel to a lowering of interstitial fluid pressure in experimental carcinoma. Lab Invest 85, 512, 2005.

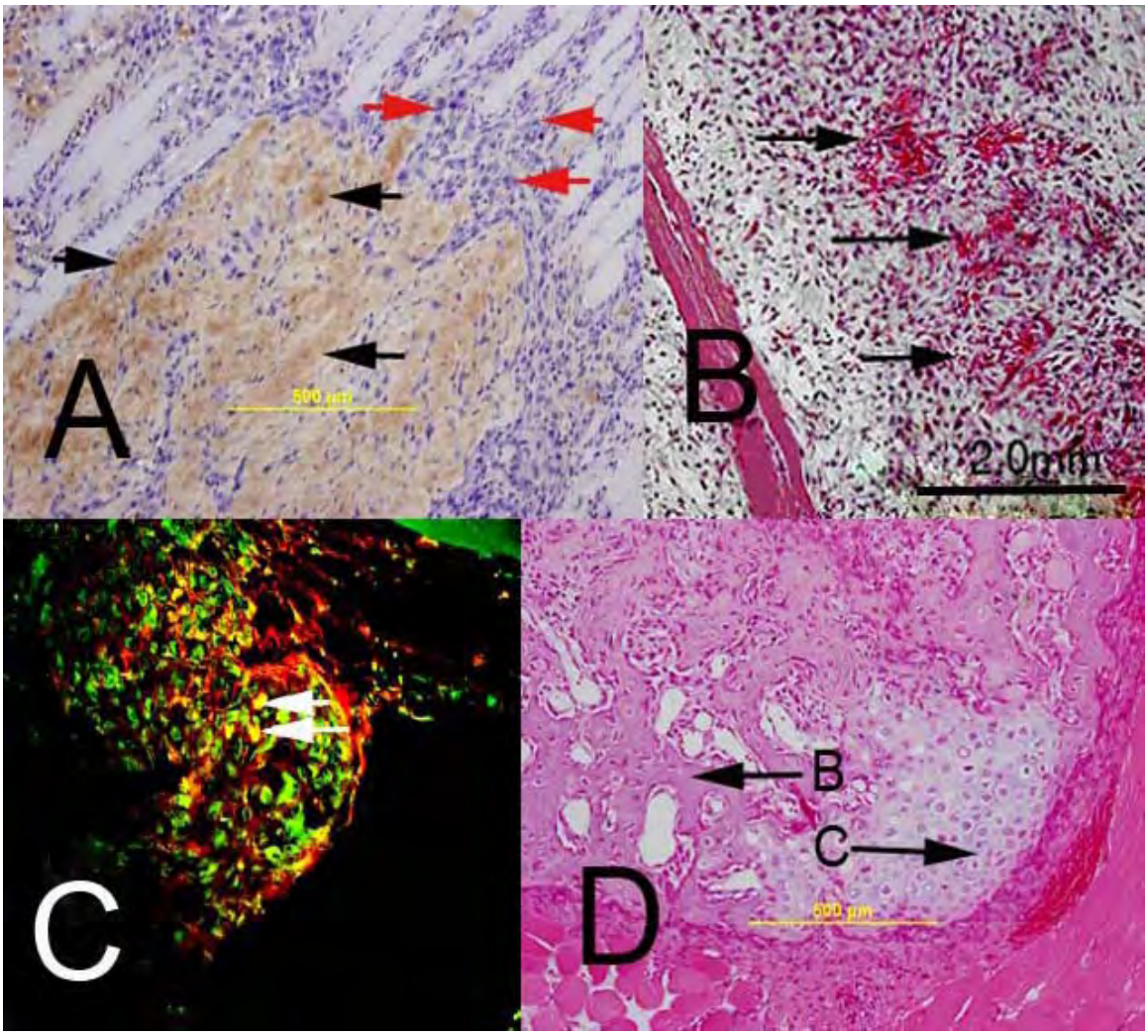

Figure 1

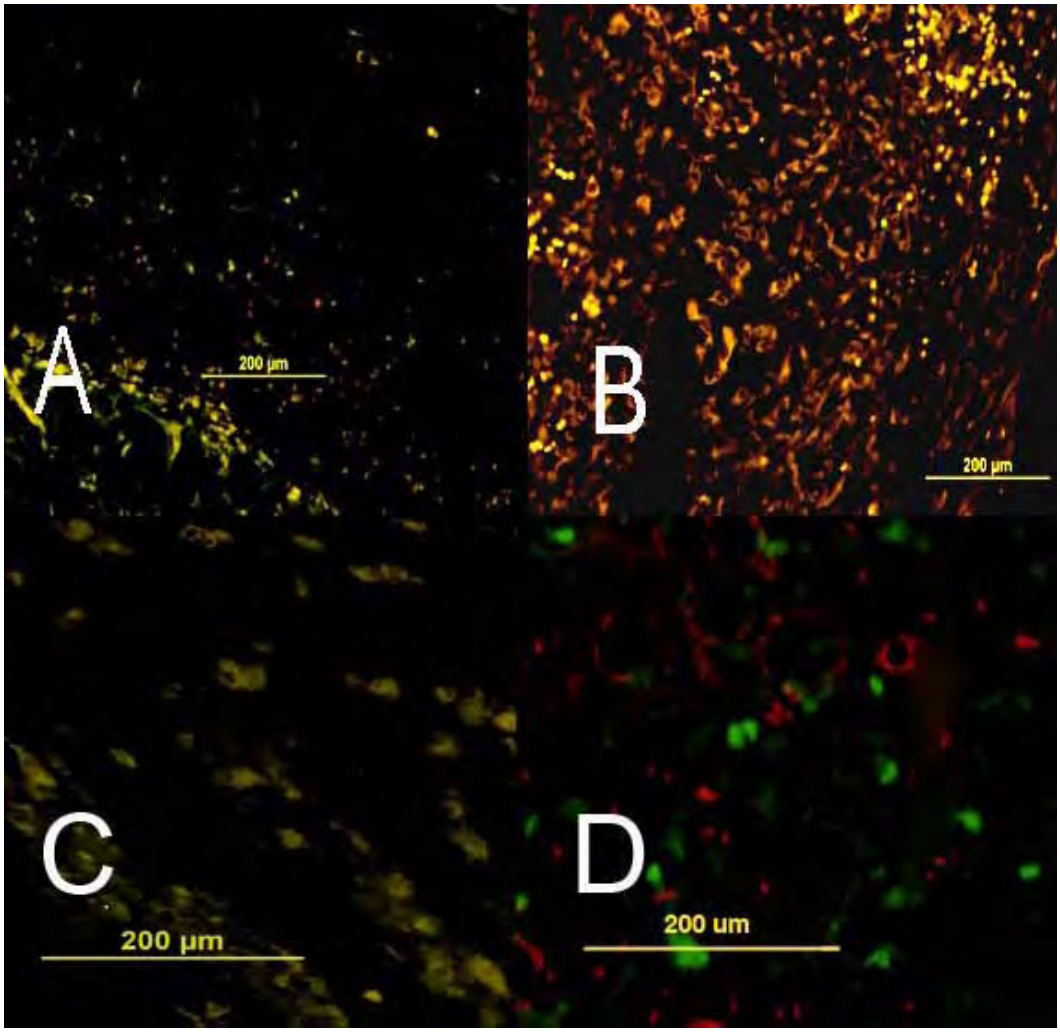

Figure 2

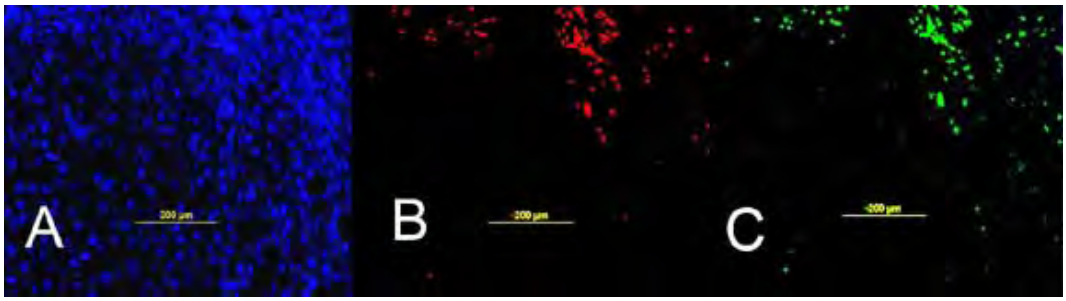

Figure 3

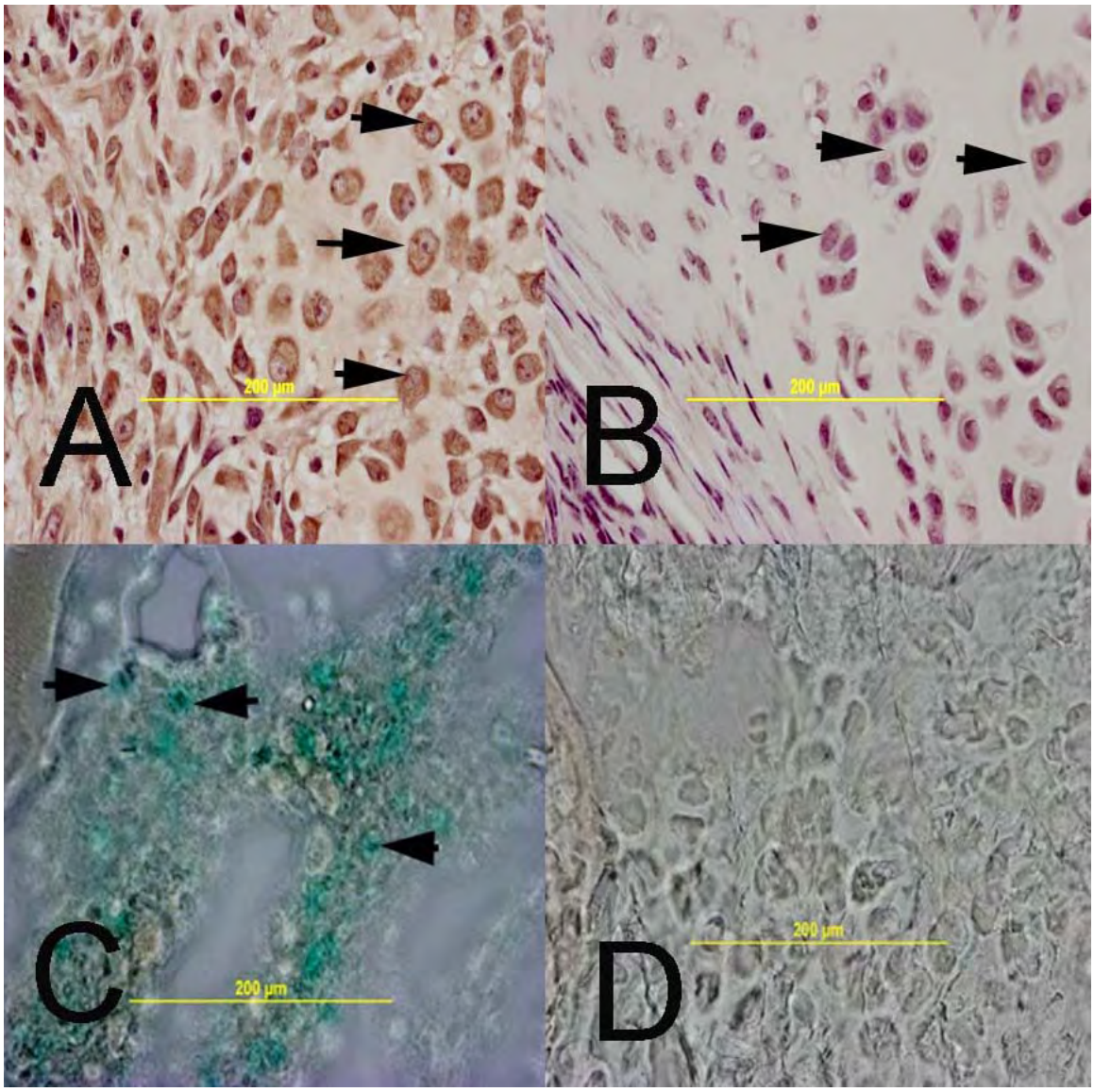

Figure 4

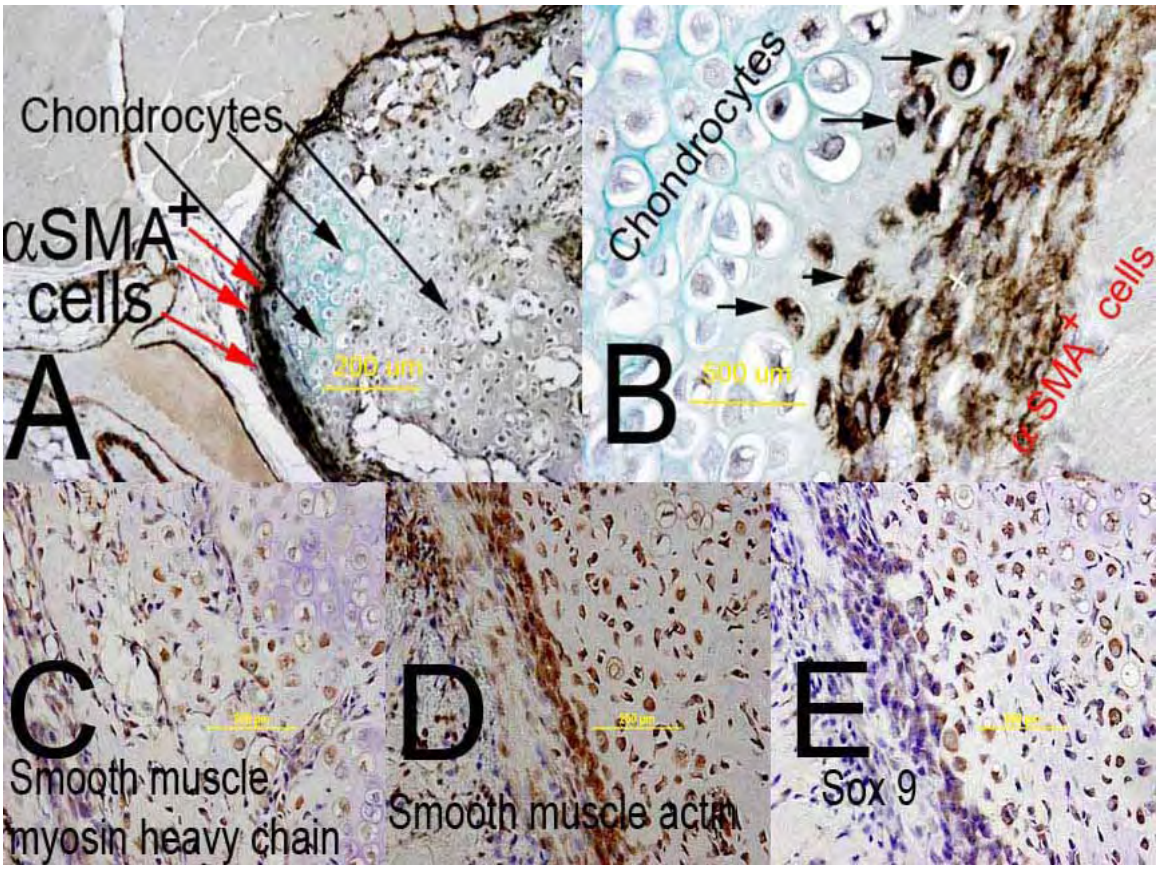
Chondrocytes
αSMA+ cells
200 um
A
Chondrocytes
500 um
B
α SMA+ cells
C
Smooth muscle myosin heavy chain
D
Smooth muscle actin
E
Sox 9

Figure 5

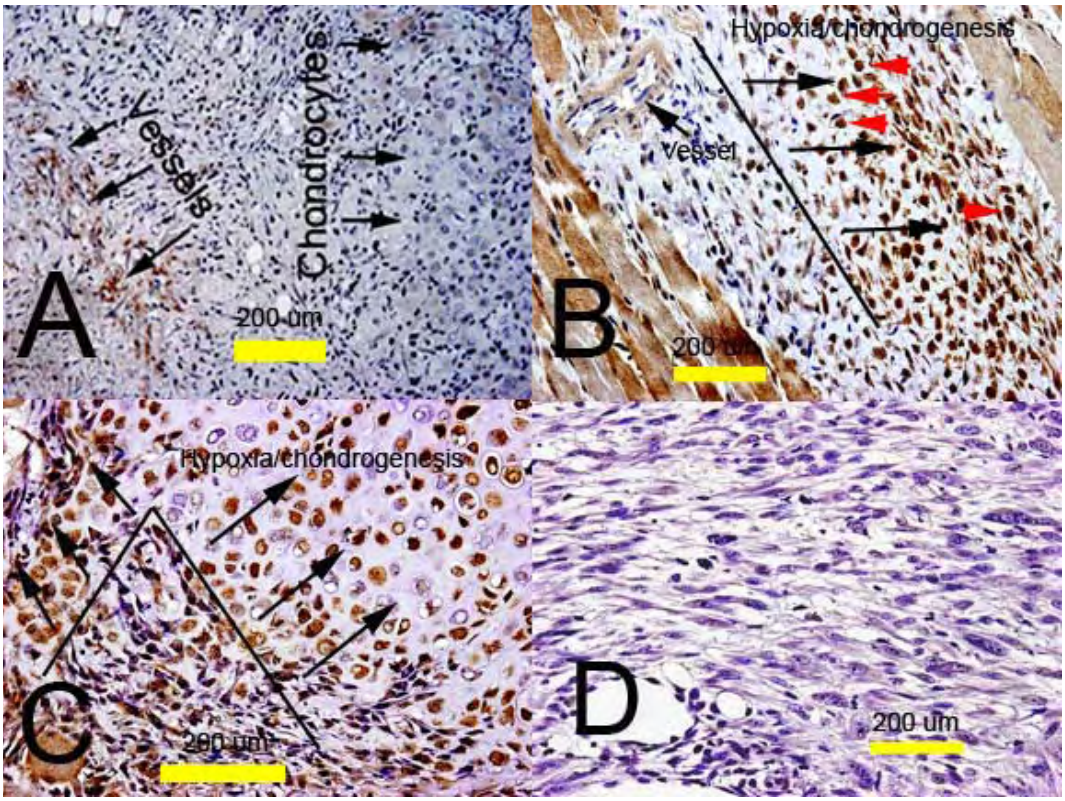
Vessels
Chondrocytes
A
200 um
Hypoxia/chondrogenesis
Vessel
B
Hypoxia/chondrogenesis
C
200 um
D
200 um

Figure 6

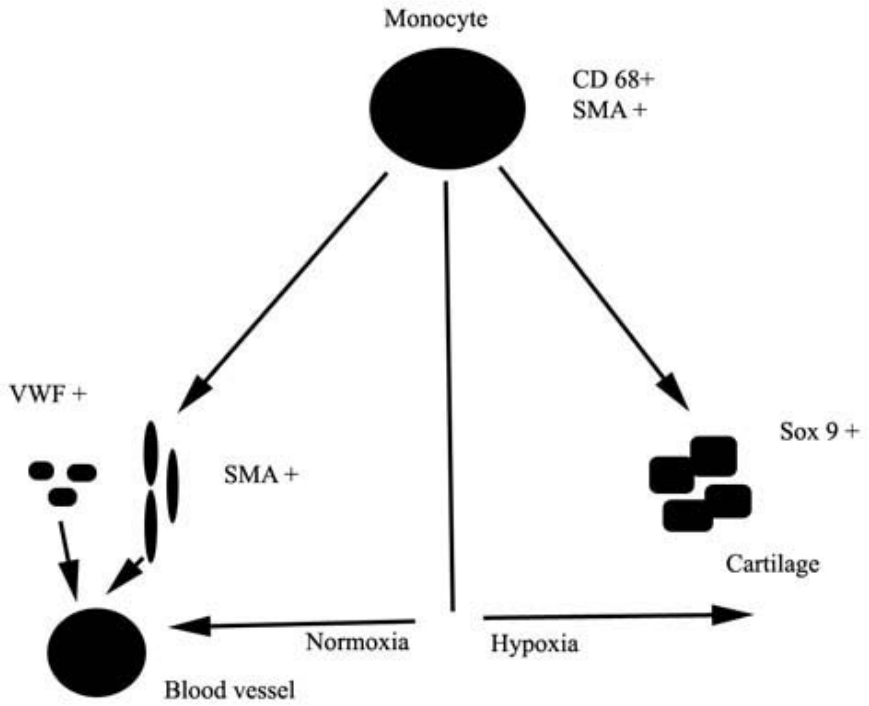
Monocyte
CD 68+
SMA +
VWF +
SMA +
Sox 9 +
Cartilage
Normoxia
Hypoxia
Blood vessel

Figure 7